Two- and Three-Liquid Phase Equilibria in Industrial Mixed-Solvent Electrolyte Solutions

Experiments and modelling of systems of importance for the extraction of caprolactam

Two- and Three-Liquid Phase Equilibria in Industrial Mixed-Solvent Electrolyte Solutions

Experiments and modelling of systems of importance for the extraction of caprolactam

Proefschrift

ter verkrijging van de graad van doctor
aan de Technische Universiteit Delft
op gezag van de Rector Magnificus Prof.dr.ir. J.T. Fokkema
voorzitter van het College voor Promoties
in het openbaar te verdedigen
op dinsdag 18 maart 2003 om 13:30 uur

door

Gerard Hendrik VAN BOCHOVE

scheikundig ingenieur
geboren te Oud-Beijerland

Dit proefschrift is goedgekeurd door de promotor:
Prof. dr. ir. J. de Swaan Arons

Toegevoegd promotor: Dr.ir. Th.W. de Loos

Samenstelling promotiecommissie:

Rector Magnificus,	voorzitter
Prof.dr.ir. J. de Swaan Arons	Technische Universiteit Delft, promotor
Dr.ir. Th.W. de Loos	Technische Universiteit Delft, toegevoegd promotor
Drs. G.J.P. Krooshof	DSM Research, Sittard
Prof. dr. W. Fürst	École Nationale Supérieure de Techniques Avancées, Paris, France
Prof. dr.ir. L.A.M. van der Wielen	Technische Universiteit Delft
Prof. dr. G.J. Witkamp	Technische Universiteit Delft
Prof. dr. G. Frens	Technische Universiteit Delft

Dit werk werd uitgevoerd bij het Laboratorium voor Toegepaste Thermodynamica en Fasenleer van de faculteit Toegepaste Natuurwetenschappen van de Technische Universiteit Delft en werd financieel ondersteund door DSM Research, Sittard.

Published and distributed by: DUP Science

DUP Science is an imprint of
Delft University Press
P.O. Box 98, 2600 MG, Delft
The Netherlands
Telephone: +31 15 27 85678
Telefax: +31 15 27 85706
E-mail: Info@library.tudelft.nl

ISBN 90-407-2394-x

Printed in The Netherlands

Table of contents

Summary

Two- and Three-Liquid Phase Equilibria in
Industrial Mixed-Solvent Electrolyte Solutions

An accurate representation of demixing in mixed-solvent electrolyte solutions remains one of the challenging research areas in chemical engineering. The simulation and design of industrial extraction processes involving electrolytes depends heavily on the availability of models that can describe the influence of ions on the phase behaviour: The presence of charged species in a mixed-solvent solution dramatically influences the phase distribution of a solute between the liquid phases. Moreover, the unexpected occurrence of three liquid phases can have a detrimental influence on the performance of an extraction process and should be anticipated. Therefore, a good understanding of the relevant phase behaviour is essential.

In the extraction process of caprolactam, the monomer of nylon-6, concentrated mixed-solvent solutions of ammonium sulfate exist. In this project a model had to be developed, that is able to represent and predict the demixing behaviour of water + caprolactam + solvent + ammonium sulfate solutions. Because of the lack of relevant experimental data in literature, experiments were to be carried out to provide the equilibrium data required to test and to adjust the model.

The experiments were carried out on liquid-liquid equilibria of ternary and quaternary systems containing caprolactam, water, an organic solvent (benzene, 1-heptanol or 2-heptanone) and ammonium sulfate at 20, 40 and 60˚C. Mixtures were prepared, stirred and then allowed to settle and to split into two liquid phases. Samples were taken and analysed by gas chromatography for the organic components, Karl-Fischer titration for water and titration with barium perchlorate for ammonium sulfate. The experiments show that the distribution of caprolactam changes with increasing temperature and salt concentration. At higher temperatures and higher salt concentrations more caprolactam is found in the organic phase.

For benzene and 2-heptanone, also three-liquid phase equilibria were encountered and determined. The pattern of the phase behaviour was studied at different temperatures and salt concentrations. A progression was found with salt concentration from two liquid phases at low salt concentrations to three liquid phases at higher salt

concentrations and to two liquid phases again at still higher concentrations. With increasing temperature the range of concentrations where three liquid phases are present, is shrinking and finally the three phase region disappears. The tricritical point of the system water + benzene + caprolactam + ammonium sulfate, where the three liquid phases are identical, was not determined but its location could be estimated from the experiments.

The experimental liquid-liquid equilibrium data could successfully be correlated using an activity coefficient model based on the extended electrolyte NRTL model. This model is built up from a NRTL contribution, a Pitzer-Debye-Hückel contribution, a Born contribution and a Brønsted-Guggenheim contribution. The modified electrolyte NRTL model developed in this PhD-project includes the solvent composition dependency of the solution properties by using mixing rules for the solution properties and taking this into account in the derivation of the activity coefficients. In this way a much better representation could be obtained of the salt concentration in the organic phase, which represented a major problem in the original model. A modified Brønsted-Guggenheim contribution was added to improve the representation of equilibrium data near the critical point of the solution. The results of the model are compared to those of the original electrolyte NRTL model for a large number of water + solvent + salt systems and for systems containing caprolactam.

The modelling of three-liquid phase equilibria puts a high demand on the consistency of the model. However, a satisfactory representation could be obtained of experimental three-liquid phase equilibrium data for the systems water + 2-heptanone + caprolactam + ammonium sulfate, water + benzene + caprolactam + ammonium sulfate and water + benzene + ethanol + ammonium sulfate.

Some additional calculations were performed using the primitive Mean Spherical Approximation (MSA) theory and using an electrolyte equation of state, incorporating MSA theory. However, the results of the calculations were markedly less good than the results presented for the modified extended electrolyte NRTL model.

Gerard van Bochove

Samenvatting

Two- and Three-Liquid Phase Equilibria in
Industrial Mixed-Solvent Electrolyte Solutions

Het nauwkeurig kunnen modelleren van de ontmenging van oplossingen bestaande uit zouten, water en één of meer organische componenten is van groot belang voor de chemische industrie. In veel processen wordt gebruik gemaakt van extractie voor de zuivering van een productstroom. Wanneer in het productieproces zouten aanwezig zijn of gevormd worden, heeft dit grote gevolgen voor de ligging van de fasenevenwichten in het extractieproces. Het goed kunnen ontwerpen, verbeteren en regelen van industriële extractieprocessen is afhankelijk van de beschikbaarheid van een fysisch model dat de invloed kan beschrijven van de zouten op het fasengedrag.

De aanwezigheid van de ionen veroorzaakt een grote verandering van de verdeling van de organische componenten over de verschillende vloeistoffasen. Bij bepaalde condities kunnen zelfs drie vloeistoffasen aanwezig zijn. Het is duidelijk dat wanneer dit onverwachts optreedt, dit een enorm effect zal hebben op het rendement van een scheidingsproces. Daarom is een goed begrip en een goede kennis van het betreffende fasengedrag essentieel.

Caprolactam is de grondstof voor nylon-6 en wordt onder andere door DSM in Nederland gemaakt. Caprolactam verlaat het productieproces als een waterige stroom van caprolactam, het bijproduct ammoniumsulfaat en diverse organische en anorganische verontreinigingen. Om een hoge zuiverheid van de caprolactam te verkrijgen, wordt onder andere gebruik gemaakt van extractie met een organisch oplosmiddel. In het extractieproces van caprolactam komen dus oplossingen voor van water, organische oplosmiddelen, caprolactam en hoge concentraties ammonium-sulfaat. Het modelleren van dit extractieproces geeft problemen door die hoge zoutconcentraties. Hiervoor is geen goed model beschikbaar.

Het doel van dit promotieonderzoek was daarom het ontwikkelen van een model dat de ontmenging van water + organisch oplosmiddel + caprolactam + ammoniumsulfaat kan beschrijven en bij voorkeur ook kan voorspellen. Dit modelleren is alleen mogelijk wanneer voldoende experimentele data beschikbaar zijn. Omdat de hoeveelheid

beschikbare experimentele data in de wetenschappelijke literatuur beperkt is, werden ook experimenten uitgevoerd om te voorzien in de benodigde evenwichtsdata.

Het experimentele gedeelte van dit onderzoek bestond uit het meten van vloeistof-vloeistofevenwichten van ternaire en quaternaire systemen van caprolactam, water, een organisch oplosmidddel (benzeen, 1-heptanol of 2-heptanon) en ammoniumsulfaat bij 20˚C, 40˚C en 60˚C. Hiervoor werden een aantal mengsels bereid en intensief geroerd en vervolgens werd gewacht tot volledig evenwicht. Van de twee of drie vloeistoffasen werden vervolgens monsters genomen, die geanalyseerd werden met behulp van gaschromatografie (organische componenten), Karl-Fischer titratie (water) en titratie met bariumperchloraat (ammoniumsulfaat).

Uit de experimenten kan worden afgeleid dat de verdeling van caprolactam over beide fasen verandert ten gunste van de organische fase bij toenemende temperatuur en zoutconcentratie. Bij hogere temperaturen neemt de oplosbaarheid van caprolactam in het organische oplosmiddel sneller toe dan de oplosbaarheid in water en zal zich dus steeds meer caprolactam bevinden in de fase met voornamelijk oplosmiddel. Omdat de oplosbaarheid van zout in de organische fase heel laag is, zal het zout in de waterfase blijven. Bij hogere zoutconcentraties treedt vervolgens het “salting-out” effect op. Door de hoge zoutconcentratie in de waterfase, zijn niet voldoende watermoleculen beschikbaar voor het oplossen van de caprolactam en de caprolactam zal dus een voorkeur hebben voor de organische fase.

Voor de systemen met benzeen of 2-heptanon als het oplosmiddel werden naast de evenwichten met twee vloeistoffasen (LLE) in een bepaald concentratiegebied ook evenwichten gevonden met drie vloeistoffasen (LLLE). Bij een bepaalde zoutconcentratie kan één van de twee vloeistoffasen in een evenwicht met twee vloeistoffasen zich splitsen in twee nieuwe fasen en wordt dus een driefasenevenwicht gevormd. Dit speciale fasengedrag werd bestudeerd bij verschillende temperaturen en zoutconcentraties. Op deze manier werd een overgang gevonden van twee vloeistoffasen bij lagere zoutconcentraties, naar drie vloeistoffasen bij hogere zoutconcentraties en weer naar twee vloeistoffasen bij nog hogere zoutconcentraties. Bij toenemende temperatuur neemt het concentratiegebied waarin drie fasen optreden af in grootte en verdwijnt het driefasengebied uiteindelijk. Het zogenaamde trikritische punt, waarbij de drie fasen dezelfde samenstelling hebben kon niet worden bepaald, maar de ligging van dit punt kon op basis van de experimenten wel worden geschat.

De experimenteel bepaalde evenwichten konden goed beschreven worden met een activiteitscoëfficiënten model op basis van het electrolyte NRTL model. Dit model bestaat uit een NRTL bijdrage, een Pitzer-Debye-Hückel bijdrage, een Born bijdrage en een Brønsted-Guggenheim bijdrage. Het oorspronkelijke model werd gewijzigd, zodat het model beter rekening houdt met het feit dat de eigenschappen van het (zoutvrije) mengsel afhankelijk zijn van de samenstelling van het mengsel van de oplosmiddelen. Dit komt met name tot uitdrukking in de afleiding van de activiteitscoëfficiënten van de oplosmiddelen. Door deze wijziging wordt het mogelijk de zoutconcentratie in de organische fase met een redelijke nauwkeurigheid te voorspellen, wat met het oorspronkelijke model veel problemen opleverde. Door een Brønsted-Guggenheim bijdrage in gewijzigde vorm toe te voegen, kan met het nieuwe model een betere weergave van het fasengedrag in de buurt van het kritische punt van het mengsel worden verkregen. Dit is van belang voor de evenwichten in de mengsels met caprolactam, waarin zich een dergelijk kritisch punt bevindt.

Met het in dit werk gepresenteerde model werden evenwichtsberekeningen uitgevoerd voor LLE voor een groot aantal oplossingen zoals die in de industrie voorkomen, te weten oplossingen van zout in water en alcohol en de oplossingen met caprolactam, zoals gebruikt in de experimenten. De resultaten met het nieuwe model werden vergeleken met het oorspronkelijke model voor deze systemen. De conclusie van deze vergelijking is dat het gewijzigde model een betere weergave geeft van de experimentele data dan het oorspronkelijke model. Dit is ook het geval wanneer voor het oorspronkelijke model wordt uitgegaan van de meer realistische aanname van partiële dissociatie van het zout, in plaats van volledige dissociatie.

Het modelleren van evenwichten met drie vloeistoffasen stelt hoge eisen aan een thermodynamisch model en daarom is hierover nauwelijks iets gepubliceerd in de wetenschappelijke literatuur. Toch kon ook hier een goede beschrijving gevonden worden van de experimentele data voor de systemen water + benzeen + caprolactam + ammoniumsulfaat, water + 2-heptanon + caprolactam + ammoniumsulfaat en water + ethanol + benzeen + ammoniumsulfaat.

Een nadeel van modellen als het electroliet NRTL model is het grote aantal aanpasbare parameters en de geringe fysische achtergrond. Daarom werd gezocht naar een model dat deze bezwaren niet of in mindere mate heeft en toch een vergelijkbare kwaliteit heeft. Enkele aanvullende berekeningen werden uitgevoerd met de Mean Spherical Approximation theorie en met behulp van een toestandsvergelijking voor

electroliet-oplossingen, die ook gebruik maakt van MSA theorie. Hoewel deze theorie een betere fysische achtergrond heeft, leverden deze berekeningen echter beduidend minder goede resultaten op dan de berekeningen met het gewijzigde electroliet NRTL model. Met betrekking tot de toestandsvergelijking moest helaas geconcludeerd worden dat door gebrek aan een aantal experimentele waarden voor ammoniumsulfaat veel van de voorspellende waarde van dit model verloren gaat.

Gerard van Bochove

1. Introduction

In this introductory chapter the incentives for the project are given. The importance of understanding liquid-liquid equilibria and the relevance of electrolyte solutions to industry are discussed. Special attention is paid to the production and extraction process of caprolactam. In the last part of this chapter, the objectives and approach for the work reported in this thesis are presented.

1.1 Electrolyte solutions in industry

Not only in the chemical and process industry, but also in daily life, phase equilibria are omnipresent and play an important role. When two mixtures are brought into contact, a transfer of components will occur. Phase equilibrium is the state in which the different phases are at the same conditions of pressure and temperature and in which their compositions are not changing anymore. At this state usually the compositions of the different phases are different. Phases that are in contact will tend to go to an equilibrium state by a change of conditions and transfer of components. This transfer of components from one phase to another is the basis of most separation technologies. Separation processes in chemical engineering include distillation, extraction, adsorption, absorption and other technologies in which two or more phases are in contact. Separation processes are essential for the industry to remove byproducts and unreacted components from a product stream. Since the separation part of a plant is often larger than the actual production part, understanding of phase equilibria is vital for designing and running a chemical process.

At phase equilibrium, the different phases can be in a different physical state. The phases can be either vapour, liquid or solid. In a distillation process a vapour phase and a liquid phase are in contact. In liquid-liquid extraction processes, two liquid phases are brought into contact and mixture components are transferred from one phase to another. Depending on the differences in solubility, solutes will distribute between both phases in a certain ratio. This principle is used to selectively remove components from a product stream. To maximise the economic efficiency of an extraction process, it is important to have a thorough knowledge of the liquid-liquid equilibria of the systems involved. Thermodynamics provides the data and theory that

are required. However, understanding of liquid-liquid demixing is not only important for extraction processes. For example, in distillation processes the unexpected occurrence of two liquid phases together with the vapour phase can have a dramatic influence on the efficiency of the distillation process.

Design and simulation of separation processes require experimental data to measure how a mixture will behave, to know which influence temperature and pressure will have on the phase behaviour, but also to know what components to use for dissolution and how minor components will affect the efficiency of a separation. In addition to experiments, a theory is required to describe the phenomena measured, to interpolate between the experimental data points and, if possible, to extrapolate to conditions outside the experimental range (Chen and Mathias, 2002). Usually, the theory is formulated as a mathematical model that contains one or more parameters that are adjusted for a better representation of reality. The ideal model is the model that does not require experimental data and still is flexible enough to use. However, in the nonideal world of phase equilibria, experimental data will always be required, to improve the performance of a model, to check its predictions, to retain the flexibility required for real time simulations, but mainly because the underlying theory is incomplete and the reality may be too complex to be captured in equations.

An example of a subject in the theory of phase equilibria that still is not fully understood is the influence of charged species on the phase behaviour of a mixture. Although theories and models of equilibria of simple solvent mixtures are available, the addition of a salt to such a solvent mixture causes a deviation from the original behaviour that cannot be described satisfactory yet with thermodynamic models. The description of the nonideality caused by the introduction of ions to a mixture of solvents is still a challenge for chemical engineers and scientists. Nevertheless, mixed-solvent electrolyte solutions exist in a large number of processes.

Examples of processes that require information on phase equilibria of mixed-solvent electrolyte solutions are numerous:

- Removal of acid gases from gas mixtures by stripping/absorption with aqueous solutions of alkanol amines (Austgen et al., 1989)
- Partitioning processes in biochemical processes, where two phases are created from one phase by addition of a compound (Cheluget et al., 1994)
- Avoidance of gas hydrate formation by methanol and salt (Zuo et al., 2001)

- Desalination of sea and brackish waters by solvent extraction (De Santis et al., 1976)
- Separation of proteins from fermentation broth by fractional precipitation or crystallization (Chen et al., 1989)
- Downstream recovery processes of antibiotics (Zhu et al., 1990)
- Precipitation and (extractive) crystallization processes to recover salt from a solution, for example $CaCl_2$ and $MgCl_2$ from 2-propanol/water (Balaban et al., 2002)
- Enhanced oil recovery of reservoir fluids (Knickerbocker et al., 1979)
- Waste water treatment
- Production processes with a salt as intermediate product
- Hydrometallurgical processes
- Distillation and extraction of miscellaneous mixtures containing salts or acids, where salt can be present as a byproduct or is added to shift a phase equilibrium towards more effective separation of components. Pfennig and Schwerin (1998) proved that even rather low concentrations of electrolytes may have strong effects on extraction systems.

An example of a production process where the salt is a major byproduct and has a large influence on the purification process is the production of ε-caprolactam. Since the desire to be able to simulate the extraction of ε-caprolactam was one of the main incentives of the current work, the production and extraction of ε-caprolactam will be discussed in more detail in the next section.

1.2 Production and extraction of caprolactam

1.2.1 Chemistry

ε-Caprolactam (further called caprolactam) is one of the most widely used chemical intermediates. Caprolactam or 6-amino-hexanoic acid-lactam is a white, hygroscopic crystalline solid at ambient temperature with a characteristic odour. It is highly soluble in water and most organic solvents and is hardly soluble in high molecular weight aliphatic hydrocarbons. The compound melts at 69°C. It can be hydrolysed, N-alkylated, O-alkylated, halogenated, but its most important reaction is polymerization. Polymerization can occur by polycondensation, polyaddition or anionic polymerization. Caprolactam is readily converted to high molecular weight

linear nylon-6 polymers. Caprolactam has already been known since the 19th century, but commercial interest started in 1938 when the first spinnable polymer was produced by polycondensation of caprolactam (Figure 1.1). Since then, caprolactam has gained importance and large-scale industrial production has increased rapidly. (Ritz et al., 1999)

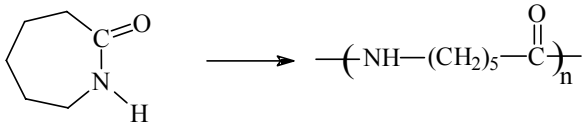

Figure 1.1: Chemical structure of caprolactam and Nylon-6.

In 2000, the world caprolactam production was about 4.2 million tons per year (Chemical Week, August 29, 2001). Caprolactam is used almost exclusively as a raw material for the production of nylon-6 fibers and resins. Fibers account for 73 percent of the nylon-6 polymer market and are made into textile (sportswear, leisure wear), carpets and industrial textiles (tire cord, ropes, nets). The resins are used in engineering plastics, principally in electronics, automotive applications and films for food packaging. The top five producers of caprolactam are BASF, DSM, Honeywell, Ube Industries and Toray Industries. These producers accounted for 43 percent of global caprolactam capacity in 2000. A recent development on the caprolactam market is the DSM/Honeywell recycling technology for converting waste nylon-6 back into caprolactam (Fisher, 2000).

1.2.2 Production

Several commercial processes exist for the manufacturing of caprolactam. Conventional caprolactam processes, that account for about 85% of the world caprolactam production, consist of three steps: production of cyclohexanone, conversion to cyclohexanone oxime and Beckman rearrangement to caprolactam. In the first step of the cyclohexanone process, cyclohexanone is produced by catalytic oxidation of cyclohexane with air or by hydrogenation of phenol. For the subsequent conversion of cyclohexanone to cyclohexanone oxime, three processes are in use: the classic HSO-process (HSO = Hydroxylamine Sulfate Oxime), DSM's HPO-process (HPO = Hydroxylamine Phosphate Oxime) and the BASF/Inventa process, based on NO reduction. In these processes different amounts of ammonium sulfate are produced

as byproduct. The resulting cyclohexanone oxime is converted to caprolactam by Beckmann rearrangement using sulfuric acid or oleum as a rearrangement medium. The reaction mixture is neutralized in ammonia and water, producing ammonium sulfate. The ammonium sulfate production, in the HSO process about four times the caprolactam production, is a major drawback of traditional processes. The ammonium sulfate is used as fertilizer, but its production is economically less interesting (Simons and Haasen, 1991).

Other commercial processes are those based on photonitrosation of cyclohexane or by nitrosation of cyclohexane carboxylic acid. These and more processes are described by Ritz et al. (1999). Recently, a new commercial process for the production of caprolactam became commercially available, DSM's Altam process, which is based on butadiene and carbon monoxide and eliminates the production of ammonium sulfate as a byproduct (Fisher, 2000).

1.2.3 Extraction

The description of the extraction of caprolactam in this section focusses on processes with ammonium sulfate as byproduct. Although newly developed processes reduce or eliminate the ammonium sulfate production, most existing plants still produce large amounts of ammonium sulfate. Thus, the relevance of the process of ammonium sulfate removal from a caprolactam product stream is still high. In addition, the process described here is representative for other extraction processes involving electrolyte solutions.

For the production of nylon-6 high purity caprolactam is required. To reduce the organic and inorganic impurities to a very low concentration level, a series of purification steps is applied. These include extraction, chemical and physical treatment and final vacuum distillation. After neutralization with water and ammonia, the product mixture is led into a settler, where it separates into two liquid phases: a lighter phase that is rich in caprolactam (up to 70% w/w) above a concentrated ammonium sulfate solution (40% w/w) phase with low concentrations of caprolactam. Both phases are transported to an extraction process. The full extraction process (as given by Simons and Faasen, 1991) is depicted in Figure 1.2.

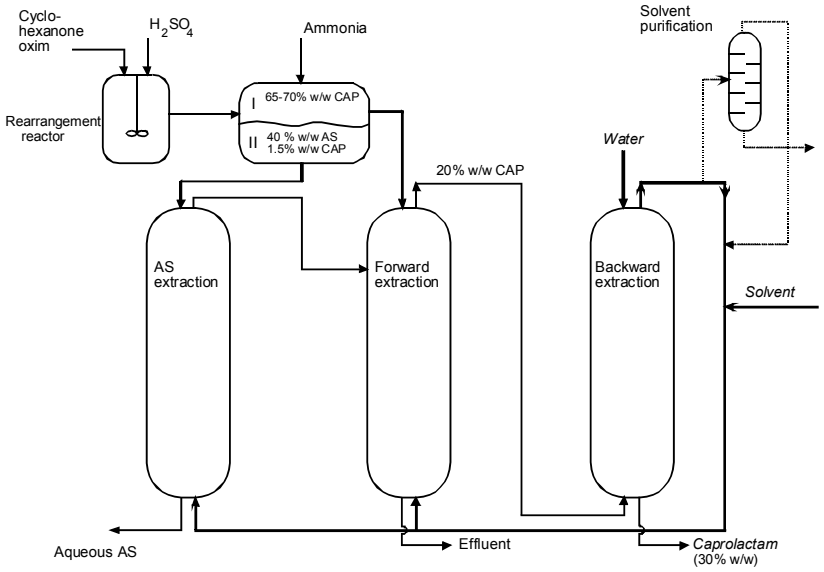

Figure 1.2: Extraction process of caprolactam (Simons and Faasen, 1991)

The ammonium sulfate rich layer is subjected to a separate extraction process with an organic solvent. The caprolactam dissolves in the organic phase (the extract), which is transported to the forward extraction. The forward extraction employs the same organic solvent as the ammonium sulfate extraction. The crude caprolactam top layer is also lead to the forward extraction. Impurities that are more soluble in water than in the organic solvent are left behind in the aqueous raffinate. The organic extract, containing about 20% w/w caprolactam, still contains impurities that dissolve better in the organic solvent than in water. These impurities are removed by a re-extraction or backward extraction with water. The organic solvent is reused after partial distillation to avoid accumulation of impurities. The resulting caprolactam-free aqueous solution is incinerated. The concentrated ammonium sulfate solution is evaporated and crystallized. Before being distilled, the caprolactam extract is subjected to a number of physicochemical purifications, such as hydrogenation and ion exchange treatment.

To simulate this extraction process, understanding of the liquid-liquid equilibria of the quaternary system water + solvent + caprolactam + ammonium sulfate is important. In the settler, the ternary system water + caprolactam + ammonium sulfate is of importance, in the first extraction column the quaternary system at high salt

concentrations, in the forward extraction the quaternary system at low salt concentrations and in the backward extraction the ternary system water + solvent + caprolactam is predominant. In summary: For simulating the complete extraction process a model is required that describes the liquid-liquid equilibria of the system water + solvent + caprolactam + ammonium sulfate over the full range of (salt) concentrations. One option is the usage of polynomials fitted to each stage in the process. However, there is a desire for one model capable of describing all stages of the process. Such a model is currently not available.

1.3 Objectives of the project

The main objective of this work is the development of a **thermodynamic model** that is able to describe demixing of the liquid phase (LLE and LLLE) in mixed-solvent electrolyte solutions from low salt concentrations up to the solubility limit of the salt. This concerns in particular LLE of the electrolyte systems that are of importance for the extraction process of caprolactam, consisting of water, an organic solvent, caprolactam and ammonium sulfate. The development of the model has to be supported by experimental data to test and adjust the model.

Since benzene, that currently is being used as the extracting solvent at DSM, is suspected of carcinogenity, there is also a need for **experimental data** with other solvents. These data should facilitate the choice of another solvent in the future, by supplying information on functional groups that can be of importance for the extracting qualities of a solvent. The measurements and usage of data sets of other solvents will also help to make the model and its parameters more generally applicable.

1.4 Research Status

In the recent literature, much attention has been paid to the thermodynamics of electrolyte solutions, both using an engineering approach or using a more fundamental approach. Not all of this literature can be used for the description of phase equilibria. Many publications focus on ion-ion interactions or are only applicable to aqueous solutions. For the description of phase equilibria, it is necessary that an expression is derived that also takes into account interactions between ions and each solvent, and

mutual interactions of solvents. Many times this is achieved by a combination of models for molecular components and a model for electrostatic interactions, like the famous Debye-Hückel theory. A survey of thermodynamic models for electrolyte solutions will be given in Chapter 2.

The number of publications on the modelling of **liquid-liquid equilibria of mixed solvent electrolyte solutions** is small, compared to the abundance of models that in some way or another deal with the thermodynamics of electrolyte solutions. An overview of the most relevant publications in this area is given below.

- Most successful so far (and in fact the only model that is widely used) is the electrolyte NRTL model of Chen et al. (1986). This model is an extension to electrolyte solutions of the NRTL model (Renon and Praunitz, 1968) to which a Pitzer-Debye-Hückel and a Born expression have been added to include the electrostatic effects.
- Cheluget et al. (1994) based their model on the Flory-Huggins theory and the Bromley equation for the electrostatic interactions and used an expression based on nonprimitive Mean Spherical Approximation theory to correct for the different reference states in both phases. The model was applied with reasonable success to water + propanol + NaCl systems.
- Zerres and Prausnitz (1994) used the Van Laar model for short range forces, a chemical model to describe ionic solvation and an extended Debye-Hückel model to account for long range electrostatic forces. They did not correct for the different reference states of the contributions. In spite of the relatively large number of adjustable binary and ternary parameters, the model represented LLE of water + alcohol + NaCl systems only with reasonable success.
- Peng et al. (1994) developed an expression based on regular solution theory and Debye-Hückel theory and applied it with moderate success to water + alcohol + salt systems. The model has only four parameters for a ternary system.
- Copeman and Stein (1987) used a perturbed MSA hard sphere equation of state to correlate LLE of water + aniline + NaCl or NH_4Cl systems. With a limited number of parameters, they were able to reproduce aniline distribution coefficients with reasonable accuracy.
- Recently, Zuo et al. (2000) applied the electrolyte equation of state of Fürst and Renon (1993) to liquid-liquid equilibria of water + alcohol + NaCl

systems. The electrolyte equation of state consists of the Soave-Redlich-Kwong equation of state combined with the primitive Mean Spherical Approximation theory.

- Thomsen and Rasmussen (2001) recently presented a poster on the application of the extended UNIQUAC model to LLE of water + alcohol + salt systems.

Not mentioned in this overview are attempts to model LLE of electrolyte solutions with models for molecular components, ignoring electrostatic interactions, or models that cannot be extended to systems with more than three components.

1.5 Approach

The work in this thesis is a continuation of the work of Wijtkamp et al. (1999), who developed the experimental procedure. As explained in the previous section, the contents of the project are twofold: 1) the collection of a set of experimental data for water + solvent + caprolactam + ammonium sulfate systems and 2) the modelling of industrial mixed solvent electrolyte solutions over a wide range of concentrations. For the experimental part, benzene, 1-heptanol and 2-heptanone were chosen as the solvents. This solvent choice is explained in Chapter 3. The experiments were carried out at temperatures from 293.1 K to 333.1 K, which covers the temperature range of the extraction process of caprolactam. A discussion of the experiments is given in Chapter 3. The experiments not only involve liquid-liquid equilibria (LLE), but also three-liquid phase equilibria (LLLE). The LLLE were encountered in the systems with benzene and 2-heptanone and determined experimentally because of the interesting phase behaviour and its challenge to the modelling.

For the modelling a choice had to be made from a small variety of models of which some had been applied to liquid-liquid equilibria and others had not been yet. Because the model would have to be applied to the simulation of an extraction process, a certain flexibility is required from the model. Complicated numerical integrations are undesirable for this purpose. Since the model has to be applied to the wide range of salt concentrations that exist within an extraction process, the model should be able to give a consistent description of the equilibria in this concentration range. Preferably, the model must be able to give results outside the experimental range of concentrations. If possible, the model should also have some predictive qualities.

Prior to the work reported in this thesis, the decision was made to start the modelling with the electrolyte NRTL model as present in Aspen Plus (Aspen Technology, 1998). The electrolyte NRTL model is an activity coefficient model based on the local composition concept. At that time, from the two types of approaches, the activity coefficient approach and the approach via equations of state (see Chapter 2), the first one could be expected to give the best quantitative results. Among existing activity coefficient models, the electrolyte NRTL has shown to give the best results, it can easily be extended to an unlimited number of molecular components, it is relatively easy to use and contains only binary parameters. DSM was using the model already, but was not satisfied with the performance of the model (see Chapter 5). They were not able to apply the model to the full range of salt concentrations. It was decided to look for improvements of this model.

The search for improvements was of two kinds: to correct some inconsistency in the derivation of the activity coefficients and to look for improvements in the model without really changing the different contributions. This is discussed in Chapter 5. A second approach was to replace the Pitzer-Debye-Hückel contribution in the electrolyte NRTL by a more physically correct contribution: the primitive Mean Spherical Approximation (MSA) model.

The second part of the modelling focussed on other models. Since the electrolyte NRTL model is relatively simple without much physical background, attempts were made to develop and use a more fundamental model, like an MSA based equation of state and to compare the two fundamentally different models and approaches. The Mean Spherical Approximation theory is a very promising theory with a much better physical background than the Debye-Hückel model, as will be shown in Chapter 6. The MSA can be solved in a primitive framework and in a nonprimitive framework. In the nonprimitive framework, solvent interactions are explicitly taken into account, where the primitive model sees the solvent mixture as a dielectric continuum, like in Debye-Hückel theories. Therefore, a strong motivation existed to apply a nonprimitive Mean Spherical Approximation model. Three options were studied in detail:

- The nonprimitive MSA model of Blum (1987)
- A perturbation of a hard sphere model (Liu et al., 1999)
- The electrolyte equation of state of Fürst and Renon (1993)

The different models are given in decreasing order of complexity and physical background. Liu et al. (2001) compared the first two options for ions and dipoles and obtained better results with the perturbation theory. However, perturbation theory requires numerical integrations, which makes it less attractive. Accordingly, initially the first option was chosen and this model was programmed. After several unsuccessful attempts to reproduce literature data and contact with one of the authors of some papers on this model (Li et al., 1996), this theory was abandoned and efforts were directed to the application of the electrolyte equation of state of Fürst and Renon (1993). The work on the MSA and its theory are reported in Chapter 6.

1.6 Organization of the thesis

In Chapter 2 some thermodynamics of electrolyte solutions that is relevant for this thesis is given, including a survey of literature and models in this field. In Chapter 3 the experimental work is discussed, including the experimental procedure and the choice of solvents. Equilibrium data are presented for both LLE and LLLE for the ternary and quaternary systems water + benzene/1-heptanol/2-heptanone + caprolactam + ammonium sulfate. Chapter 4 describes the computational procedures. In Chapter 5, theory and modelling results for the Electrolyte NRTL model are presented and a modification is proposed. Special attention is also paid to partial dissociation and different thermodynamic frameworks. Chapter 6 summarizes the work on the Mean Spherical Approximation theory. Finally, conclusions and recommendations are given in Chapter 7.

12

2. Thermodynamic theory

In this chapter some relevant thermodynamic background for the work in this thesis is presented. A short summary on phase equilibria is provided. A discussion is given of what makes electrolyte solutions different from nonelectrolyte solutions and an overview is given of thermodynamic models for electrolyte solutions in literature.

2.1 Thermodynamics of phase equilibria

A very important part of the modelling of separation processes is the modelling of phase equilibria. The phase equilibria of most relevance for this thesis are liquid-liquid equilibria (LLE) and liquid-liquid-liquid equilibria (LLLE). These types of equilibria have in common that the overall mixture has to split up into two or three liquid phases to reach a stable state, called equilibrium. This equilibrium can be represented by thermodynamic equations. Excellent descriptions on this subject can be found in the books by Smith and Van Ness (1987) and the book by Prausnitz et al. (1999).

There are two fundamentally different methods for phase equilibrium calculations: calculations based on **activity coefficient models** (for example the NRTL model) and calculations based on **equations of state** (for example the Soave-Redlich-Kwong equation of state). In the equation of state approach, an equation of state (EOS) is used to describe all phases. This can be the case for vapour-liquid equilibria, but also for liquid-liquid equilibria and implies that the EOS has to be able to represent both vapour and liquid phases. This is not valid for most simpler equations of state (Liu and Watanasiri, 1999). The main advantage of an equation of state approach is the applicability to higher temperatures and pressures. In general, equations of state are not suitable for polar components and less good in describing the liquid phase than the vapour phase. At atmospheric pressure excess Gibbs energy models give a better description of the liquid phase. The EOS approach has not been applied widely for electrolyte solutions. Only recently some progress has been achieved in the development of an electrolyte equation of state (Fürst and Renon, 1992).

In the activity coefficient approach, an activity coefficient model is used for the liquid phase(s). When calculating vapour-liquid equilibria, an equation of state is used for the vapour phase. In principle, activity coefficient models are excess Gibbs energy models.The activity coefficient γ_i is related to the molar excess Gibbs energy G^E, by:

$$RT \ln \gamma_i = \left(\frac{\partial n G^E}{\partial n_i} \right)_{T,P,n_j} \tag{2.1}$$

The excess Gibbs energy of a solution is the difference between the actual Gibbs energy and the Gibbs energy of the ideal solution at the same temperature T, pressure P and composition. A large variety of models exists for the description of the excess Gibbs energy of mixtures of molecular components, for example the UNIQUAC and the NRTL model. Most electrolyte models are also models for the excess Gibbs energy. They are discussed later in this chapter.

2.2 Equilibria of two or three liquid phases

A liquid mixture will split into two separate liquid phases if this way the Gibbs energy is lowered. In many cases, two liquids will have limited mutual solubilities and will show demixing in a certain concentration range. As was illustrated with the extraction process of caprolactam, liquid-liquid equilibria play an important role in separation processes. Limited miscibility is also of interest in another context. The unexpected presence of two liquid phases can be a serious problem in for example distillation and pumping. LLE did not receive as much attention as vapour-liquid equilibria, since LLE are more difficult to correlate, the temperature effect is more pronounced and economically VLE play a bigger role in industry than LLE. Nevertheless, many references do exist for LLE data, both for nonelectrolyte and electrolyte solutions. (Sørensen et al., 1979)

Apart from two-liquid phase equilibria, systems can show three or more liquid phases. At fixed temperature and pressure the maximum number of phases that can be present at equilibrium equals the number of components. Hildebrand (1949) reports as a curiosity on a system of seven liquid layers in stable equilibrium for a system consisting of seven components, but in practice only LLE and LLLE are of any importance.

The practical importance of liquid-liquid-liquid equilibria is in particular obvious for the systems in enhanced oil recovery processes, where capillary forces in reservoir pores are reduced by surfactant flooding. Also, for improving the performance of an extraction process, the understanding of the phase behaviour of systems exhibiting three liquid phases can be essential (Garcia-Sanchez, 1996). LLLE received considerable interest, mainly inspired by the possibility of a tri-critical point and as a test for theories of critical phenomena. A tri-critical point is the point where the three phases become identical.

Despite the degree of interest, the amount of three-liquid phase equilibrium data is limited (Bocko, 1980). For electrolyte solutions most LLLE data were determined for systems with surfactants (Kahlweit, 1988). However, some studies have been made for other electrolyte systems, exhibiting three liquid phases. Quaternary equilibrium data have been published for water + benzene + ethanol + ammonium sulfate (Lang and Widom, 1975) and water + octane + 1-propanol + sodium chloride (Negahban, 1986). For these systems the patterns of the three-liquid phase equilibria with increasing salt concentration are similar to those investigated by Knickerbocker et al. (1979, 1982) for a variety of water + hydrocarbon + alcohol + salt systems.

The phase behaviour of the system water + benzene + ethanol + ammonium sulfate (Lang and Widom, 1975) can be used to describe the phenomena of similar systems. A thorough discussion of this system was given by Rowlinson and Swinton (1982) and is used in section 3.7 to describe the experimentally observed phase behaviour.

In Figure 2.1 the tetrahedron is given that represents the system water + benzene + ethanol + ammonium sulfate and similar systems exhibiting a three-phase region: The three-phase region is bounded by a continuous curve, composed of the LLLE phase compositions and also called the three-phase coexistence curve, and two critical tie-lines. It has the form of a stack of infinitely many closely spaced and differently sized three-phase triangles, terminated at the top and bottom by two critical tie-lines. A typical mixture that will demix into three phases is given by a point inside a triangle. The compositions of the three liquid phases are given by the vertices of the triangle. At the limiting tie-lines, two of the three phases are critical and in equilibrium with the third phase (Bocko, 1980).

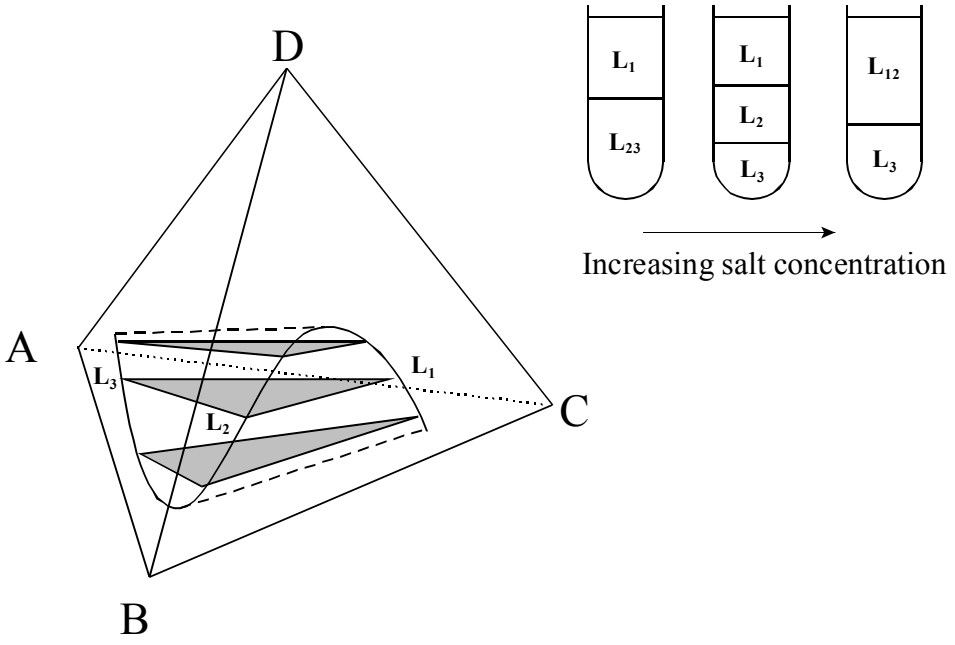

Figure 2.1: Schematic picture of the characteristic three-liquid phase pattern, as found for water + benzene + ethanol + ammonium sulfate (Figure after Lang and Widom, 1975)

The phase behaviour pattern observed for LLLE in quaternary electrolyte solutions, is a progression with salt concentration (D) from two liquid phases L_1 and L_2 at low salt concentrations, a three-liquid phase region at higher salt concentrations and again a two-liquid phase region at still higher salt concentrations. The compositions of the three phases follow the three-phase coexistence curve. The three-phase region is limited by the two critical tie-lines (in Figure 2.1 represented by dashed lines), where two of the three phases become identical. In this pattern, temperature can play a similar role as the salt concentration.

With increasing temperature the size of the LLLE region is decreasing. At a given pressure, a point with a certain temperature and composition exists, where the two critical tie-lines merge and the three coexisting phases become identical. This is the tri-critical point. In the publication by Lang and Widom (1975) an attempt was made to locate this tri-critical point for the system water + benzene + ethanol + ammonium sulfate.

2.3 Electrolyte thermodynamics

2.3.1 Electrolyte solutions

Two main characteristics distinguish salt containing solutions from solutions with other solutes: Firstly, the salts (partially) dissociate into cations and anions if the solvent is polar enough to allow this. Secondly, the presence of the charged species has a strong nonideal effect on the thermodynamic properties of the solution. The strong nonideal behaviour of electrolyte solutions is caused by the long range forces between the ions. In electrolyte systems both molecular and ionic species are present, resulting in molecule-molecule interactions, molecule-ion interactions and ion-ion interactions. The ion-ion interactions are dominated by the electrostatic Coulomb interactions, except at high electrolyte concentrations. Electrostatic interactions are inversely proportional to the distance of separation, while other inter-molecular interactions are inversely proportional to a higher power of the distance of separation (Stokes, 1991). The influence of the presence of a salt on the thermodynamic properties can be illustrated by:

- Freezing point depression
- Boiling point elevation / vapour pressure lowering
- Osmosis
- Salting-in or salting out effects.

The latter one is of importance for liquid-liquid equilibria. Salting-in or salting out occurs when the solubility of a component in a solvent is altered by the presence of a salt. Salting out is the phenomenon that many non-electrolytes are less soluble in a salt solution than in the corresponding pure solvent. This effect is commonly utilized to separate a hydrophilic organic component from an aqueous solution or to precipitate a protein. Salting-out is related to the hydration behaviour of the salt causing the salting-out effect. It may be explained as a result of association of the solvent with the ions, leaving less free solvent molecules for the solvation of the non-electrolyte solute. A kind of competition may exist for available solvent molecules. Salting-out can also be explained by the lowering of the dielectric constant in the direct neighbourhood of an ion. This leads to an increase in the activity coefficient and the formation of dielectric holes around the ions. The dielectric holes or cavities have a much lower polarizability and other ions are repelled from these cavities. The cavities thus act as a shield around the ions (Conway, 1981).

2.3.2 Conventions

True or apparent mole fractions
Associated with the dissociation is the use of true mole fractions, where the ions are counted as molecules, instead of so-called apparent mole fractions counting the undissociated salt molecules.

Mean ionic properties
Because thermodynamic measurements usually deliver properties for the ion pair instead of for the individual ions, it is customary to define a mean ionic activity coefficient $\gamma_{\pm}$ for the electrolyte by:

$$\gamma_{\pm} = \left(\gamma_{+}^{\upsilon_{+}} \cdot \gamma_{-}^{\upsilon_{-}}\right)^{\left(\upsilon_{+}+\upsilon_{-}\right)^{-1}} \qquad \textbf{(2.2)}$$

where v_i is the stoichiometric coefficient and γ_i is the single-ion activity coefficient for a salt that dissociates as: $M_{v+}X_{v-} \rightarrow v_+ M^{z+} + v_- X^{z-}$

For the electrolyte the condition for liquid-liquid equilibria is equated as:

$$\left(x_{\pm}\gamma_{\pm}\right)^{I} = \left(x_{\pm}\gamma_{\pm}\right)^{II} \qquad \textbf{(2.3)}$$

where $x_{\pm}$ is the mean ionic mole fraction and is calculated in the same way as the mean ionic activity coefficient. Mean ionic activity coefficients have been tabulated for many salts at low temperatures and atmospheric pressure. Experimental data for mean ionic activity coefficients are important for calculating thermodynamic properties, like Gibbs energies of formation of solid phases, but also to test the applicability of solution models to multicomponent solutions. Mean ionic activity coefficients can be determined experimentally with different methods. They can be obtained from freezing point lowering, vapour pressure depressions, via isopiestic measurements and from electrochemical cell measurements (Pitzer, 1995).

Reference state
An important issue in the modelling of electrolyte solutions is the reference state of the ionic activity coefficients. For primitive electrolyte models, like the Debye-Hückel theory, the reference state is the infinite dilution of the ions in the dielectric medium. For mixtures of more than one solvent, this reference state is composition dependent. For nonelectrolyte models, like the NRTL model, the pure liquid at system pressure

and temperature is used as the reference state. Thus, different reference states are used for ionic and neutral species. When an excess Gibbs energy model like the NRTL model is used to describe the short range interactions between ions and solvents in addition to an electrostatic contribution, conflicting reference states exist for the ions. In general, then the short range contribution is normalized to infinite dilution in pure water or in the mixed solvent. If different reference states are used for the contributions to the activity coefficients, problems will arise in the calculation of liquid-liquid equilibria and salt solubilities as discussed by Zuo et al. (2000b).

2.3.3 Debye-Hückel model

The Debye-Hückel model (Debye and Hückel, 1924) was the first model to describe long-range interactions of the ions and it still is the common element of many electrolyte models. Most electrolyte models contain a Debye-Hückel term or one of its modifications. The Debye-Hückel model can be derived either from electrostatics (Poisson's equation) or from classical mechanics. Both derivations are described extensively in literature (for instance: Lee, 1988). Major assumptions are: the solvent is replaced by a dielectric background, the ions have no diameter or volume and the salt concentration is low. A short description will now be given of the classical derivation from electrostatics.

In the Debye-Hückel theory the ions are point charges and the solvent is replaced by a dielectric continuum, according to the McMillan-Mayer theory. For charged hard spheres the interaction potential u_{ij} between ion 1 and ion 2 is given by the Coulomb interaction:

$$u_{ij} = \frac{z_i z_j e^2}{\varepsilon r_{ij}} \tag{2.4}$$

where e is the charge of one electron, z is the valence of the ion and ε is the dielectric constant (calculated by $\varepsilon = 4\pi \cdot 8.8542 \times 10^{-12} \cdot \varepsilon_r$).

The ions are assumed to be point charges and thus have no hard core (the diameter of the ions σ is taken to be zero) or volume: It is assumed that the different behaviour of electrolyte solutions can be described by the Coulomb interaction only. Starting point of the derivation of the Debye-Hückel model is the insertion of Boltzmann's

distribution law into Poisson's equation, which is a relation between the distribution of charges and the electrostatic potential ψ. The resulting equation is called the Poisson-Boltzmann equation and describes the distribution of charge around an ion by assuming a Boltzmann distribution:

$$\nabla^2\psi(r) = -\frac{1}{\varepsilon}\sum_i z_i e\rho_i \exp\left(\frac{z_i e\psi(r)}{kT}\right) \tag{2.5}$$

The Debye-Hückel theory further assumes that $kT >> z_i e\psi$, so that the exponential term can be linearized:

$$\nabla\psi(r) = \kappa^2\psi(r) \tag{2.6}$$

$$\kappa^2 = \frac{e^2}{\varepsilon kT}\sum_i \rho_i z_i^2 = \frac{2I}{\varepsilon kT} \tag{2.7}$$

where κ is the Debye-Hückel shielding parameter and I is the ionic strength. The reciprocal of this parameter is called the Debye-length and is an indication of the range of electrostatic interaction between the ions. The electrostatic potential of the ions is shielded by the ionic atmosphere and decreases by a factor 1/exp(1) over the Debye length. The expression for the activity coefficient is written as:

$$\ln\gamma_i = -\frac{z_i^2 e^2\kappa}{8\pi\varepsilon kT} \tag{2.8}$$

Several modifications have been proposed to extend the range of applicability to higher concentrations:

- Extended Debye-Hückel: In contrary to the original Debye-Hückel model, in the extended model the charge density within a radius a from the centre of the ion is assumed to be zero, resulting in:

$$\ln\gamma_i = -\frac{z_i^2 e^2}{8\pi\varepsilon kT}\frac{\kappa}{1+\kappa a} \tag{2.9}$$

  Often the radius a is referred to as the closest approach parameter and is treated as an empirical constant.
- Pitzer-Debye-Hückel: Pitzer (1980) suggested an extension of the Debye-Hückel model. It actually is the long range contribution for ion-ion interaction from the so called Pitzer ion interaction model. It contains one adjustable parameter, the closest approach parameter ρ. The dependence on the

composition is given by the true mole fraction based ionic strength I_x. The equation, which was derived using the McMillan-Mayer theory, gives some recognition to the repulsive forces between ions (Chen et al. 1982).

$$\ln \gamma_i^{PDH} = -\left(\frac{2\pi N_A d}{M_S}\right)^{\frac{1}{2}}\left(\frac{e^2}{\varepsilon kT}\right)^{\frac{3}{2}} \cdot \left(\frac{2z_i^2}{\rho}\ln\left(1+\rho\sqrt{I_x}\right)+\frac{z_i^2\sqrt{I_x}-2I_x^{3/2}}{1+\rho\sqrt{I_x}}\right) \quad \textbf{(2.10)}$$

$$I_x = \frac{1}{2}\sum x_i z_i^2 \quad \textbf{(2.11)}$$

where d is the solution density, N_A is Avagadro's number and M_S is the solvent molecular weight.

- Many other attempts been made to improve the applicability of the Debye-Hückel model. The basic form of these equations is usually (just like the extended Debye-Hückel):

$$\ln \gamma_i = \frac{A\left|z_+ z_-\right|\sqrt{I}}{1+B\sqrt{I}} + C \cdot I \quad \textbf{(2.12)}$$

$$I = \frac{1}{2}\sum \rho_i z_i^2 \quad \textbf{(2.13)}$$

where I is the ionic strength and A, B and C are parameters that are dependent on the physical properties.

2.4 Frameworks for electrolyte thermodynamics

2.4.1 McMillan-Mayer ensemble

In statistical thermodynamics, macroscopic properties of a system are calculated from the microscopic nature of the system. One way to do this is the ensemble method introduced by Gibbs. An ensemble is defined as a great number of independent systems identical in nature, but differing in state. By making a statistical count of all possible states, average properties can be calculated corresponding to the macroscopical state of the system.

Several ensembles are distinguished in statistical thermodynamics (Lee, 1988):

- If the number of particles N, the total volume V and the internal energy are kept constant, the system is called a microcanonical ensemble.
- In a canonical ensemble every system has the same number of particles, volume and temperature. The work function of this ensemble is the Helmholtz energy.
- If all systems have the same (constant) volume, temperature T and chemical potential μ, a grand canonical ensemble is produced. In a grand canonical ensemble the internal energy and the number of particles may vary. Macroscopically it corresponds to an open system, with heat and mass transfer across the boundaries.
- An ensemble with a constant number of particles, constant pressure P and constant temperature T is called an N,P,T-ensemble, also referred to as a **Lewis-Randall ensemble** or isothermal-isobaric ensemble. This ensemble is related to the Gibbs-energy.

A special ensemble is the **McMillan-Mayer (MM) ensemble** for solutions (McMillan and Mayer, 1945), also called the **primitive model** of electrolytes. The McMillan-Mayer ensemble is based on the grand canonical ensemble and is used for the description of electrolyte solutions. The solvent molecules, unlike in the grand canonical ensemble, do not appear explicitly. The assumption is made that the solvent molecules form a dielectric continuum, a uniform background. The ions are considered as charged spheres or points in a continuous medium. This reduces the level of difficulty considerably. "Averaged" quantities are used where the solvent molecules have been 'smoothed out' and are replaced by a dielectric continuum. For example the MM partition function in the grand canonical ensemble is defined as the quotient of the partition function Ξ for a solution (II) and the one of the reference state (I), namely the pure solvent(s) at the same T. The relative quantity is denoted with *.

$$\Xi^{*,II} = \frac{\Xi^{II}}{\Xi^{I}} = \frac{\exp\left(\beta^{II} \cdot p^{II} \cdot V^{II}\right)}{\exp\left(\beta^{I} \cdot p^{I} \cdot V^{I}\right)} = \exp\left(\beta \cdot \Pi \cdot V\right) \qquad \textbf{(2.14)}$$

where V is the volume of pure solvent (I) or pure solvent + solutes (II) and Π is the osmotic pressure. Characteristic of models derived in the McMillan-Mayer ensemble is that an excess Helmholtz energy is derived, whereas a Lewis-Randall ensemble yields an expression in terms of an excess Gibbs energy. If a pressure is obtained, this is the osmotic pressure and not the system pressure.

The Debye-Hückel theory and the (primitive) MSA model for electrolytes are derived in the McMillan-Mayer framework. In both theories, the Ornstein-Zernike integral equation (Equation 2.15) is worked out for a mixtures of only ions, without considering the solvent molecules.

$$h_{ij}(r_{ij}) = g_{ij}(r_{ij}) - 1 = C_{ij}(r_{ij}) + \rho \int h_{ik}(r_{ik}) C_{ik}(r_{ik}) dr_k \qquad \textbf{(2.15)}$$

where ρ is the numeric density, h_{ij} is the total correlation function, g_{ij} the pair correlation function or radial distribution function and r_{ij} is the distance between ion i and j. The properties of the solvent mixture are only introduced in the equation via the direct correlation function C_{ij} in the interaction potential u_{ij}. This is illustrated for example for the Debye-Hückel model, where the direct correlation function is assumed to be equal to:

$$C_{ij} = -\frac{u_{ij}}{kT} = -\frac{z_i z_j e^2}{\varepsilon k T r_{ij}} \quad for \quad r_{ij} > 0 \qquad \textbf{(2.16)}$$

and where ε is the dielectric constant of the mixture and z_i is the charge number. Obviously, the direct correlation function is zero for uncharged species. In Chapter 6, the statistical mechanics used here, will be discussed more extensively in relation with the Mean Spherical Approximation theory. Then, besides the primitive MSA model, the nonprimitive MSA will be described. Electrolyte theories that do not use the McMillan-Mayer framework are called nonprimitive models, as opposed to primitive models.

Many theories have been derived in the primitive or MM model to describe the single-solvent and multi-solvent systems. Until 1982 they merely focussed on properties of the salt rather than of the solvents and were not applicable to correlate the effects of salts on phase equilibria in multi-solvent systems. However, in 1982 the electrolyte NRTL model (Chen et al.,1982) and in 1984 the extended UNIQUAC model (Sander, 1984) were published and these models were able to predict phase equilibria for electrolyte systems. They combine a long range electrostatic term with another model such as NRTL and UNIQUAC for the short range interactions. UNIQUAC and NRTL are Lewis-Randall models, whereas the models for long range electrostatic interaction are McMillan-Mayer models. This seems to lead to some inconsistency, as discussed in the next section.

2.4.2 Conversion to Lewis-Randall systems

As stated in the previous section, the McMillan-Mayer ensemble is related to the excess Helmholtz energy and the Lewis-Randall (LR) ensemble is related to the excess Gibbs energy. In the McMillan-Mayer ensemble, the independent variables are temperature, volume, mole numbers of **solute** species and chemical potential of the solvent mixture. In the Lewis-Randall ensemble, the independent variables are temperature, pressure and mole numbers of **all species**. In the McMillan-Mayer ensemble the solvent is only present as background. Therefore, thermodynamic properties as derived from the MM-framework are not fully identical to those derived from the LR-framework.

In many electrolyte models, the excess Gibbs energy is the sum of an electrostatic contribution (usually derived in the MM-ensemble as an excess Helmholtz energy) and a short-range contribution (usually derived in the LR-ensemble). Experimental data are commonly obtained at constant pressure, temperature and total mole number and thus are obtained in the LR-framework. The combination of the two frameworks in one model or the comparison of data and modelling results obtained in different frameworks has given rise to a lot of discussion in literature.

According to Friedman (1972) for an electrolyte solution the relation between the MM excess Helmholtz energy A^{ex} (MM) and the LR excess Gibbs energy G^{ex} is given by:

$$\frac{A^{ex}}{nRT} = \frac{G^{ex}}{nRT} + \ln\frac{V_{LR}(n,T,P+\Pi)}{V_{LR}(n_s,T,P)} + \frac{1}{nRT}\int_{P}^{P+\Pi} V_{LR}(n,T,P)dP - \frac{\Pi \cdot V_{LR}(x,T,P+\Pi)}{nRT} \qquad \textbf{(2.17)}$$

where V_{LR} is the volume of solution per kilogram of solvent for a electrolyte solution in the LR state and n_s is the concentration of solvents in the same solution without salt. In Equation (2.17) all the correction terms are LR functions and they have to be estimated from tabulated (experimental) data of thermodynamic functions. However, these data are often missing. Also, the formulas given by Friedman to convert variables like the activity coefficients from Lewis-Randal to McMillan-Mayer systems are very complex.

In 1987 Cardoso and O'Connell (1987) published a paper addressing this issue, proposing a more simple conversion that approaches the results by Friedman. They

state that the Gibbs-Duhem equation for a Lewis-Randall model and for a McMillan-Mayer model is, respectively:

$$VdP = \sum_{i=solvents} n_i d\ln\gamma_i + \sum_{j=solutes} n_j d\ln\gamma_j \qquad \textbf{(2.18)}$$

$$VdP = \sum_{j=solutes} n_j d\ln\gamma_j \qquad \textbf{(2.19)}$$

The electrostatic contribution to the activity coefficients should be calculated using the osmotic pressure formalism, which finally leads to the following expressions:

$$\ln\gamma_i(T,P,x) = \ln\gamma_i^{'}(T,P,x) - \frac{<v_i> P_{osm}^{LRE}}{RT} \qquad \textbf{(2.20)}$$

$$\ln\gamma_j(T,P,x) = \ln\gamma_j^{'}(T,P,x) + \ln\gamma_j^{LRE}(T,P,x) \qquad \textbf{(2.21)}$$

where i refers to solvents and j refers to ions, γ' is the activity coefficient found from the Lewis-Randall (excess Gibbs) model, LRE refers to the long range (electrostatic) contribution from the McMillan-Mayer theory and $<v_i>$ is the average partial molar volume. It should be noted that for ordinary electrolyte solutions of a single solvent, neglecting of this conversion has almost no effect. The same formulas as given in Equation (2.20) and (2.21) were given by Lee (2000) in a paper that discusses more thoroughly the conversion between the two ensembles.

Although these and other papers discuss the correctness and the necessity to treat electrolyte models applying this conversion, it has not been used in publications where the models are applied to equilibrium data. In most papers the conversion is mentioned but ignored and the long range electrostatic model is treated as an excess Gibbs energy model.

2.5 Electrolyte models

A wide variety of electrolyte models has been published in literature, ranging from fundamental models to multi-parameter equations with hardly any physical background. Overviews of models for electrolyte solutions have been given by a number of authors. Several methods have been used in these overviews to distinguish the different models: The models are divided in excess Gibbs energy models and equations of state based on the Helmholtz energy (Liu and Watanasiri, 1999), in

fundamental models and engineering models (Loehe and Donohue, 1997) or in empirical models and molecular models (Renon, 1986).

Anderko et al. (2002) grouped electrolyte models in three classes. They distinguished models that assume full dissociation, undissociated salt or speciation-based models. Models that treat electrolytes on an undissociated basis are analogous to nonelectrolyte mixture models and are particularly suitable for supercritical and high-temperature systems, in which ion-pairs dominate. However, the majority of models assumes full dissociation. Models that use partial dissociation are computationally more intensive. They especially have advantages for calculations other than phase equilibria, when pH is important and in electrochemical processes (Anderko et al., 2002).

Other overviews of electrolyte models have been given by Rafal et al. (1993) and by Prausnitz et al. (1999). The latter divided the variety of electrolyte models into more fundamental models (integral equations, perturbation theories, fluctuation solution theories) and engineering equations (physical models, local composition models, solvation models). This categorization will be followed here. For a complete survey of electrolyte models, the reviews enumerated above can be used, in particular the paper by Loehe and Donohue (1997). In the next subsections a selective compilation is given, with emphasis on models that can be used for phase equilibrium calculations.

2.5.1 Theoretical models

Perturbation theory is based on the idea that the properties of a fluid can be described as those of a simpler fluid (usually a hard sphere fluid) plus some corrections to account for nonidealities. Some work has been published in the field of electrolyte solutions ranging from rather simple models to complex equations, differing in the interactions that are accounted for (dipole-dipole, ion-dipole, dispersion, quadrupolar, induced interaction energies) and in the order to which the perturbation expansion is evaluated. Usually a perturbation by the Mean Spherical Approximation (MSA) is used to account for nonidealities resulting from ionic interactions.Using perturbation theory, Jin and Donohue (1988) derived an equation of state that was used with success to model mean ionic activity coefficients and some VLE for aqueous solutions. Many MSA perturbed equations of state have been published recently (see also Chapter 6).

Chapter 6 presents a discussion on the Mean Spherical Approximation theory. The Mean Spherical Approximation is a closure relation to the integral equation of Ornstein and Zernike. It was solved both in the primitive model (Blum, 1975) and in the nonprimitive model of electrolytes (Blum and Wei, 1987). Unlike the Debye-Hückel theory, it takes into account the size of the ions. The primitive MSA model reduces to the Debye-Hückel theory for point charges at infinite dilution of the ions. This is also valid for the nonprimitive MSA model in the case of zero diameters of the solvents. Liu et al. (2001) compared internal energies for the primitive MSA, nonprimitive MSA and the perturbation theory for electrolytes with molecular simulation data for ion-dipole mixtures and found unsatisfactory result for any of these. As discussed in Chapter 6, the primitive MSA was used in combination with other models to give good results for VLE and mean ionic activity coefficients. Fürst and Renon (1993) published an equation of state that combines the Soave-Redlich-Kwong EOS with the MSA. Successful application of this EOS in modeling VLE and LLE of mixed solvent electrolyte solutions was reported by Zuo et al. (2000a, 2000b).

2.5.2 Semi-empirical models

An important class of electrolyte models are those based on the local composition concept. In the local composition concept, the solvent molecules are assumed to be present in cells, consisting of a central molecule surrounded by a layer of molecules, that can be of the same kind or different. The local composition X_{ij} is the mole fraction of molecules *i* in the direct neighbourhood of a molecule *j*. Examples of nonelectrolyte models based on the local composition concept are the UNIQUAC model (Abrams and Prausnitz, 1975), the NRTL model (Renon and Prausnitz, 1968) and the Wilson model (Wilson, 1964). Based on any of these, electrolyte models were proposed.

The models based on the Non Random Two Liquid (**NRTL**) theory will be presented in more detail in Chapter 5. Most important among these models is the electrolyte NRTL model of Chen et al. (1982, 1986) and its modifications, based on the two main assumptions of like-ion repulsion and local electroneutrality. Other electrolyte models based on the NRTL model are the model of Cruz and Renon (1978), the NRTL-NRF model of Hagtalab and Vera (1988) and the model of Liu et al. (1989a).

The **UNIQUAC** (Universal Quasi-Chemical) models for electrolytes are made up of three parts. The first part is the so called configurational or combinatorial part. This

is a contribution due to differences in sizes and shapes of the molecules. The second part is the residual part and accounts for the interactions between the molecules. The third part is a Debye-Hückel contribution. The electrolyte UNIQUAC models are algebraically more complex than the electrolyte NRTL models and usually need more binary parameters. The UNIQUAC model utilizes knowledge of molecular surfaces and volumes of the pure components, which makes it applicable to mixtures of widely different molecular sizes (Walas, 1985).

Sander et al. (1984, 1986) extended the UNIQUAC equation to electrolytes. A salt concentration dependence of the (ionspecific) interaction energy parameters is introduced here. The model of Sander was applied to VLE and SLE. Based on the model of Sander, Thomsen et al. (1996) published an extended UNIQUAC model for electrolyte solutions and applied it successfully to SLE, VLE and also LLE (Thomsen and Rasmussen, 2001). Haghtalab and Mokhtarani (2001) developed a UNIQUAC-NRF model for LLE in salt containing polymer solutions. Yan et al. (1999) replaced the UNIQUAC contribution in the LIQUAC model of Li et al. (1994). The LIQUAC model consists of a Debye-Hückel term, an UNIQUAC contribution and a middle range virial contribution. The model of Yan was applied successfully to a large amount of VLE of mixed solvent electrolyte solutions. Balaban et al. (2002) combined the UNIQUAC model with a Pitzer-Debye-Hückel term and included hydration and solvation.

Another local composition model for electrolyte solutions worth mentioning here is the model for LLE and VLE of Zerres and Prausnitz (1994), that combines the **Van Laar** model with a solvation model and a Debye-Hückel contribution. The model for LLE of Cheluget et al. (1994) is constructed from a **Flory-Huggins** contribution, a Debye-Hückel contribution and a contribution accounting for solvation. In the ion-interaction model of Pitzer (1973) the excess Gibbs energy is given by a virial series in the salt concentration. This model has been applied widely for geochemical systems and systems of interest in industry and can be used up to very high salt concentrations. Disadvantage of this model is that it is only applicable to aqueous systems (Prausnitz et al., 1999).

3. Experimental work

Chapter 3 gives a description of the experiments carried out to support the modelling work. The procedure and setup are described and the results are given for the liquid-liquid equilibria and liquid-liquid-liquid equilibria that were experimentally determined for various systems containing caprolactam.

3.1 Introduction

To test existing and new models for electrolyte solutions on their applicability to liquid-liquid equilibria of systems containing caprolactam, it appeared necessary to extend the amount of equilibrium data available with some complete data sets in the temperature and electrolyte concentration range of the extraction process. At present, benzene is used as the extracting solvent. Some data of water + benzene + caprolactam + ammonium sulfate systems were already present at DSM Research and have also been published in graphical form by De Haan and Niemann (1999). However, the use of benzene in extraction processes has to be reconsidered because of new legislation due to the suspected carcinogenity of benzene. Thus, a second objective for the experimental work is to investigate the influence of the solvent on the phase behaviour in water + solvent + caprolactam + ammonium sulfate systems.

In literature, experimental data can be found for a number of solvents that can be used for the extraction process of caprolactam. Unfortunately, these data are usually not given at different temperatures or cannot be used because only the caprolactam distribution is given. In Table 3.1 a survey is given of liquid-liquid equilibrium data reported for systems with caprolactam. Many of the organic solvents are chlorinated compounds, which are now not suitable any more to serve as extracting solvents due to environmental considerations. Regarding the LLE data for the systems water + benzene + caprolactam and water + caprolactam + ammonium sulfate, it was observed that some results from the different sources are sometimes deviating from each other or from data available at DSM Research. More attention will be paid to this issue later in this chapter.

Table 3.1: LLE data for water (W) + caprolactam (C) in literature

System	Temperature °C	Source
W + C + benzene	20	Tettamanti et al. (1960a)[a]
	20	Morachevskii et al. (1960)
W + C + nitrobenzene	20	Tettamanti et al. (1960a)
W + C + trichloroethene	20	Tettamanti et al. (1960a)
W + C + trichloroethene + $(NH_4)_2SO_4$	20	Tettamanti et al. (1960b)
W + C + $(NH_3)_2SO_4$	20	Tettamanti et al. (1960b)[a]
	20	Shubtsova et al. (1975b)
	30, 50	Vecera et al. (1955)
	40	Gucwa et al. (1976)
W + C + carbon tetrachloride	20	Morachevskii et al. (1960)
W + C + dichloroethane	20	Morachevskii et al. (1960)
W + C + toluene	25	Pajak et al. (1991)
W + C + phenol	25	Shubtsova et al. (1975a)

[a] These data are not in accordance with experimental results presented in this thesis.

3.2 Solvent selection

Since experimental work is rather time consuming, it is important to make a prior prediction of the phase behaviour of the solvent in systems with caprolactam. Two criteria are important: The solubility of caprolactam in the solvent must be high enough, the solvent must have a large concentration range of demixing with water and the solvent should not be any halogenated or toxic compound. Again, data are scarce. In Table 3.2 a survey is given of reported solubilities of caprolactam for some organic solvents.

To obtain a better base for a solvent choice, a study was carried out by Wijtkamp (1996), who used the UNIFAC-LBY method in ASPEN Plus to predict the phase behaviour for different solvents in water + solvent + caprolactam systems. Based on these estimations and the limited amount of literature data available, solvents were selected. An important criterium for this selection has also been the wish to limit the selection to components having only one functional group, to leave the opportunity open to develop a group contribution method for the interaction parameters. The components thus selected were, besides benzene, 1-heptanol and 2-heptanone. Some

experiments have been performed with cyclohexane (Van Bochove, 1998), but these experiments were stopped because the solubility of caprolactam in cyclohexane was too low.

Table 3.2: Solubility of caprolactam in various solvents at 293 K.

Solvent	Weight %
1,2-Dichloroethane[a]	95
1,4-Dichlorobutane[a]	85
Water[a]	82
Cyclohexanol[a]	82
Methyl ethyl ketone[a]	53
Benzene[b]	41
Cyclohexanone[a]	35
Toluene[a]	26
Ethylacetate[a]	24
p-Xylene[a]	14
Cyclohexane[a]	2

[a] Snell-Ettre, 1969
[b] Morachevski et al., 1960

3.3 Experimental setup

The apparatus used, consisted of a stirred glass vessel with a thermostated water jacket and sample points for each phase. A schematic representation of the equilibrium cell is found in Figure 3.1. The temperature was kept constant using a constant temperature bath (RC 6 Lauda). Water was used as the thermostatic fluid and the temperature inside the vessel was controlled to within ± 0.1 K. The temperature was measured with an ASL F25 Precision Thermometer. Liquid mixtures were prepared by weighing the pure components (with purities as given in Table 3.3) such that almost equal volumes were obtained for the different liquid phases. The mixtures were stirred for about 4 hours and then allowed to settle for at least 12 hours to ensure that equilibrium was reached and the phases were completely separated. Subsequently, samples were taken through the sealed sample ports using a syringe. For the LLLE glass vessels with three sample ports were used and the time to settle was prolonged to two or sometimes many more days.

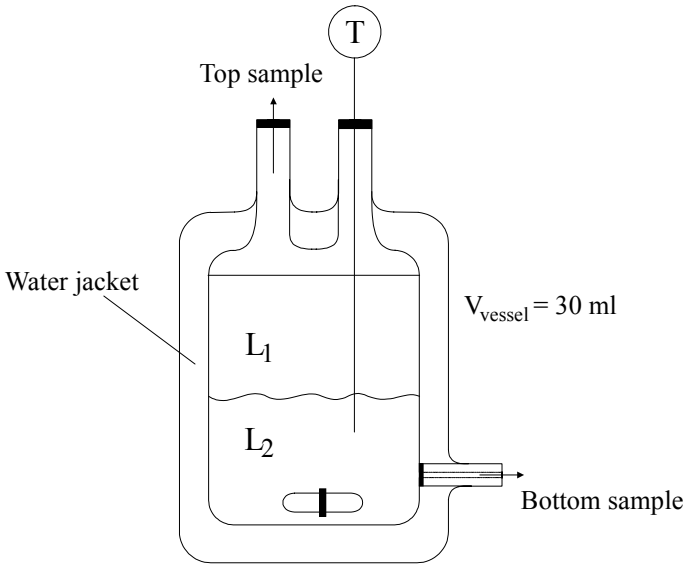

Figure 3.1: Vessel used for the LLE experiments

The concentrations of the organic components were determined by gas chromatography. The analyses were carried out by a HP 5890 Series II gas chromatograph with an HP 7673 automatic sampler connected to an HP 3396 Series II integrator. The injected volume was 0.5 µl. The column was a 30 m × 0.53 mm DB5 (J&W Scientific). Helium was used as the carrier gas. The temperature was programmed at 100˚C for 5 minutes, then increased to 200˚C at 10˚C min^{-1}, kept at this temperature for 5 minutes. Finally, the temperature was further increased to 250˚C at 25˚C min^{-1} to remove any remaining traces of the sample. The sampling was performed using split injection with a split ratio of 1:55 and an injection temperature of 225˚C. Detection was performed by a flame ionization detector operating at a temperature of 260˚C. Methanol (Merck, 99.5%) was used for the dilution and toluene (Janssen Chimica, 99.5%) was taken as the internal calibration standard.

Periodically, calibration lines were determined by preparing and measuring a series of standards with different ratios of the organic component and toluene. The ratio of the areas of the GC peaks of the organic component and toluene as calculated by the integrator is an almost linear function of the ratio of the concentrations. Linear regression was applied to calculate this calibration function. By addition of a fixed

amount of toluene to the dilution of every sample, the concentration of the organic component can be calculated from the ratio of the peak areas and the exact amount of toluene added. The use of an internal standard makes the result less dependent on variations in the injected volume.

For the determination of the water content Karl-Fischer analysis (Riedel de Haen, 1994) was used with a Mettler DL 35 Karl Fisher Titrator with Hydranal Titrant 2 or Hydranal Titrant 5 (Riedel de Haën) as titrant and Hydranal solvent (Riedel de Haën) as the solvent medium. For the water determination in the systems with 2-heptanone a different titrant had to be used because of a reaction between 2-heptanone and the titrant. Water is formed, which is then titrated as well. Therefore, Hydranal Composite 5K (Riedel de Haën) was used as the titrant and Hydranal Working Medium K (Riedel de Haën) as the solvent. The titrants were calibrated using Hydranal Standard sodium tartrate-2-hydrate (Riedel de Haën) with a water content of 15.66 ± 0.02%. The results were corrected by "drift" measurements . The drift or background consumption is the consumption due to moisture penetrating the equipment.

Ammonium sulfate contents were determined by photometric titration with barium perchlorate using a Mettler DL 21 Titrator. The titration is based on the reaction of the barium ions with the sulfate ions to form barium sulfate. The titrant was a 0.005 mol l^{-1} bariumperchlorate solution in 2-propanol/water (Merck) and thorin (Merck), 0.2 wt % in water, was used as absorption indicator. The samples were diluted with 2-propanol (Baker Analyzed, 99%). A 0.2 M perchloric acid (Fluka) solution was used to adjust the pH of the solution. The end-point of the titration was determined using a Mettler DP 550 Phototrode.

The sum of all the mass fractions in a sample was typically between 0.99 and 1.01 wt/wt with an average deviation from 1 of 0.003 to 0.007 for the different systems. For the individual mass fractions, error analyses were carried out. The GC-analyses were repeated at least three times for every sample. The water analyses were repeated at least five times and the salt titrations were repeated at least three times. Based on these repetitions, the average statistical error can be calculated. The results, based on a 95% confidence interval, are given in the last column of Table 3.3. These values may vary slightly in the different systems investigated.

Table 3.3: Chemicals used in the experiments and the average relative statistical error of the analyses, based on a 95% confidence interval.

Component	Source	Stated purity	Relative error (wt%)
Caprolactam	DSM	99.5 %	1.5
Benzene	J.T. Baker	99.0 %	0.7
1-Heptanol	Merck	99.0 %	0.7
2-Heptanone	Aldrich	98.0 %	0.5
Ammonium sulfate	Merck	99.5 %	3.0
Water	-	-	1.7

3.4 The complete system

For the benefit of a better understanding of the experimental results, it may be useful first to consider the entire system of water + solvent + caprolactam + ammonium sulfate at lower temperatures. A schematic drawing is given in Figure 3.2.

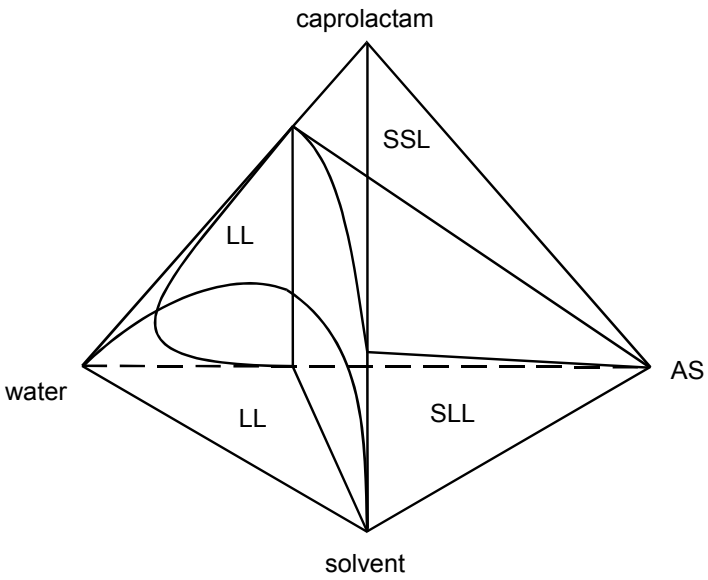

Figure 3.2: Schematic representation of the quaternary system water + solvent + caprolactam + ammonium sulfate (AS). Only ternary phase boundaries are shown in this figure.

In the figure a tetrahedron is given which represents the four component system. Every vertex of the tetrahedron represents a pure component. In the right part of the figure, one or two solids are formed: caprolactam and ammonium sulfate. In the diagram only one part is important for the extraction, the region(s) where liquid-liquid equilibria (LLE) are found. This region is formed by three ternary LLE planes and the solubility limits of ammonium sulfate and caprolactam. In the diagram, for simplicity only ternary LLE are shown. With certain solvents different LLE regions may be found enclosing a region of liquid-liquid-liquid equilibria (LLLE). This phase behaviour is explained in section 3.7 by means of the experimental data on the LLE and LLLE for the different systems.

3.5 Experiments: Liquid-liquid equilibria

This section gives the results for the experimental LLE of the different systems measured. All data are given as normalized **mass fractions** w_i: all mass fractions have been adjusted to let the sum of all mass fractions in a sample be equal to one by dividing the measured mass fraction by the sum of all measured mass fractions in a sample:

$$w_i = \frac{w_i^{measured}}{\sum_j^{nc} w_j^{measured}} \qquad \textbf{(3.1)}$$

Although data were already available in literature (see Table 3.1) and from DSM Research (Navis, 1996 and De Haan and Niemann, 1999), some experiments were also carried out with the systems **water + caprolactam + ammonium sulfate** (AS) at 293.1 K and 313.1 K and **water + benzene + caprolactam** at 293.1 K (Haase, 1997). This was done to validate the experimental procedure and to check the results with those obtained at DSM-Research and in literature.

3.5.1 Water + caprolactam + AS

Experimental LLE data are reported for the system water + caprolactam + ammonium sulfate at 293.1 K and 313.1 K. All measurements were carried out in duplicate to provide information on the reproducibility of the experiments. The LLE data are

tabulated in Table 3.4. In Figure 3.3 the experimental results are visualized and compared with literature data by Navis (1996) and Shubtsova et al. (1975b).The results of the experiments showed that the equilibrium cell and the analyses were giving good and reproducible results, which are in good agreement with LLE data given in literature.

Table 3.4: Liquid-liquid equilibrium data for the system water (W) + caprolactam (C) + ammonium sulfate (A) at 293.1 K and 313.1 K. Data are in mass fractions.

Temperature	Aqueous phase I			Aqueous phase II		
	W	C	A	W	C	A
293.1 K	0.595	0.310	0.095	0.673	0.148	0.180
	0.533	0.420	0.047	0.693	0.071	0.236
	0.487	0.480	0.033	0.677	0.050	0.273
	0.384	0.600	0.016	0.641	0.026	0.336
	0.334	0.658	0.008	0.598	0.016	0.386
	0.310	0.684	0.006	0.583	0.008	0.410
313.1 K	0.578	0.340	0.082	0.687	0.141	0.173
	0.496	0.465	0.039	0.702	0.064	0.234
	0.463	0.506	0.032	0.686	0.046	0.268
	0.374	0.611	0.015	0.653	0.020	0.327
	0.326	0.664	0.009	0.610	0.012	0.378
	0.284	0.711	0.005	0.565	0.006	0.429

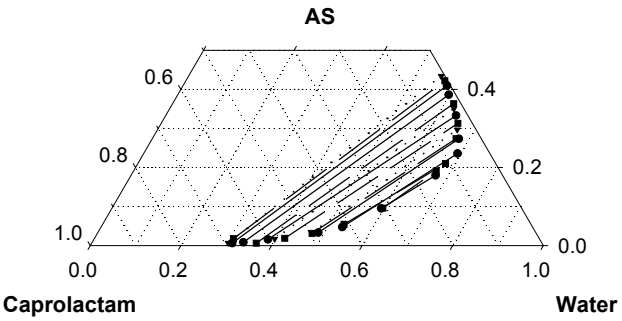

Figure 3.3: Comparison of LLE data as given in Table 3.4 (●, solid lines) with data from Shubtsova et al. (1975a) (■, dashed lines) and Navis (1996) (▼, dotted lines) for the system water + caprolactam + ammonium sulfate at 293.1 K.

3.5.2 Water + benzene + caprolactam

In this section, the LLE data are given for the (salt-free) system water + benzene + caprolactam at 293.1 K. Table 3.5 gives the experimental LLE data and in Figure 3.4 the results are compared to the data as given by Navis (1996) and Morachevskii et al. (1960). Once again a good agreement with literature is found, ensuring that the equilibrium cell and the analyses were giving reliable results.

Table 3.5: Liquid-liquid equilibrium data for the system water (W) + benzene (B) + caprolactam (C) at 293.1 K. Data are given in mass fractions.

Organic phase			Aqueous phase		
W	B	C	W	B	C
0.001	0.951	0.048	0.798	0.003	0.199
0.021	0.806	0.173	0.504	0.033	0.463
0.017	0.813	0.170	0.502	0.033	0.465
0.071	0.577	0.352	0.253	0.168	0.579
0.070	0.578	0.352	0.259	0.172	0.569

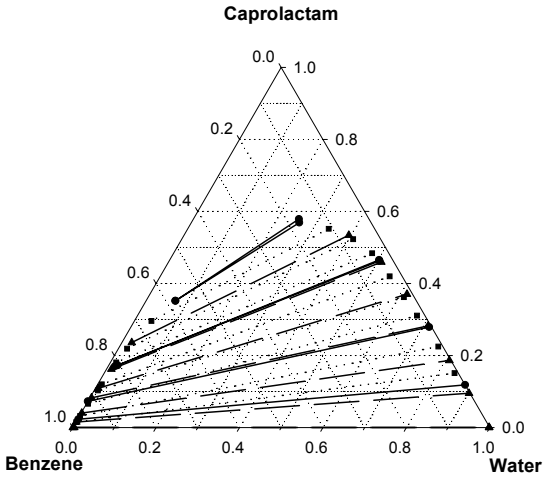

Figure 3.4: Comparison of the LLE data in Table 3.5 (●, solid lines) with experimental data from Navis (1996) (▲, dashed lines) and from Morachevskii et al. (1960) (■, dotted lines) for the system water + benzene + caprolactam at 293.1 K

3.5.3 Water + 1-heptanol + caprolactam + AS

For the systems containing 1-heptanol as the solvent, LLE data were measured for the ternary system water + 1-heptanol + caprolactam and the quaternary system water + 1-heptanol + caprolactam + ammonium sulfate, each at 293.1, 313.1 and 333.1 K. Results are given in Table 3.6 to 3.9. Graphical representations can be found in Figure 3.5 to 3.7. Figure 3.5 and 3.6 illustrate the influence of the temperature on the tie-lines and the solubilities of caprolactam in water and 1-heptanol. With increasing temperature, the solubility of caprolactam in the organic phase increases faster than in the aqueous phase.

Table 3.6: Liquid-liquid equilibrium data for the system water (W) + 1-heptanol (H) + caprolactam (C) at 293.1 K, 313.1 K and 333.1 K. Data are in mass fractions.

Temperature	Organic phase			Aqueous phase		
	W	H	C	W	H	C
293.1 K	0.058	0.942	0.000	1.000	0.000	0.000
	0.106	0.743	0.152	0.860	0.000	0.140
	0.147	0.611	0.242	0.768	0.007	0.225
	0.228	0.452	0.320	0.670	0.021	0.309
	0.324	0.321	0.355	0.582	0.071	0.348
	0.417	0.217	0.366	0.512	0.128	0.360
313.1 K	0.061	0.939	0.000	1.000	0.000	0.000
	0.100	0.757	0.143	0.910	0.000	0.090
	0.175	0.561	0.265	0.786	0.008	0.205
	0.212	0.488	0.299	0.736	0.015	0.249
	0.256	0.418	0.326	0.699	0.028	0.273
	0.417	0.239	0.344	0.554	0.121	0.325
333.1 K	0.061	0.939	0.000	1.000	0.000	0.000
	0.121	0.702	0.178	0.900	0.000	0.100
	0.184	0.538	0.279	0.815	0.010	0.176
	0.217	0.480	0.302	0.774	0.017	0.209
	0.250	0.419	0.331	0.747	0.018	0.235
	0.313	0.346	0.341	0.690	0.043	0.268
	0.437	0.221	0.342	0.593	0.120	0.302

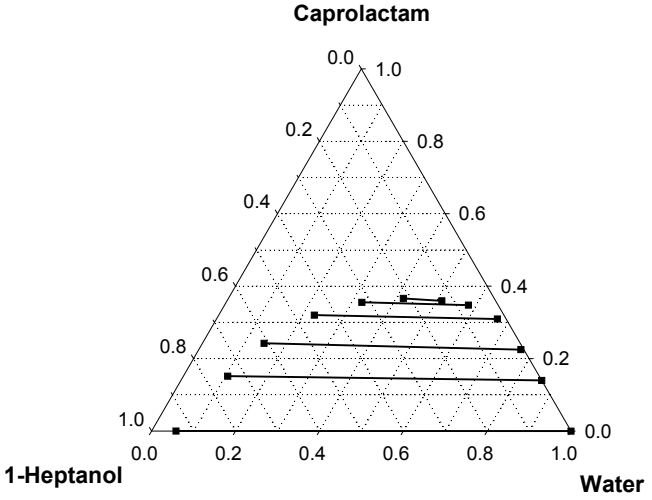

Figure 3.5: Experimental LLE tie-lines for the system water + 1-heptanol + caprolactam at 293.1 K.

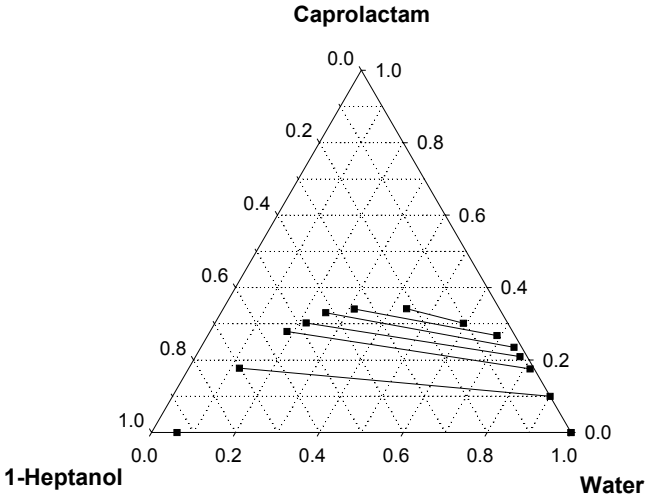

Figure 3.6: Experimental LLE tie-lines for the system water + 1-heptanol + caprolactam at 333.1 K.

Table 3.7: Liquid-liquid equilibrium data for the system water (W) + 1-heptanol (H) + caprolactam (C) + ammonium sulfate (A) at 293.1 K. Data are in mass fractions.

Organic phase				Aqueous phase			
W	H	C	A	W	H	C	A
0.076	0.818	0.106	0.000	0.864	0.000	0.047	0.088
0.106	0.710	0.183	0.000	0.827	0.000	0.122	0.052
0.169	0.537	0.295	0.000	0.729	0.006	0.218	0.048
0.069	0.849	0.081	0.000	0.773	0.000	0.010	0.217
0.077	0.796	0.127	0.000	0.824	0.000	0.032	0.144
0.126	0.615	0.259	0.000	0.771	0.000	0.085	0.144
0.070	0.797	0.133	0.000	0.722	0.000	0.010	0.269
0.106	0.623	0.272	0.000	0.702	0.000	0.017	0.281
0.124	0.565	0.311	0.000	0.706	0.000	0.026	0.269

Table 3.8: Liquid-liquid equilibrium data for the system water (W) + 1-heptanol (H) + caprolactam (C) + ammonium sulfate (A) at 313.1 K. Data are in mass fractions.

Organic phase				Aqueous phase			
W	H	C	A	W	H	C	A
0.000	0.056	0.944	0.000	0.000	0.950	0.000	0.050
0.139	0.088	0.772	0.000	0.058	0.895	0.000	0.047
0.256	0.135	0.609	0.000	0.134	0.814	0.003	0.049
0.369	0.231	0.399	0.002	0.220	0.722	0.009	0.050
0.000	0.052	0.948	0.000	0.000	0.857	0.000	0.143
0.149	0.083	0.767	0.000	0.026	0.813	0.000	0.161
0.294	0.134	0.572	0.000	0.077	0.785	0.000	0.139
0.413	0.233	0.352	0.003	0.117	0.740	0.000	0.143
0.000	0.044	0.956	0.000	0.000	0.689	0.000	0.311
0.181	0.073	0.746	0.000	0.009	0.687	0.000	0.304
0.335	0.115	0.550	0.000	0.020	0.703	0.000	0.277
0.463	0.201	0.334	0.002	0.038	0.708	0.000	0.255

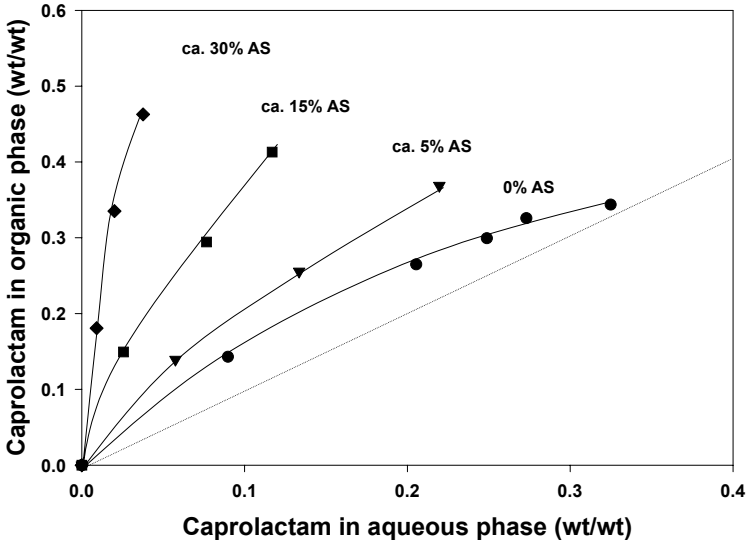

Figure 3.7: Experimental caprolactam distribution curves in water + 1-heptanol at 313.1 K for different weight percents of ammonium sulfate in the aqueous phase. Lines are interpolated.

Table 3.9: Liquid-liquid equilibrium data for the system water (W) + 1-heptanol (H) + caprolactam (C) + ammonium sulfate (A) at 333.1 K. Data are in mass fractions.

Organic phase				Aqueous phase			
W	H	C	A	W	H	C	A
0.000	0.057	0.943	0.000	0.000	0.954	0.000	0.046
0.149	0.098	0.753	0.000	0.054	0.899	0.002	0.045
0.302	0.164	0.534	0.000	0.134	0.808	0.004	0.055
0.392	0.354	0.247	0.008	0.254	0.664	0.034	0.048
0.000	0.056	0.945	0.000	0.000	0.854	0.000	0.146
0.185	0.095	0.720	0.000	0.031	0.820	0.000	0.148
0.354	0.161	0.484	0.001	0.066	0.772	0.000	0.162
0.450	0.373	0.164	0.013	0.137	0.713	0.000	0.150
0.000	0.047	0.953	0.000	0.000	0.709	0.000	0.291
0.206	0.084	0.709	0.000	0.010	0.695	0.000	0.296
0.410	0.146	0.444	0.001	0.019	0.679	0.000	0.303
0.512	0.240	0.245	0.004	0.032	0.684	0.000	0.284

Figure 3.7 illustrates the large influence of the salt concentration on the distribution of caprolactam between the organic phase and the aqueous phase. At higher concentrations of salt more caprolactam tends to dissolve in the organic phase. In other words: due to an increasing salt concentration the caprolactam solubility in the aqueous phase is decreasing.

3.5.4 Water + 2-heptanone + caprolactam + AS

With 2-heptanone as the solvent, LLE of the ternary system water + solvent + caprolactam were measured at 293.1, 313.1 and 333.1 K. The LLE of the quaternary system with ammonium sulfate were measured at 293.1 and 313.1 K. For this system also equilibria with three liquid phases were found as will be discussed in the next section. The experimental LLE data are given in Table 3.10 to 3.12. Figure 3.8 shows for 2-heptanone the same temperature effect on the caprolactam distribution as found for 1-heptanol. At higher temperatures the caprolactam distribution is changing in favour of the organic phase.

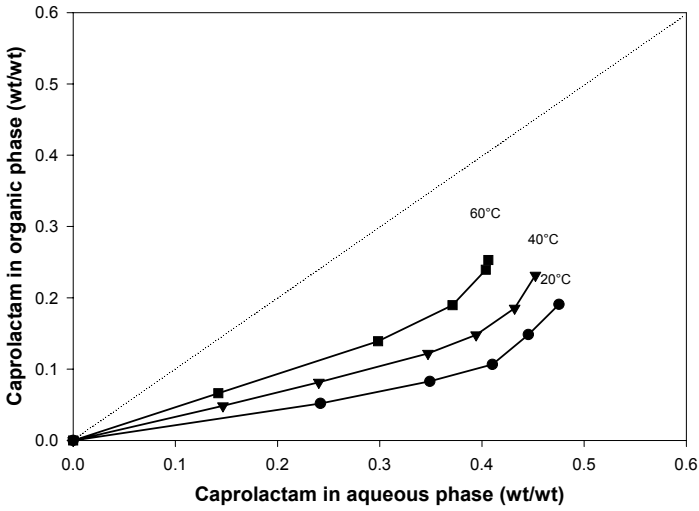

Figure 3.8: Caprolactam distribution between the aqueous phase and the organic phase in water + 2-heptanone mixtures. Markers are experimental data, lines are interpolated.

Table 3.10: Liquid-liquid equilibrium data for the system water (W) + 2-heptanone (H)+ caprolactam (C) at 293.1 K, 313.1 K and 333.1 K. Data are in mass fractions.

Temperature	Organic phase			Aqueous phase		
	W	H	C	W	H	C
293.1 K	0.013	0.987	0.000	0.998	0.002	0.000
	0.025	0.923	0.052	0.743	0.015	0.242
	0.030	0.887	0.083	0.617	0.034	0.349
	0.036	0.857	0.107	0.536	0.053	0.410
	0.048	0.803	0.148	0.458	0.097	0.446
	0.066	0.743	0.191	0.371	0.154	0.476
	0.105	0.635	0.259	0.294	0.253	0.453
313.1 K	0.015	0.985	0.000	0.997	0.003	0.000
	0.024	0.928	0.049	0.842	0.011	0.147
	0.033	0.885	0.082	0.736	0.023	0.241
	0.046	0.832	0.122	0.608	0.045	0.347
	0.058	0.794	0.148	0.529	0.077	0.394
	0.074	0.740	0.186	0.449	0.119	0.432
	0.102	0.667	0.232	0.372	0.176	0.452
333.1 K	0.016	0.984	0.000	0.997	0.003	0.000
	0.029	0.905	0.066	0.849	0.009	0.142
	0.052	0.809	0.139	0.672	0.029	0.299
	0.070	0.740	0.190	0.549	0.080	0.371
	0.095	0.652	0.253	0.446	0.146	0.406
	0.107	0.654	0.239	0.454	0.142	0.404

Graphical representations of the results presented in Table 3.12 can be found in Figure 3.9 and 3.10. From these figures it can be observed that an increasing salt concentration dramatically changes the phase diagram for the system water + 2-heptanone + caprolactam. With 30 wt% ammonium sulfate in the bottom phase, nearly all caprolactam and organic solvent are present in the organic phase. At these high salt concentrations the caprolactam solubility, but also the 2-heptanone solubility, in the bottom phase is very low.

Table 3.11: Liquid-liquid equilibrium data for the system water (W) + 2-heptanone (H) + caprolactam (C) + ammonium sulfate (A) at 293.1 K. Data are given in mass fractions.

Organic phase				Aqueous phase			
W	H	C	A	W	H	C	A
0.022	0.924	0.054	0.000	0.776	0.006	0.150	0.069
0.035	0.850	0.115	0.000	0.652	0.017	0.266	0.064
0.056	0.763	0.181	0.000	0.555	0.040	0.341	0.065
0.034	0.854	0.112	0.000	0.722	0.004	0.132	0.142
0.046	0.803	0.151	0.000	0.647	0.014	0.228	0.111
0.435	0.069	0.473	0.024	0.698	0.000	0.065	0.237
0.049	0.780	0.171	0.000	0.685	0.000	0.042	0.273
0.108	0.597	0.295	0.000	0.678	0.000	0.038	0.284
0.222	0.335	0.440	0.004	0.675	0.000	0.033	0.292
0.269	0.222	0.504	0.005	0.666	0.000	0.027	0.307
0.416	0.053	0.511	0.020	0.673	0.000	0.037	0.290

Table 3.12: Liquid-liquid equilibrium data for the system water (W) + 2-heptanone (H) + caprolactam (C) + ammonium sulfate (A) at 313.1 K. Data are given in mass fractions.

Organic phase				Aqueous phase			
W	H	C	A	W	H	C	A
0.029	0.903	0.068	0.000	0.813	0.004	0.115	0.068
0.043	0.832	0.125	0.000	0.721	0.012	0.215	0.052
0.071	0.720	0.210	0.000	0.631	0.025	0.268	0.075
0.102	0.633	0.265	0.000	0.567	0.046	0.332	0.056
0.127	0.563	0.310	0.000	0.518	0.071	0.370	0.041
0.043	0.834	0.123	0.000	0.765	0.003	0.101	0.131
0.111	0.612	0.277	0.000	0.672	0.013	0.201	0.114
0.142	0.534	0.324	0.000	0.714	0.006	0.146	0.134
0.144	0.513	0.342	0.001	0.693	0.010	0.171	0.127
0.047	0.781	0.172	0.000	0.676	0.000	0.014	0.309
0.105	0.581	0.314	0.000	0.695	0.000	0.027	0.278
0.175	0.387	0.437	0.001	0.682	0.000	0.024	0.293
0.253	0.208	0.535	0.004	0.680	0.000	0.024	0.295
0.299	0.126	0.568	0.007	0.669	0.000	0.022	0.309

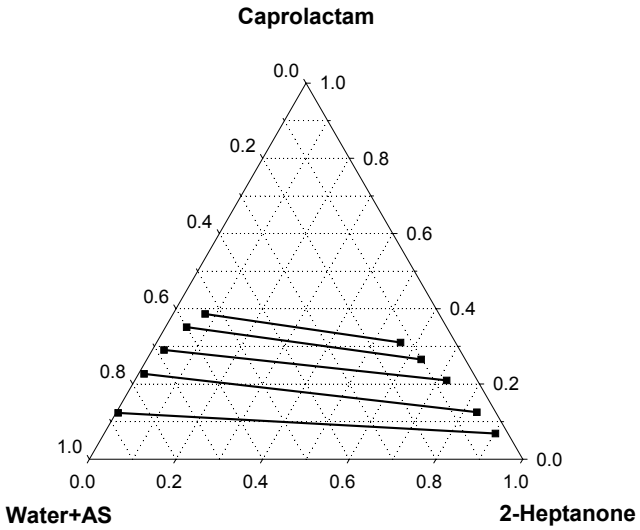

Figure 3.9: Experimental phase diagram for the system water + 2-heptanone + caprolactam at 313.1 K with an ammonium sulfate concentration in the bottom phase of around 6 wt%.

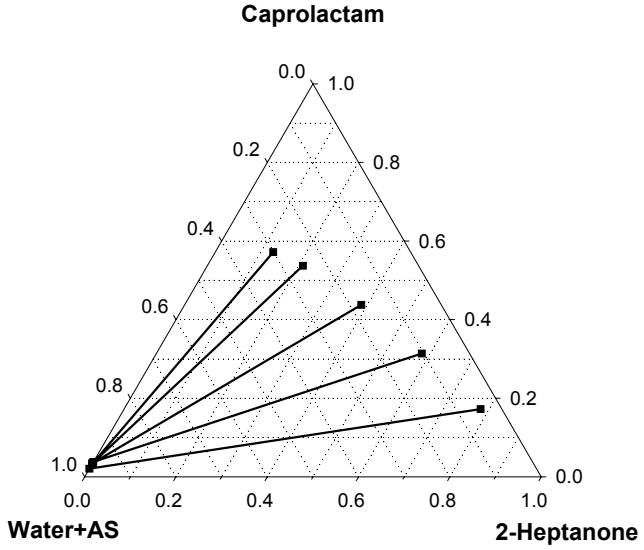

Figure 3.10 Experimental phase diagram for the system water + 2-heptanone + caprolactam at 313.1 K with an ammonium sulfate concentration in the bottom phase of around 30 wt%.

3.6 Experiments: Liquid-liquid-liquid equilibria

3.6.1 Water + 2-heptanone + caprolactam + AS

During the experiments on the LLE in the quaternary system of water + 2-heptanone + caprolactam + AS, equilibria of three liquid phases were observed at 293.1 K. As stated in Chapter 2, the modelling of this kind of equilibria represents a major challenge and can be seen as a severe test for the abilities of a model to describe liquid demixing. Therefore, the decision was made to measure LLLE data at 293.1 K for the system with 2-heptanone. These data are given in Table 3.13. At 313.1 K no stable LLLE were found.

The results are visualized in Figures 3.11 to 3.13. The figures illustrate the progression with increasing salt concentration from one critical tie-line at low salt concentrations to another critical tie-line at higher salt concentrations, as discussed in Chapter 2. At the low salt concentration two liquid phases can exist and most of the caprolactam will be in the bottom phase, at higher salt concentrations three liquid phases exist and most of the caprolactam is found in the middle phase. At high salt concentrations two liquid phases are present and the top phase will contain most of the caprolactam. In the drawing below, these phenomena are schematically represented:

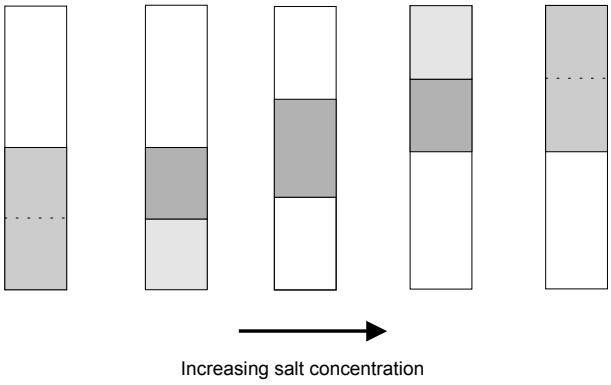

Figure 3.11: Schematic representation of the LLLE phase behaviour. The darkness of the phases represents the caprolactam concentration

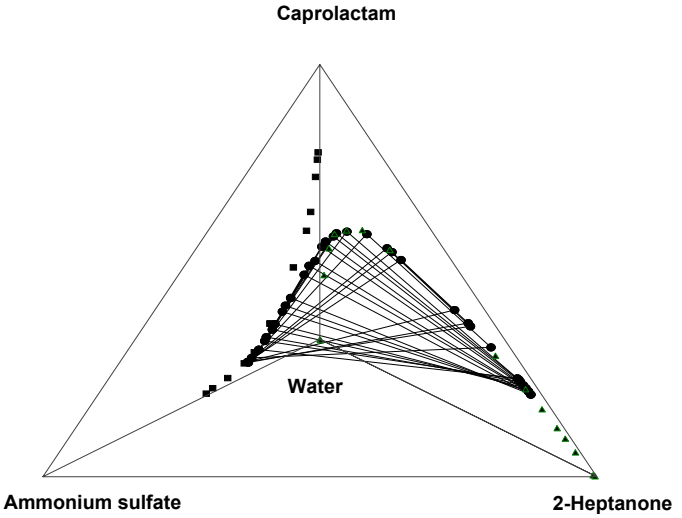

Figure 3.12: Experimental LLLE triangles for the system water + 2-heptanone + caprolactam + ammonium sulfate at 293.1 K (●) and the LLE-binodals of two of the ternary subsystems (■,▲)

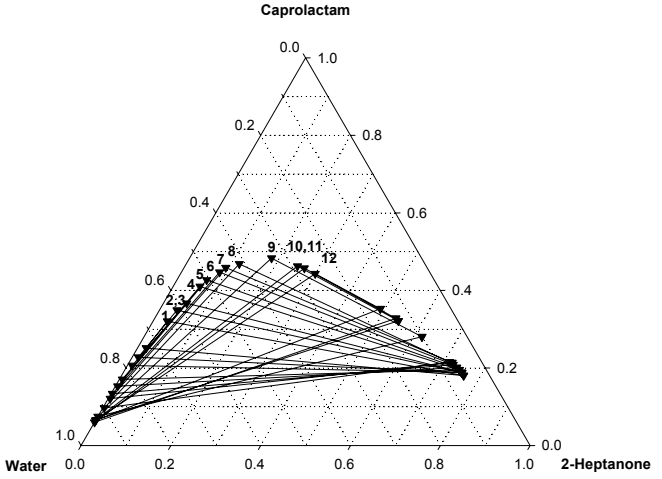

Figure 3.13: Projection of experimental LLLE in the system water + 2-heptanone + caprolactam + ammonium sulfate at 293.1 K. The numbers refer to the experimental data in Table 3.13

Table 3.13: Liquid-liquid-liquid equilibrium data of the system water (W) + 2-heptanone (H) + caprolactam (C) + ammonium sulfate (A) at 293.1 K. Data are given in mass fractions.

Phase	No.	W	H	C	A
Top phase	1	0.058	0.762	0.181	0.000
	2	0.058	0.754	0.188	0.000
	3	0.059	0.753	0.189	0.000
	4	0.060	0.745	0.195	0.000
	5	0.063	0.736	0.201	0.000
	6	0.067	0.724	0.209	0.000
	7	0.067	0.719	0.214	0.000
	8	0.072	0.713	0.215	0.000
	9	0.101	0.618	0.281	0.000
	10	0.133	0.545	0.321	0.001
	11	0.135	0.536	0.328	0.001
	12	0.157	0.489	0.352	0.002
Middle phase	1	0.592	0.029	0.293	0.086
	2	0.566	0.036	0.323	0.075
	3	0.543	0.048	0.343	0.066
	4	0.504	0.057	0.390	0.049
	5	0.485	0.063	0.409	0.042
	6	0.452	0.082	0.432	0.033
	7	0.435	0.090	0.446	0.029
	8	0.406	0.116	0.460	0.018
	9	0.331	0.181	0.478	0.010
	10	0.285	0.249	0.460	0.006
	11	0.272	0.267	0.455	0.006
	12	0.256	0.298	0.441	0.005
Bottom phase	1	0.640	0.017	0.221	0.122
	2	0.655	0.012	0.197	0.136
	3	0.671	0.009	0.177	0.143
	4	0.685	0.005	0.142	0.167
	5	0.694	0.004	0.126	0.176
	6	0.694	0.002	0.108	0.196
	7	0.698	0.004	0.097	0.202
	8	0.699	0.002	0.075	0.223
	9	0.697	0.000	0.057	0.246
	10	0.690	0.000	0.049	0.261
	11	0.698	0.000	0.045	0.258
	12	0.694	0.000	0.048	0.258

3.6.2 Water + benzene + caprolactam + AS

From data at DSM-Research it was known that a LLLE-region also existed in the systems with benzene. Of the latter systems a more extensive study was made of LLLE at temperatures from 293.1 K to 330.1 K. In this way, also an estimation could be made of the location of the tricritical point. The experimental data at the different temperatures are given in Table 3.14 and 3.15. The results are graphically represented in Figures 3.15 to 3.19.

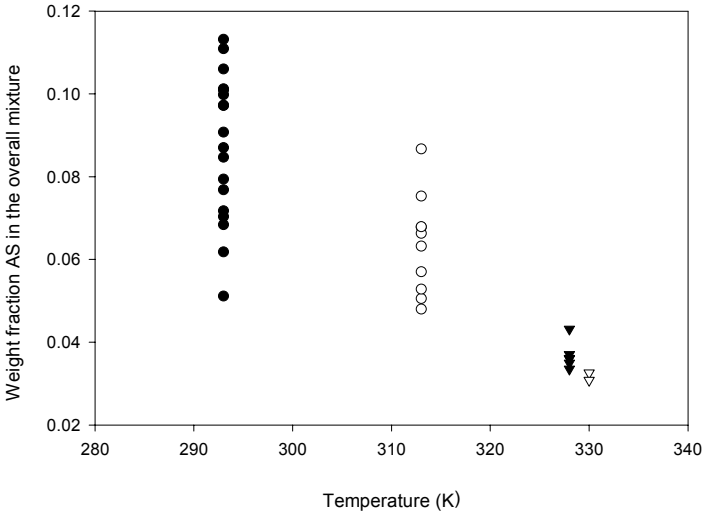

Figure 3.14: Overall salt concentrations for the experiments in Table 3.14 and 3.15. Data are given in weight fractions.

Figure 3.14 gives the overall salt concentrations of the mixtures at which the experiments were performed and for which LLLE were found. From this figure it is possible to estimate the location of the tricritical point. As discussed in Chapter 2, the tricritical point is the temperature and composition where the three phases become identical and the two critical tie-lines merge and have a zero length. Extrapolation of the overall salt concentrations with temperature leads to an estimated tricritical point around 331 K at a salt concentration around 0.027 wt/wt. Experimentally, no LLLE were found above 331 K.

Table 3.14: Liquid-liquid-liquid equilibrium data of the system water (W) + benzene (B) + caprolactam (C) + ammonium sulfate (A) at 293.1 K. Data are given as mass fractions.

Phase	No.	W	B	C	A
Top	1	0.027	0.724	0.249	0.000
	2	0.028	0.720	0.252	0.000
	3	0.029	0.702	0.269	0.000
	4	0.031	0.691	0.278	0.000
	5	0.032	0.683	0.285	0.000
	6	0.036	0.664	0.300	0.000
	7	0.042	0.638	0.320	0.000
	8	0.046	0.625	0.329	0.000
	9	0.050	0.616	0.334	0.000
	10	0.057	0.587	0.356	0.000
	11	0.059	0.580	0.361	0.000
	12	0.075	0.528	0.397	0.000
	13	0.091	0.477	0.431	0.000
	14	0.103	0.459	0.438	0.000
Middle	1	0.582	0.019	0.332	0.066
	2	0.539	0.024	0.382	0.055
	3	0.519	0.027	0.402	0.052
	4	0.491	0.030	0.434	0.045
	5	0.471	0.038	0.455	0.035
	6	0.429	0.049	0.494	0.027
	7	0.400	0.061	0.519	0.020
	8	0.389	0.072	0.521	0.018
	9	0.364	0.090	0.531	0.014
	10	0.337	0.111	0.542	0.010
	11	0.327	0.120	0.543	0.009
	12	0.284	0.156	0.553	0.007
	13	0.258	0.182	0.555	0.005
	14	0.240	0.200	0.555	0.004
Bottom	1	0.670	0.005	0.185	0.140
	2	0.684	0.003	0.151	0.162
	3	0.689	0.003	0.146	0.163
	4	0.696	0.002	0.128	0.174
	5	0.695	0.002	0.106	0.198
	6	0.705	0.001	0.090	0.204
	7	0.700	0.001	0.068	0.232
	8	0.699	0.001	0.066	0.235
	9	0.702	0.000	0.057	0.241
	10	0.700	0.000	0.050	0.249
	11	0.704	0.000	0.048	0.248
	12	0.696	0.000	0.044	0.259
	13	0.703	0.000	0.042	0.254
	14	0.695	0.000	0.039	0.265

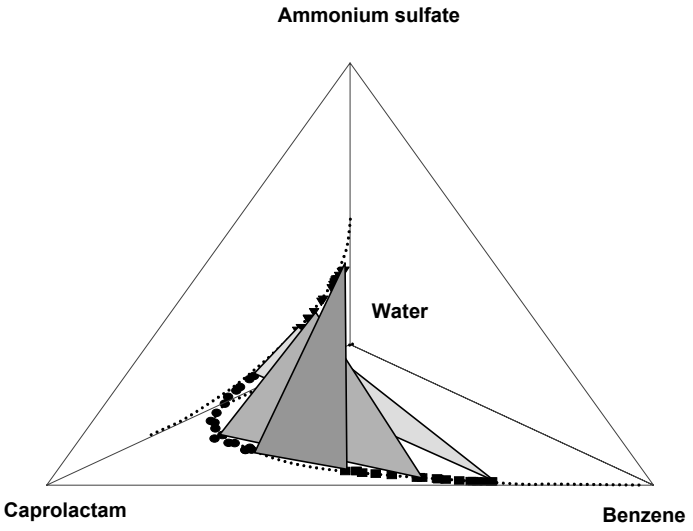

Figure 3.15: Top (■), middle (▼) and bottom (●) phase compositions and some tie-triangles of LLLE in the system water + benzene + caprolactam + ammonium sulfate at 293.1 K.

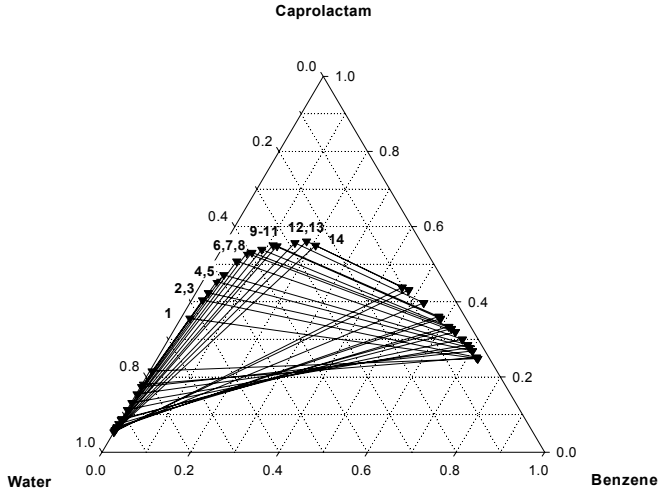

Figure 3.16: Projection of experimental LLLE in the system water + benzene + caprolactam + ammonium sulfate at 313.1 K. The labels refer to the LLLE data in Table 3.13

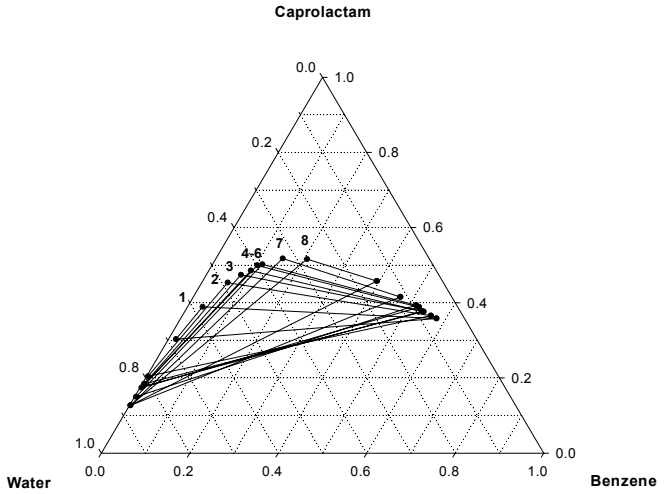

Figure 3.17: Projection of experimental LLLE for the system water + benzene + caprolactam + ammonium sulfate at 313.1 K. The labels refer to the LLLE data in Table 3.15.

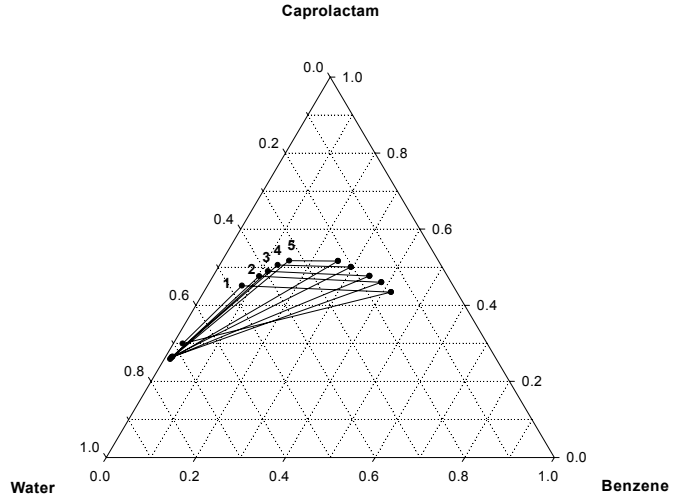

Figure 3.18: Projection of experimental LLLE for the system water + benzene + caprolactam + ammonium sulfate at 328.1 K. The labels refer to the LLLE data in Table 3.15.

Table 3.15: Liquid-liquid-liquid equilibrium data of the system water (W) + benzene (B) + caprolactam (C) + ammonium sulfate (A) at 313.1 to 330.1 K. Data are given in mass fractions.

Temperature	Phase	No.	W	B	C	A
313.15	Top phase	1	0.064	0.578	0.358	0.000
		2	0.072	0.562	0.366	0.000
		3	0.084	0.540	0.376	0.000
		4	0.087	0.536	0.378	0.000
		5	0.088	0.524	0.388	0.000
		6	0.092	0.515	0.393	0.000
		7	0.117	0.468	0.416	0.000
		8	0.149	0.393	0.457	0.001
	Middle phase	1	0.543	0.032	0.366	0.059
		2	0.471	0.057	0.438	0.034
		3	0.438	0.077	0.464	0.021
		4	0.411	0.093	0.476	0.020
		5	0.391	0.100	0.490	0.019
		6	0.379	0.111	0.495	0.015
		7	0.328	0.150	0.512	0.010
		8	0.276	0.206	0.513	0.006
	Bottom phase	1	0.620	0.016	0.276	0.089
		2	0.687	0.003	0.177	0.133
		3	0.688	0.004	0.156	0.152
		4	0.690	0.005	0.149	0.156
		5	0.696	0.003	0.147	0.153
		6	0.690	0.003	0.122	0.185
		7	0.708	0.002	0.103	0.188
		8	0.710	0.002	0.104	0.185
328.15	Top phase	1	0.147	0.417	0.434	0.001
		2	0.156	0.383	0.460	0.001
		3	0.174	0.348	0.476	0.001
		4	0.203	0.295	0.500	0.002
		5	0.225	0.258	0.515	0.003
	Middle phase	1	0.458	0.075	0.438	0.029
		2	0.412	0.101	0.467	0.021
		3	0.388	0.114	0.481	0.016
		4	0.360	0.128	0.499	0.014
		5	0.328	0.147	0.509	0.015
	Bottom phase	1	0.622	0.019	0.274	0.085
		2	0.653	0.013	0.239	0.095
		3	0.654	0.013	0.238	0.096
		4	0.654	0.014	0.241	0.091
		5	0.657	0.012	0.233	0.097
330.15	Top phase	1	0.203	0.316	0.478	0.003
		2	0.232	0.245	0.518	0.004
	Middle phase	1	0.453	0.052	0.457	0.039
		2	0.420	0.067	0.49	0.022
	Bottom phase	1	0.595	0.026	0.315	0.064
		2	0.603	0.025	0.306	0.065

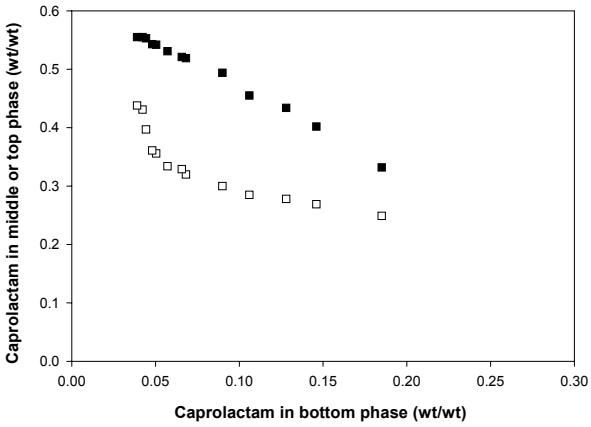

Figure 3.19: Caprolactam distribution for the LLLE in the system water + benzene + caprolactam + ammonium sulfate at 293.1 K.

3.7 Discussion

3.7.1 Liquid-liquid equilibria

Some general trends can be noticed when comparing the data for the different systems presented in the tables and figures. A saturated solution of ammonium sulfate in water is immiscible with a saturated solution of caprolactam, but can be brought to a critical point by adding more water. Similarly, for all the systems water + solvent + caprolactam given, the water and the solvent are hardly miscible but reach a critical point when enough caprolactam is added. As expected, at higher temperatures the solubility of caprolactam in both the organic solvent and water increases. However, the solubility of caprolactam in the organic solvent increases more rapidly than the solubility in water, as can be seen from the change in the slope of the tie-lines. The region in which demixing occurs becomes smaller at higher temperatures.

The two ternary systems, water + solvent + caprolactam and water + caprolactam + ammonium sulfate form two of the four triangular faces of the tetrahedron by which the quaternary system is represented (Figure 3.2, 3.12, 3.15). By adding salt to the first ternary system, its critical point moves to the interior of the tetrahedron. When

solvent is added to the second ternary system, its critical point is also moved to the interior.

At higher salt concentrations, more caprolactam will go into the organic phase. At salt concentrations of 30 wt% and higher almost all caprolactam is found in the organic phase. In this case the aqueous phase hardly contains any organic solvent. This is an illustration of "salting out" behaviour. Due to the large number of ions that need to be hydrated, not enough water molecules are available for the hydration/solvation of the solute. From the experiments, it can also be observed that with higher temperatures and salt concentrations, also the salt concentration in the organic phase increases, which is always accompanied by increasing water concentrations in the organic phase.

Figure 3.20 gives the caprolactam distribution for the solvents benzene, 1-heptanol and 2-heptanone. Comparison of the liquid phase behaviour of the different solvents shows that 2-heptanone and benzene behave in a more or less similar way, although the two phase region is smaller for 2-heptanone. The phase behaviour of 1-heptanol is quite different, because 1-heptanol has a higher solubility for caprolactam than water.

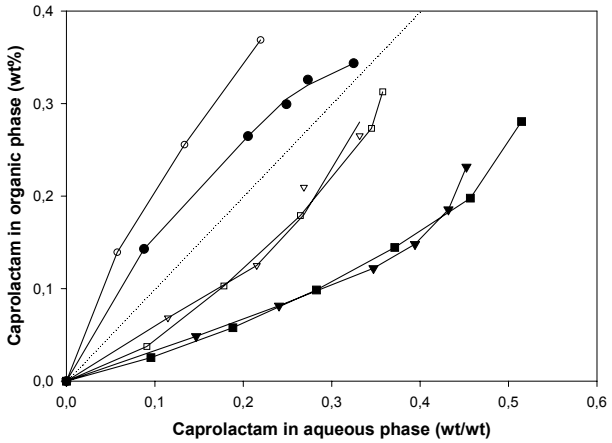

Figure 3.20: Caprolactam distribution curve for 1-heptanol (circles), benzene (squares) and 2-heptanone (triangles) in water + solvent systems at 313.1 K. Solid markers are for salt-free systems, open markers are for systems with around 5 wt% salt in the bottom phase.

With respect to the extraction process of caprolactam, it can be seen that the forward extraction is favoured by an increase in temperature. At higher temperatures more caprolactam will be transferred to the organic phase. For the backward extraction the opposite is found. A lower temperature favours the transfer of caprolactam to the water phase. From the solvents other than benzene, 2-heptanone seems more suitable than 1-heptanol. The two phase region is larger for 2-heptanone. The presence of salt in the system has a positive influence on the extraction. The salt is only present in the forward extraction step. The salting-out effect causes more caprolactam to dissolve in the organic phase and thus reduces the amount of solvent required.

3.7.2 Liquid-liquid-liquid equilibria

Both for the systems water + benzene + caprolactam + ammonium sulfate and water + 2-heptanone + caprolactam + ammonium sulfate, a three-liquid phase region was determined. The observed phase behaviour can be explained on the basis of the discussion on the system water + benzene + ethanol + ammonium sulfate by Rowlinson and Swinton (1982), as summarized in Chapter 2:

The two ternary subsystems water + solvent + caprolactam and water + caprolactam + ammonium sulfate, form two of the four triangular faces of the tetrahedron by which the quaternary system is represented (Figure 3.2). By adding salt to the critical point of the first ternary system, the critical point moves to the interior of the tetrahedron. When solvent is added to the second ternary system, its critical point is also moved to the interior. The critical points at different salt or solvent concentrations can be seen as a critical line. These two critical lines can form a continuous curve from one face to another. In this case one two-liquid phase region is found and a continuous transition is found for the slope of the LLE tie-lines from one triangular face or ternary subsystem to the other one.

If the quaternary system (water + benzene or 2-heptanone + caprolactam + ammonium sulfate) is below its tri-critical point, the two critical lines do not meet, but have an end-point. At this end-point, the two critical phases are in equilibrium with a third phase. The tie-lines thus formed are the two critical tie-lines that bound the three phase region. Between the two end-points, there is a stack of three-phase triangles. The compositions of the LLLE follow the three-phase composition curve. This is visualized in Figure 3.21.

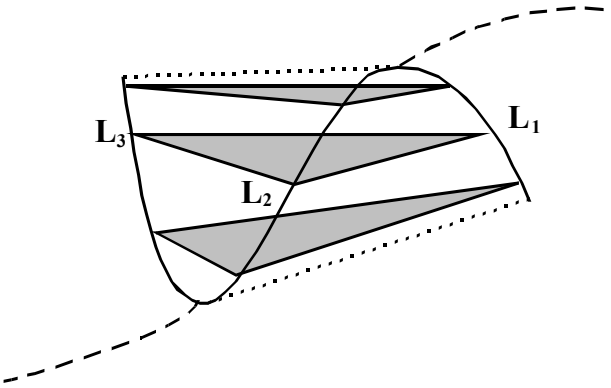

Figure 3.21: The three-liquid phase body in the interior of the composition tetrahedron. Dashed lines are critical lines, dotted lines are critical tie-lines. (Figure after Rowlinson and Swinton, 1982)

The experiments illustrate the progression from two liquid phases to three liquid phases to two liquid phases. With decreasing salt concentrations the bottom and middle phase become identical; with increasing salt concentrations the top and middle phase become identical. In the tetrahedron, the three-phase region is bounded by a curve that connects the phase compositions of the different phases over the full range of concentrations and the two critical tie-lines. It is difficult to represent the LLLE in a three-dimensional figure, but for the two systems an attempt has been made in Figure 3.12 and 3.15. It can be seen that both systems obey the same pattern. Figure 3.22 demonstrates for the LLLE with benzene how the three-liquid phase region is enclosed by a two-phase region of which the limits are given for the ternary subsystems.

Since the LLLE for the system with benzene as the solvent were studied at more temperatures, it is possible to examine the temperature effect. With increasing temperature, the size of the three-phase body is decreasing. Especially the composition of the bottom phase is influenced by a change in temperature. The salt concentration in the three phases is lower at higher temperatures. The salt content for the overall mixture had to be decreased dramatically in order to find three phases. This is clarified in Figure 3.13, where the salt concentrations of the overall mixtures for the various experiments are made visible. The range of concentrations at which still three phases are found, is shrinking to almost zero at 330.1 K.

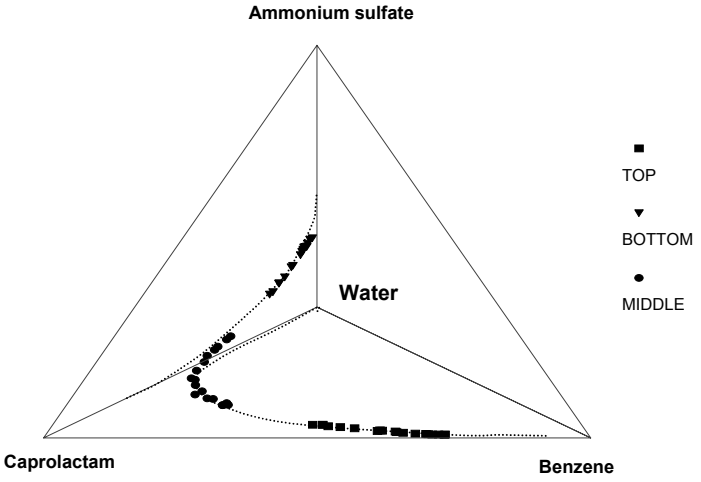

Figure 3.22: Tetrahedron showing the compositions of all phases in the LLLE measured (markers) and the binodal curves (dotted lines) for two of the ternary subsystems at 293.1 K

In literature, there is only one example of a comparable system that was investigated at different temperatures. This is the system water + benzene + ethanol + ammonium sulfate, studied by Lang and Widom (1975). Figure 3.23 shows their results at 294 K. These results are comparable with the results for the system water + 2-heptanone + caprolactam + ammonium sulfate and water + benzene + caprolactam + ammonium sulfate at 293.1 K. Figure 3.24 shows their results at 318 K. It can be seen that the temperature influence is larger for the system water + benzene + ethanol + ammonium sulfate. Lang and Widom calculated the tri-critical point for the system water + benzene + ethanol + ammonium sulfate at 322.0 K and were even able to measure one three phase triangle at 321.7 K.

Regarding the extraction process of caprolactam, it seems unlikely that three liquid phases are encountered in the extraction process. For three phases a salt concentration of at least 5 wt % is required plus a caprolactam concentration of around 30 wt%. This condition is not met in the extraction columns. Nevertheless, it is important to be aware of the possibility of three liquid phases instead of two liquid phases, when modifying the separation process.

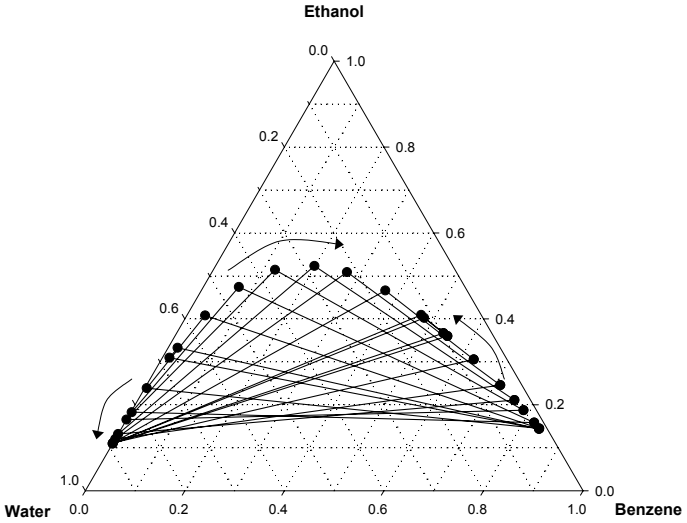

Figure 3.23: Projection of LLLE in the system water + benzene + ethanol + ammonium sulfate at 294.0 K (Lang and Widom, 1975). The arrows indicate the progression with increasing salt concentration. Concentrations are in weight fractions.

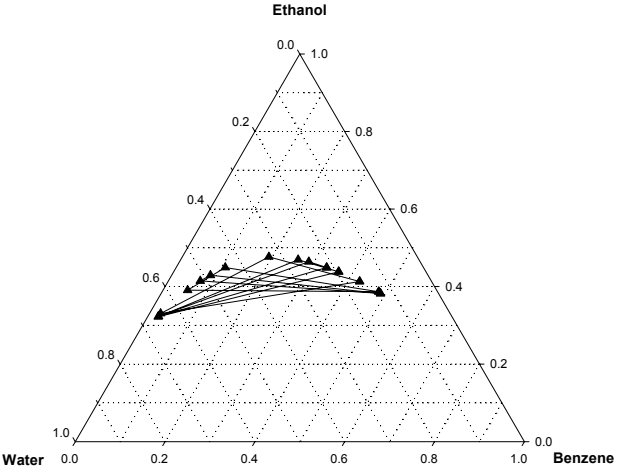

Figure 3.24: Projection of LLLE in the system water + benzene + ethanol + ammonium sulfate at 318.0 K (Lang and Widom, 1975). Concentrations are in weight fractions.

4. Computations

In this chapter the computational procedures will be described that were used in the modelling work that will be discussed in the next chapters. The two most important parts deal with the regression and with the flash calculations. Some information will be given on the structure of the Fortran program used.

4.1 Flash calculations

In the work presented in this thesis, different types of flash calculations were used, like liquid-liquid, liquid-liquid-liquid and vapour-liquid flash calculations. However, all these calculations make use of the same basic subroutines. The principles for the flash calculation will be given here. The programming of the flash routine was based for a large part on the approach followed by the group of Heidemann (Phoenix, 1998), as described very clearly in the thesis of Koak (1997).

The basic conditions for phase equilibria are equal pressure, equal temperature and equality of the chemical potentials μ_i.

$$\mu_{i,\alpha} = \mu_{i,\beta} = ... = \mu_{i,np} \qquad \textbf{(4.1)}$$

or in terms of fugacities :

$$f_{i,\alpha} = f_{i,\beta} = .. = f_{i,np} \ , \ i = 1..nc \qquad \textbf{(4.2)}$$

where *nc* is the number of components and *np* is the number of phases at equilibrium. For liquid-liquid equilibria this can be rewritten either in terms of fugacity coefficients ϕ_i (in the equation of state approach) or in terms of activity coefficients γ_i (in the approach via excess Gibbs energy models) as:

$$\begin{aligned} (x_i\phi_i)_{phase\,1} &= (x_i\phi_i)_{phase\,2} \\ (x_i\gamma_i)_{phase\,1} &= (x_i\gamma_i)_{phase\,2} \end{aligned} \qquad \textbf{(4.3)}$$

In a flash calculation the equilibrium conditions have to be solved for each component and the mole balances have to be satisfied. In addition, for a multiphase equilibrium a stability test has to be included to check whether a different number of phases would

yield a more stable solution. Some phases postulated may actually not be present at equilibrium. In the algorithm used here, the calculation of the equilibrium phases is combined with the so-called Gibbs tangent plane distance stability criterion of Michelsen (1982) for phases not present at equilibrium, defined as:

$$D = \sum_{i=1}^{nc} n_{ik} \left(\mu_{ik}(\bar{x}_k) - \hat{\mu}_i \right) \geq 0 \qquad \textbf{(4.4)}$$

where D is the tangent plane distance for a phase k with a certain composition to be tested. If this condition is satisfied, the Gibbs energy surface at composition x_k lies at any point above the tangent plane that defines equilibrium. In other words: If D=0, the Gibbs energy of the overall mixture is at its global minimum at the composition of phase k. The stationary points of D satisfy the condition:

$$\mu_{ik} = \hat{\mu}_i + \theta_k RT \qquad \textbf{(4.5)}$$

where θ_k is zero if phase k is present at equilibrium; θ_k is given by (Phoenix et al., 1998):

$$\theta_k = D_k = -RT \sum_{i}^{nc} X_{ik} \qquad \textbf{(4.6)}$$

In this equation X_{ik} is a composition variable, equivalent to the mole fraction after normalizing. For computational convenience, the equilibrium condition can be expressed as:

$$\sum_{k=1}^{np} \left(f_{ik} - f_i^{avg} - \theta_i \right) = 0 \quad with \quad f_i^{\text{avg}} \equiv \sum_{k=1}^{np} \beta_k f_{ik} \qquad ,i = 1..nc \qquad \textbf{(4.7)}$$

where f_i^{avg} is the average fugacity and β_k is the total number of moles of phase k relative to the number of moles in the mixture. Obviously, at equilibrium the average fugacity is equal to the individual fugacities. By using an average fugacity, the algorithm does not make use of one of the phases as the reference phase, as is often done. To further facilitate the calculations distribution coefficients K_{ik} are introduced:

$$x_{ik} = K_{ik} z_i \exp(\theta_k) \qquad \textbf{(4.8)}$$

with:

$$K_{ik} = \frac{\phi_i^{avg}}{\phi_{ik}} = \frac{f_i^{avg}}{f_{ik}} \frac{x_{ik}}{z_i} \qquad \textbf{(4.9)}$$

where z_i is the overall mole fraction of component i in the mixture, x_{ik} is the mole fraction of component i in phase k and ϕ_{ik} is the fugacity coefficient (or activity coefficient) of component i in phase k.

The algorithm consists of an inner and an outer loop. In the inner loop the mole balances are solved. Two types of mole balances have to be satisfied: Firstly, the sum of the mole fractions x_{ik} in every phase k has to be equal to unity. Secondly, for every component the total amount of a component in the different phases should correspond to the overall composition:

$$\sum_{k=1}^{np} \beta_k x_{ik} = z_i \qquad \textbf{(4.10)}$$

Combining Equation (4.8), (4.9) and (4.10) gives the equation to calculate the mole fractions for a given K_{ik} and β_k,

$$x_{ik} = \frac{K_{ik} z_i}{\sum_{p=1}^{np} \beta_k K_{ip}} \exp(\theta_k) \qquad \textbf{(4.11)}$$

The sum for the mole fractions in a phase is then given by equation (4.12). This equation has to be solved for every phase by adjusting β. In the inner loop K's are assumed to be constant.

$$h_k = 1 - \sum_{i=1}^{nc} X_{ik} = 0 \qquad \textbf{(4.12)}$$

The solution for the equation above is found by multi-dimensional Newton-Raphson iteration.

$$\overline{\beta}^{new} = \overline{\beta}^{old} - \lambda \overline{A}^{-1} \overline{h}^{old} \qquad \textbf{(4.13)}$$

where A^{-1} is the inverse matrix of A containing the partial derivatives of h to β_j (i.e. the Jacobian elements). In this work, analytical derivatives were used. The equation above is then solved using LU-decomposition, a mathematical technique to solve a set of linear algebraic equations described by Press (1997). By controlling the step size λ, it is prevented that more than one β_k moves to zero in one iteration step or that a β_k gets a negative value.

The method described here corresponds to minimizing the objective function $Q(\beta)$ as defined by Michelsen (1994):

$$Q(\beta) = \sum_{k}^{np} \beta_k - \sum_{i}^{nc} z_i \ln\left(\sum_{k}^{np} \beta_k K_{ik} \right) \tag{4.14}$$

The derivative for this equation to β_k is equal to h_k. Equation (4.14) is calculated after each iteration step to check the progression of the calculation and to adjust the step size λ when the iteration tends to diverge.

In the inner loop the distribution coefficients (and thus the fugacity coefficients) are considered concentration independent. In the outer loop the chemical equilibrium is calculated with the direct substitution method by minimizing:

$$\sum_{k}^{np} \sum_{i}^{nc} g_{ik}^2 = \sum_{k}^{np} \sum_{i}^{nc} \left(\ln f_{ik} - \ln f_i^{avg} - \theta_k \right)^2 \tag{4.15}$$

where f_{ip} is the fugacity of component i in phase p and f_i^{avg} is the average fugacity of component i in the equilibrium phases and θ_p is given by:

$$\theta_k = -D_k / RT = -\ln \sum_i X_{ik} \tag{4.16}$$

In the outer loop the inner loop is called (the mole balance is solved), the fugacity coefficients at the new composition are calculated and the new distribution coefficients are calculated from:

$$\ln K_{ij}^{new} = \ln K_{ij}^{old} - g_{ij} \tag{4.17}$$

If the compositions of two phases become identical, the number of phases is reduced by one. This loop is terminated when the expression in Equation (4.15) is smaller than a given tolerance.

4.2 Regression

The adjustable parameters for the models were obtained by regression of the experimental data using Levenberg-Marquardt optimization. The basic part for the Levenberg-Marquardt routine was obtained from DSM Research. A detailed description of the numerical method will not be given here, for more information see

for example Press et al. (1997). The Levenberg-Marquardt method is a modification of the well-known Gauss-Newton method. The Gauss-Newton method is a least squares estimation method that linearizes the nonlinear regression problem. In the program only numerical derivatives are used for this linearization. The Gauss-Newton method solves the linearized problem and uses the resulting regression parameters to get a new estimation. Subsequently the system is linearized around the new estimations. The process is repeated until the sum of squared errors does not decrease anymore and the regression parameters do not change either. The Levenberg-Marquardt method is a method to prevent the problem from becoming singular and thus hardly solvable.

Of great importance for the results of a regression are the initial values (starting values). A wrong set of initial parameters may lead to a local minimum of the objective function. This was avoided by always using different sets of initial values for the adjustable parameters. Also, the scaling of all parameters to a range between 1 and 10 has a positive result on the quality of the results of the regression. On the other hand the choice of the objective function is very important. In the regressions different objective functions were used in combinations or in sequence to reach an optimal result. In general, two types of objective functions can be used, respectively absolute and relative objective functions.

An example of an absolute objective function for mean ionic activity coefficients is given below, where *nd* is the number of data points, $\gamma_{\pm}^{exp}$ is the experimental value and $\gamma_{\pm}^{calc}$ is the value calculated with the model:

$$F_{OBJ} = \sum_{i}^{nd} \left(\gamma_{\pm}^{\mathrm{exp}} - \gamma_{\pm}^{\mathrm{calc}} \right)^2 \qquad \textbf{(4.18)}$$

A relative objective function is obtained when the expression between brackets is divided by $\gamma_{\pm}^{exp}$. Relative objective functions proved to be useful for mean ionic activity coefficients, vapour pressures and for starting regressions without good initial values. A relative objective function was found to give easier a set of parameters where at least convergence of the flash calculation for all data points could be obtained. The main disadvantage of the relative objective function is that too much weight is given to small data values, like the low concentrations that often exist in the phases in the liquid-liquid equilibria studied in this work. This usually leads to results far from the best results obtainable.

An objective function often used for multiphase equilibria in this work is the objective function F_{OBJ} defined below:

$$F_{OBJ} = \sum_{l}^{nd} \sum_{k}^{np} \sum_{i}^{nc} [W_{ki} \cdot (x_{lki}^{\exp} - x_{lki}^{\text{calc}})^2] + F_P \qquad \textbf{(4.19)}$$

where x_i is the mole or weight fraction of component i, W_{ki} is a weighting factor and where the summations are over the number of data points (*nd*), the number of phases (*np*) and the number of components (*nc*) respectively. The extra contribution F_P is a penalty function that is dependent on the number of data points where the flash routine could not reach convergence with the given number of phases. In Equation (4.19) both weight and mole fractions can be used. Weight fractions often give better results for salt containing solutions, but in principle increasing the weighting factors for the salt has a similar effect.

4.3 Partial dissociation

In Chapter 5 partial dissociation of the salt is introduced. The ionic equilibrium obeys the following dissociation reaction for the systems involved:

$$M_mX_n \rightarrow m\ M^{p+} + n\ X^{q-}$$

The extent of dissociation is given by the dissociation fraction α. The equilibrium compositions are calculated from the dissociation constant K:

$$K = K_x \cdot K_\gamma = \frac{\gamma_M^m \cdot \gamma_X^n}{\gamma_{M_mX_n}} \cdot \frac{x_M^m \cdot x_X^n}{x_{M_mX_n}} \qquad \textbf{(4.20)}$$

The mole fractions of the salt and the ions are given by:

$$x_{M_mX_n} = \frac{x_s \cdot (1-\alpha)}{1 + (m+n-1) \cdot x_s \cdot \alpha} \qquad \textbf{(4.23)}$$

$$x_M = \frac{m \cdot x_s \cdot \alpha}{1 + (m+n-1) \cdot x_s \cdot \alpha} \qquad \textbf{(4.22)}$$

$$x_X = \frac{n \cdot x_s \cdot \alpha}{1 + (m+n-1) \cdot x_s \cdot \alpha} \qquad \textbf{(4.21)}$$

Insertion of these mole fractions in the equation for the dissociation constant and rewriting, leads to:

$$\alpha = \left(1 - \frac{K_\gamma(T,x)}{K} \cdot \frac{m^m n^n x_s^{m+n} \alpha^{m+n}}{\left[1 + (m+n-1)x_s\alpha\right]^{m+n-1}} \right) \tag{4.24}$$

where x_S is the salt weight fraction.

The procedure programmed to solve the dissociation fraction is a loop in which the mole fractions are calculated at a given α, then the activity coefficients are calculated and α is calculated using Equation (4.24) and compared with its previous value. For better convergence the "secant method" is used to determine the new α. The secant method is a root finding method, comparable to the bisection method.

4.4 VLE calculations using an equation of state

For the work on the electrolyte equation of state of Fürst and Renon (1993) in Chapter 6, a volume solver was required. The procedure programmed for VLE calculations using the electrolyte equation of state is as follows:

For solutions that do not contain electrolytes, the electrolyte equation of state reduces to a cubic equation of state. In this case, having calculated the required parameters and using the appropriate mixing rule, the volume can be solved analytically. To do this, the equation of state is rewritten to the form "$0 = x^3 + bx^2 + cx + d$" and then the molar volume is solved by Cardan's method as given for example by Perry (1997). The cubic equation solver produces three roots. The largest root is the molar volume of the vapour phase, the smallest root is the molar volume of the liquid phase.

In the case electrolytes are present the calculations are more complicated. In the vapour phase, the salt concentration can be ignored and Cardan's method can still be used. For the liquid phase the electrostatic contribution will affect the molar volume. For the electrolyte equation of state seven roots for the molar volume can be found, including five real roots. Calculating all roots is computationally too intensive. However, it was found that the correct solution could be obtained if Cardan's method was used to calculate the liquid molar volume for the nonelectrolyte part of the equation. This value is then used as the initial value for the iterations and to calculate

the pressure for the full equation including electrostatic contributions. Consequently, a Newton-Raphson iteration can be used:

$$v^{new} = v^{old} - \frac{P^{calc} - P}{(\partial P / \partial v)} \tag{4.25}$$

As can be seen, the derivative of the pressure to the molar volume is required here. Once the molar volumes are calculated, the fugacity coefficients can be found. The fugacity coefficients are derived from the equation of the pressure by:

$$RT \ln \varphi_i = \int_V^\infty \left[\left(\frac{\partial P}{\partial n_i} \right)_{T,V,n_j} - \frac{RT}{V} \right] dV - RT \ln Z \tag{4.26}$$

This equation requires the derivatives for all the contributions of the pressure to the mole numbers. With the fugacity coefficients thus obtained, the vapour-liquid equilibrium is calculated by a flash routine. For constant-temperature-constant-pressure VLE calculations the flash routine used is the flash routine as discussed in section 4.1. For the bubble point or dew point calculations and the vapour pressure depression calculations other subroutines were programmed. For the dew and bubble point calculations the composition of one of the phases is fixed and the temperature or pressure is calculated. For the vapour pressure (depression) calculations only the pressure is adjusted. In that case the calculations are started with an estimation of the vapour pressure and the pressure is updated by:

$$P^{new} = P^{old} \exp\left(\ln f_1^L - \ln f_1^V \right) = P^{old} \cdot \frac{x_1 \varphi_1^L}{\varphi_1^V} \tag{4.27}$$

where L refers to the liquid phase and V refers to the vapour phase

4.5 Structure of the Fortran program

For the modelling a program was written in Fortran 95. The program reads the property data, the experimental data sets and some program options from an input file. The program options include the choice of the model and the optimization function. The program is able to use many data sets with different components and can do LLE, LLLE and VLE calculations and regressions, in addition to the calculation of vapour pressure depressions and mean ionic activity coefficients. The main structure of the program is given in Figure 4.1.

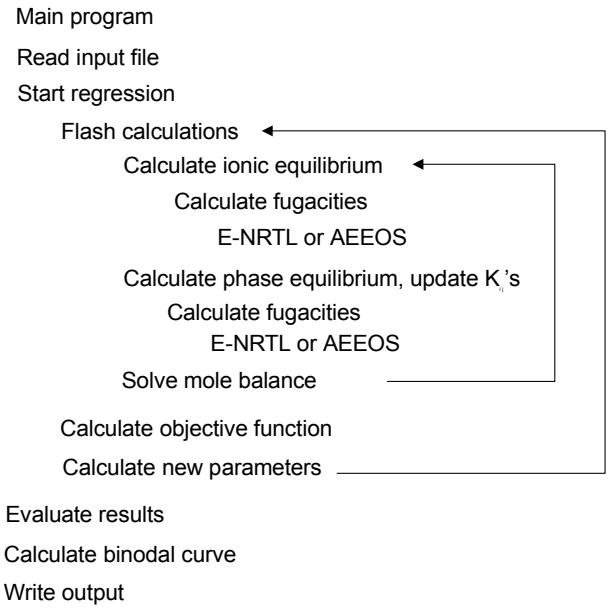

Figure 4.1: Schematic structure of the Fortran program used for the calculations

5. Electrolyte NRTL model

A large part of the modelling described in this thesis is concerned with the application of the electrolyte NRTL model to both the experimental LLE and LLLE data given in chapter 3 as well as to experimental LLE data from literature. In this chapter an overview is given of the original and the extended electrolyte NRTL model and their modifications. A modification of the extended electrolyte NRTL is proposed and used to correlate the experimental data.

5.1 NRTL model

The Non Random Two Liquid (NRTL) equation is based on the concept of local compositions. Local compositions, different from overall compositions, are assumed to account for the short range order and nonrandom molecular orientations that result from differences in molecular size and intermolecular forces. Local mole fractions are given as X_{ji}, which is the local mole fraction of molecule j in the immediate neighbourhood of molecule i. In the NRTL model, the local mole fraction of molecules j in the neighbourhood of molecule i, X_{ji}, relative to the local mole fraction of molecule i in the direct neighbourhood of another molecule i, X_{ii}, is assumed to be given by:

$$\frac{X_{ji}}{X_{ii}} = \frac{x_j}{x_i}\frac{\exp(-g_{ji}/RT)}{\exp(-g_{ii}/RT)} \qquad \textbf{(5.1)}$$

where g_{ji} is a symmetric energy parameter characteristic of the i-j interaction (g_{ij}=g_{ji}).

The original NRTL model was proposed by Renon and Prausnitz (1968). They used the idea of local compositions as suggested by Wilson (1964). They combined Equation (5.1) with the two-liquid theory, which assumes two kinds of cells in a binary mixture: one with molecule 1 in the centre, the other with molecule 2 in the centre. The residual Gibbs energy for a central molecule 1 is then given by the sum of the interaction energies between the central molecule and the surrounding molecules:

$$g^{(1)} = X_{11} \cdot g_{11} + X_{21} \cdot g_{21} \qquad \textbf{(5.2)}$$

The molar excess Gibbs energy is the sum of the changes in the residual Gibbs energy of transferring molecules i from a pure liquid to the centre of a cell and is written as:

$$G^E = x_1 X_{21}(g_{21} - g_{11}) + x_2 X_{12}(g_{12} - g_{22}) \quad \textbf{(5.3)}$$

Combining equation (5.1)- (5.3) and realizing that the local mole fractions must sum to unity, gives the Non Random, Two-Liquid (NRTL) equation. Although the NRTL model shows a large similarity to the Wilson equations, it can, unlike the Wilson equation, predict liquid-liquid demixing. The NRTL equation for the excess Gibbs energy can easily be generalized to a multi-component mixture to give the following expression:

$$\frac{G^E}{RT} = \sum_{i=1}^{n} x_i \frac{\sum_{j=1}^{n} \tau_{ji} G_{ji} x_j}{\sum_{j=1}^{n} G_{ji} x_j} \quad \textbf{(5.4)}$$

where:

$$\tau_{ji} = \left(g_{ji} - g_{ii}\right)/RT \quad \textbf{(5.5)}$$

$$G_{ji} = \exp\left(-\alpha_{ji}\tau_{ji}\right) \quad \textbf{(5.6)}$$

The nonrandomness factor α was introduced in Equation (5.1) by Renon and Prausnitz (1968). This α is an empirical constant related to the nonrandomness in the mixture and accounts for the fact that the different molecules are not fully statistically distributed through the liquid. If $\alpha = 0$ the mixture is completely random and the Margules equation is obtained. The NRTL model contains three adjustable parameters for each binary system, which can be found by data regression: two binary interaction parameters τ_{ij} and τ_{ji} (which are equal to the differences of the dimensionless interaction energies) and the nonrandomness factor $\alpha_{ij}=\alpha_{ji}$.

Although the nonrandomness factor α_{ij} was vaguely related by Renon and Prausnitz (1968) to the reciprocal of the coordination number (the number of molecules i just touching the central molecule j), the range of numerical values found in literature shows that it may be regarded as an empirical constant. In literature, values from 0.01 to 100 can be found from correlations of experimental data. Walas (1985) examined the parameters published for a large number of VLE systems and found for α a large

variation with an average of 0.3 for nonaqueous mixtures and 0.4 for aqueous-organic systems. For liquid-liquid equilibria of molecular components the nonrandomness factor is often fixed at 0.20. The parameters (g_{ji}-g_{ii}) and (g_{ij}-g_{jj}) appear to be linear functions of temperature (Prausnitz et al., 1999).

The advantages of the Non Random Two Liquid theory are its algebraic simplicity, the applicability of the model to mixtures that give liquid phase splitting, the applicability to multicomponent systems using only binary parameters and the fact that no specific volume or surface area data are required like in the UNIQUAC model. The main disadvantage is the large number of adjustable parameters for multicomponent mixtures (although the parameters can often be obtained from binary systems.) Also, in the case of liquid-liquid equilibria the NRTL overpredicts the area under the binodal curve compared with experiments (Walas, 1985).

5.2 Electrolyte NRTL model (Chen)

The NRTL model has been extended to electrolyte solutions, first by Cruz and Renon (1978) and later by Chen et al. (1982, 1986). The two models are based on different assumptions of the structure of electrolyte solutions. In the model of Cruz and Renon (1978), the local composition of cations and anions in a cell with a cation in the centre, as well as the local composition of anions and cations around an anion is assumed to be zero. The ions are always completely surrounded by solvent molecules, even at higher salt concentrations. The excess Gibbs energy is the sum of two terms, one accounting for long range forces between ions (based on Debye-Hückel and Born theory) and a term for short range forces between all species (derived from the NRTL model).

The short range contribution in the model of Chen et al. (1982) is based on two assumptions, of which the first is the like-ion repulsion assumption. This means that the ions in the centre of a cell are never surrounded by ions of the same sign. In addition, Chen uses the local electroneutrality assumption: around a central solvent molecule, the net local ionic charge is zero. Three types of cells are assumed. Besides cells with a solvent molecule in the centre, also cells with a cation c or an anion a in the centre are considered. Unlike in the model of Cruz and Renon, ions can be surrounded partially by oppositely charged ions.

The electrolyte NRTL local composition contribution results in the following equation for a multi-solvent system with one salt (Aspen Technology, 1998):

$$\frac{G^E}{RT} = \sum_m X_m \frac{\sum_j X_j G_{jm} \tau_{jm}}{\sum_k X_k G_{km}} + X_c \frac{\sum_j X_j G_{jc} \tau_{jc}}{\sum_k X_k G_{kc}} + X_a \frac{\sum_j X_j G_{ja} \tau_{ja}}{\sum_k X_k G_{ka}} - x_c \ln\left(\gamma_c^\infty\right) - x_a \ln\left(\gamma_a^\infty\right)$$

where:

(5.7)

$$X_j = C_j x_j \qquad (C_j = Z_j \; for \; ions, C_j = 1 \; for \; solvents)$$
$$\alpha_{jc} = \alpha_{ja} = \alpha_{cj} = \alpha_{aj} = \alpha_{j,ca}$$
$$\tau_{jc} = \tau_{ja} = \tau_{j,ca}$$
$$\tau_{cj} = \tau_{aj} = \tau_{ca,j}$$

The last two terms in the expression for the excess Gibbs energy are added, because an infinite dilution of completely dissociated electrolytes in water is taken as the reference state. This was done to make the symmetrically normalized $G^{E,lc}$ compatible with the unsymmetric reference condition (normalized to mole fractions of unity for solvent and zero for electrolytes) of the electrostatic contribution. In the Chen model, the long range forces between the ions are accounted for by a Pitzer-Debye-Hückel contribution (Pitzer, 1980):

$$\frac{G^{E,PDH}}{RT} = -\left(\sum_n^{nc} x_n\right) \frac{4 A_x I_x}{\rho} \ln(1 + \rho \sqrt{I_x}) \qquad \textbf{(5.8)}$$

with:

$$I_x = \frac{1}{2} \sum_i^{ion} x_i z_i^2 \qquad \textbf{(5.9)}$$

$$A_x = \frac{1}{3} \sqrt{\frac{1000}{M_s}} \sqrt{2\pi N_A d} \left(\frac{e^2}{\varepsilon k T}\right)^{3/2} \qquad \textbf{(5.10)}$$

where ρ is the closest approach parameter. The Pitzer-Debye-Hückel model is a primitive model. Therefore, the reference state of the electrostatic contribution is the infinite dilution in the dielectric continuum. If more than one solvent is present in the

mixture, the reference state becomes composition dependent. In case of liquid-liquid equilibria of mixed solvents, two phases with a different solvent composition are at equilibrium. To obtain the same reference state for the electrostatic contribution on both sides of the equilibrium condition, an expression is required that accounts for the net electric work to transfer the ions from the dielectric medium formed by one phase to the dielectric medium formed by the other phase. In practice, infinite dilution in water is chosen as the reference state for both phases.

To achieve equal reference states, Austgen et al. (1989) added a Born expression. The Born model is in fact a solvation model and gives the solvation energy of an ion in a dielectric medium, relative to vacuum. Born assumed that the enthalpy of hydration of ions is dominating the electrostatic energy, which is mainly determined by the dielectric constant of the surrounding medium and the size and charge of the ion (Grunwald, 1997). By taking the difference between the solvation energies of water and the mixed solvent, an equation is obtained that gives the desired energy of transfer of ions from the mixed solvent to pure water. The Born contribution is given by:

$$\frac{G^{E,Born}}{RT} = \frac{e^2}{2kT}\left(\frac{1}{\varepsilon} - \frac{1}{\varepsilon_w}\right)\sum_i^{ion} \frac{x_i z_i^2}{r_i} \qquad \textbf{(5.11)}$$

where r_i is the Born radius. In some cases, the problem of the different reference states in mixed solvents is avoided. Mock et al. (1986) found the long range contribution to have only little effect on phase equilibrium calculations and dropped the Pitzer-Debye-Hückel term. They applied the NRTL local composition contribution to VLE data and a limited number of LLE data of mixed solvent electrolyte solutions with reasonable success.

There have been a number of attempts to improve the performance of the electrolyte NRTL model (Jaretun and Aly, 2000; Haghtalab and Vera, 1988; Liu et al., 1989a). Some extensions of the electrolyte NRTL model were published by Chen and co-workers from Aspen Technology. The extended electrolyte NRTL model of Liu and Watanasiri (1996) is discussed in the next section. Abovsky et al.(1998) introduced salt concentration dependency of the water + salt interaction parameters. Taking water as the "key solvent" the interaction parameters were made a function of the water concentration and thus indirectly of the salt concentration. Abovsky applied the model successfully to mean ionic activity coefficients at high salt concentrations (up to 25 mol/kg). Chen et al. (1999) extended the electrolyte NRTL model to include hydration of the ions and partial dissociation. To describe hydration, they derived an expression

from the hydration theory of Robinson and Stokes (1959). The model was applied to mean ionic activity coefficients of water + salt systems.

The electrolyte NRTL is used widely, not in the least because of its presence in Aspen PLUS. It is one of the few models that can be applied to LLE of mixed-solvent electrolyte solutions. A disadvantage is the large number of adjustable parameters. Another disadvantage of the electrolyte NRTL is that it is not so suitable for multi-salt solutions. It can be seen in Equation (5.7) that the parameters for the electrolyte are defined for the ion-pair rather than for the ions. This reduces the number of binary interaction parameters required in the case of only one salt. However, to apply the model to multi-electrolyte solutions, many more parameters are required. To some extent this can be solved by making the parameters ion-specific instead of salt-specific as shown by Liu et al. (1989b).

5.3 Extended electrolyte NRTL model (Liu and Watanasiri)

The extended electrolyte NRTL model for the excess Gibbs energy G^E is built up from four contributions: a local composition NRTL contribution (NRTL), a Pitzer-Debye-Hückel contribution (PDH), a Born contribution and a Brønsted-Guggenheim contribution (BG).

$$G^E = G^{E,NRTL} + G^{E,PDH} + G^{E,Born} + G^{E,BG} \tag{5.12}$$

The Brønsted-Guggenheim contribution was added to the electrolyte NRTL model by Liu and Watanasiri (1996), especially for the modelling of liquid-liquid equilibria, to account for inadequacies in the Born term and the Pitzer-Debye-Hückel term:

$$\frac{G^E_{BG}}{RT} = \frac{100}{T} \sum_m x_m M_m \sum_c \sum_a \beta_{ca} x_c x_a \tag{5.13}$$

where m refers to molecular components. Unfortunately, they seem to have made a mistake in converting the equation (originally expressed in molalities) to the expression expressed in mole fractions. In 1983, Christensen et al. already added the Brønsted-Guggenheim contribution to the UNIQUAC model, for one salt written as:

$$\frac{G^{E,BG}}{RT} = \frac{1000}{\sum_m x_m M_m} \cdot \frac{\beta_{ca}}{T} x_a x_c \tag{5.14}$$

where β_{ca} is the Brønsted-Guggenheim interaction parameter. Christensen added the Brønsted-Guggenheim contribution, because the (original) UNIQUAC model and the Debye-Hückel model alone were incapable of giving a satisfactory fit of mean ionic activity coefficients. The Brønsted-Guggenheim equation was proposed by Guggenheim (1935), based on the theory of specific interactions of Brønsted. This empirical equation for aqueous electrolyte solutions should take better into account specific differences between ions of the same valence type than the Debye-Hückel theory.

5.4 Shortcomings of the electrolyte NRTL models

The electrolyte NRTL model of Chen (Aspen Technology, 1998) and the extended electrolyte NRTL model of Liu and Watanasiri (1998) were both used to represent the experimental data from Chapter 3 and a number of experimental data sets from literature. In both cases, the results appeared to be unsatisfactory. (In this section, only some results will be highlighted. A more extensive discussion of the modelling procedure and results for the Chen model will be given later in this chapter). Liu and Watanasiri (1996) applied their **extended electrolyte NRTL model** to only four data sets of water + alcohol + NaCl, where the alcohol was 1-propanol, 2-propanol, 1-butanol and 2-butanol. Using the same data sets, attempts were made in this work to reproduce their results. These attempts were unsuccessful:

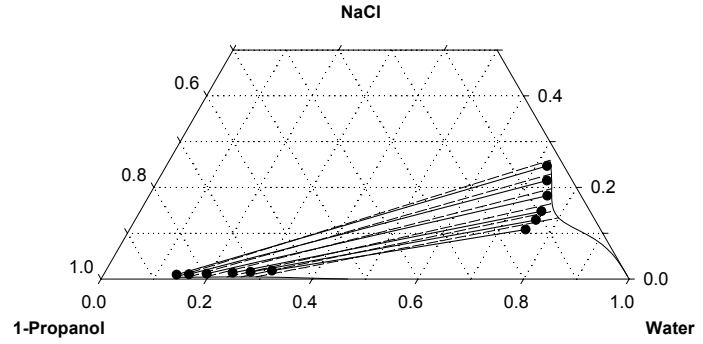

Figure 5.1: The curve in the figure shows the extrapolation of the results of Liu and Watanasiri (1996) to lower salt concentrations for LLE in the system water + 1-propanol + NaCl (De Santis, 1976) at 298.1 K. Markers and dashed lines represent experimental LLE, solid lines have been calculated.

The modelling with the extended electrolyte NRTL model was not extended to other data sets. Figure 5.1 gives the results for LLE in the system water + 2-propanol + NaCl at 298.1 K (De Santis, 1976) in weight fractions and shows the calculated binodal line. The results were calculated using the binary interaction parameters given by Liu and Watanasiri (1996). When the binodal line is calculated, it was found that it does not even approach a plait point. Instead, the model seems to predict demixing of the binary system water + 2-propanol. However, with the given set of NRTL parameters, no binary demixing is found for water and 2-propanol.

A second deficiency of the model of Liu and Watanasiri is that it was found to give mean ionic activity coefficients that deviate largely from the experimental values for any value of the Brønsted-Guggenheim parameter not equal to zero. This implies that it is impossible to simultaneously model liquid-liquid equilibria and mean ionic activity coefficients with the Brønsted-Guggenheim contribution as used by Liu and Watanasiri. This is also valid for Equation (5.14) as used by Christensen et al. (1983).

When the original **electrolyte NRTL model** of Chen and Evans (1986) is applied to the same system, water + 2-propanol + NaCl, the "opening" of the binodal curve is not found. However, calculations in the neighbourhood of the plait point failed. Figure 5.2 visualizes the results for the model of Chen for the system water + 2-propanol + NaCl. The adjustable parameters (Appendix III, Table III.1) were obtained from regression with several data sets of water + alcohol + salt systems.

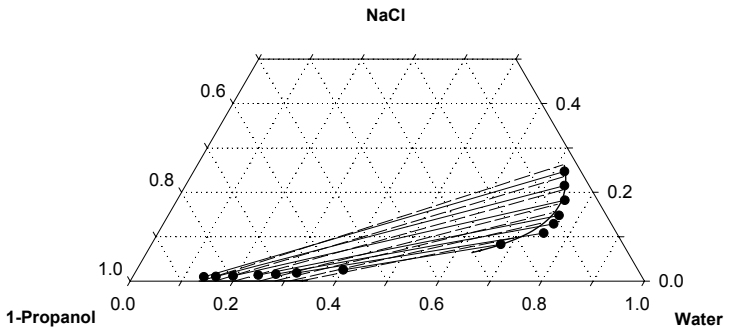

Figure 5.2: Correlation of LLE in the system water + 1-propanol + NaCl at 298.1 K (De Santis, 1976) using the electrolyte NRTL model of Chen and Evans (1986). Markers and dashed lines are experimental LLE, solid lines have been calculated. Units are weight fractions.

The representation in Figure 5.2 illustrates two problems with the original electrolyte NRTL model of Chen. Firstly, with the Chen model it is not possible to carry out flash calculations in the neighbourhood of the plait point. At no concentration, the concentrations of the two phases at the calculated equilibrium will approach each other. Secondly, the Chen model has difficulties in representing the salt concentration in the organic phase. The salt concentration in the organic phase is always too low. This is not only valid for the system water + 1-propanol + NaCl, but as well for other ternary systems studied. In Figure 5.3, a similar diagram is given for the system water + caprolactam + ammonium sulfate at 293.1 K.

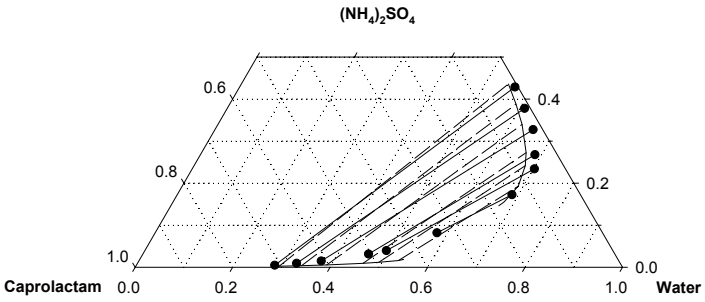

Figure 5.3: Correlation of LLE in the system water + caprolactam + ammonium sulfate at 293.1 K by the electrolyte NRTL of Chen and Evans (1986). Markers and dashed lines are experimental data, solid lines have been calculated.

The modification of Abovsky et al. (1998) with concentration dependent interaction parameters does not give a significant improvement, when it is applied to systems of water + alcohol + NaCl at 298.1 K. To test this modification, the (water) concentration dependency was used for the water + NaCl NRTL binary interaction parameters. The new model performed only slightly better for LLE. For the mean ionic activity coefficients the improvement was larger. The problems observed for the original electrolyte NRTL model, are not solved by this modification.

It has been suggested that the salt concentration in the organic phase is too low, because full dissociation is assumed. This appeared not to be true. This issue will be addressed in section 5.8. Assuming partial dissociation in the organic phase, does not improve the representation of the experimental data for the organic phase, despite the fact that this assumption increases the number of adjustable parameters.

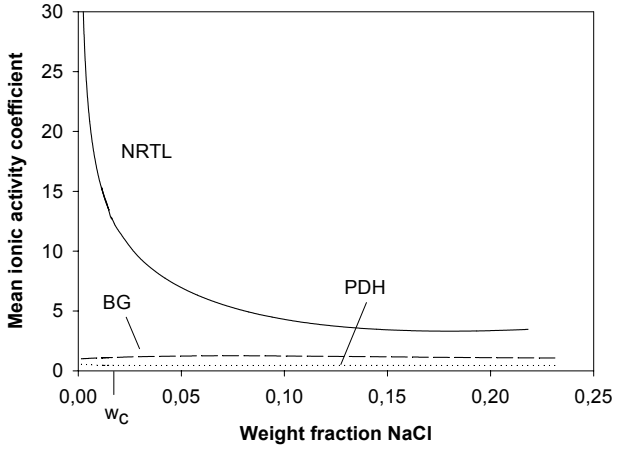

Figure 5.4: Mean ionic activity coefficients at the compositions along the binodal curve for the system water + 1-propanol + NaCl at 298.1 K (see Figure 5.2), calculated after regressions of the LLE without the Born contribution. w_c is the estimated location of the plait point.

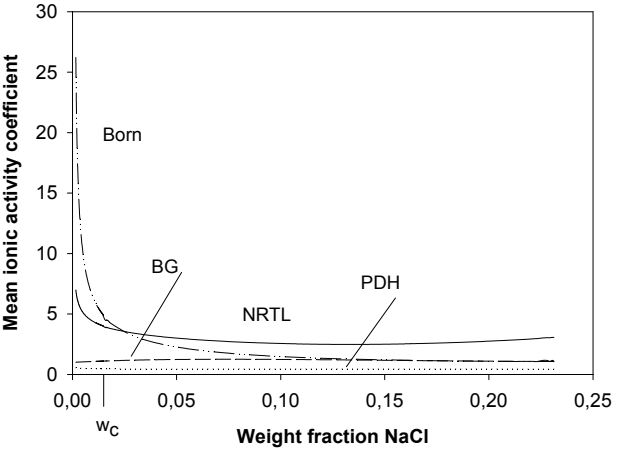

Figure 5.5: Mean ionic activity coefficients at the compositions along the binodal curve for the system water + 1-propanol + NaCl at 298.1 K, calculated after regressions of the LLE with the Born contribution. w_c is the estimated location of the plait point.

To improve the description of the experimental LLE data for mixed solvent electrolyte solutions two modifications were proposed, that are discussed in the following section. In literature, also some discussion is going on with respect to the Born contribution. For example, Anderko et al. (2002) discuss this issue. They found that the Born contribution did not contribute to the accuracy of their model. Anderko could reproduce Gibbs energies of transfer of ions without applying the Born term. According to Zerres and Prausnitz (1994), the Born contribution gives poor results when compared with experiments and sometimes the Born equation gives a partial Gibbs energy that is qualitatively incorrect with the wrong sign. They stated that a contribution to change the reference state was not necessary and used different reference states for the long-range and short-range contributions. This was later disproved by Zuo et al. (2000b). These authors applied a Born contribution in their electrolyte equation of state.

In this study some attention was paid to this matter. Figure 5.4 and 5.5 show some results of fitting liquid-liquid equilibria for the system water + 1-propanol + NaCl at 298.1 K. The figures give the individual contributions to the mean ionic activity coefficients for the points on the binodal curve. In the results of Figure 5.4 the Born contribution was not included; in Figure 5.5 it was used. The figures make clear that changes in the adjustable parameters of the NRTL contribution simply compensate for shortcomings in other contributions. If the Born term is missing, different adjustable parameters will be found, that lead to a larger NRTL contribution. In the model presented in the next section, a Born contribution was used. Even though the Born equation may not be very accurate, it is believed it is more physically correct to include this contribution and to have the same reference state for the short-range and long-range contribution.

5.5 Modifications of the Electrolyte NRTL model

The extended Debye-Hückel equation for the excess Gibbs energy, proposed by Pitzer (1980), generalised to mixed solvents and used in the electrolyte NRTL model to account for the long-range contribution, was given in Equation (5.8). The activity coefficients can be derived from this equation and have been given in literature (Chen and Evans, 1986; Aspen Technology, 1998). In this work a different equation was derived for the solvent activity coefficient, assuming that the Pitzer-Debye-Hückel model is indeed an excess Gibbs energy model and not an excess Helmholtz energy

model. A more extensive discussion on this assumption will follow later. The new equations for the solvent activity coefficients include an additional contribution, due to the solvent composition dependence of the solution properties. This contribution is usually ignored in electrolyte thermodynamics, but must be included in a proper derivation of the solvent activity coefficient if a solvent composition dependent dielectric constant is used in the model. If the model is used to describe liquid-liquid equilibria of water + organic solvent + salt systems, the difference in the dielectric constants of the solvents will be large and a physically correct description will require the use of a solvent composition dependent dielectric constant. The activity coefficients for the ionic species remain unchanged. The activity coefficients for the ions and solvents are given respectively by:

$$\ln \gamma_i^{PDH} = A_x \left[\frac{2I_x^{3/2} - z_i^2 \sqrt{I_x}}{1 + \rho \sqrt{I_x}} - \frac{2 z_i^2}{\rho} \ln\left(1 + \rho \sqrt{I_x}\right) \right] \tag{5.15}$$

$$\ln \gamma_j^{PDH} = \frac{2 A_x I_x^{3/2}}{1 + \rho \sqrt{I_x}} + \frac{4 n I_x A_x}{\rho} \ln(1 + \rho \sqrt{I_x}) \cdot \left[\frac{1}{2M_s} \frac{M_j - M_s}{\sum_k n_k} - \frac{1}{2d} \frac{\partial d}{\partial n_j} + \frac{3}{2\varepsilon} \frac{\partial \varepsilon}{\partial n_j} \right] \tag{5.16}$$

where i refers to ions and j and k refer to any solvent. I_x and A_x have been defined in Equation (5.9) and (5.10). For the Born contribution to the solvent activity coefficient, the same applies as for the Pitzer-Debye-Hückel contribution: if the solvent composition dependence of the dielectric constant is correctly taken into account in the derivation, a contribution will appear in the activity coefficient of the solvent molecules from the derivatives of the dielectric constant to the solvent composition:

$$\ln \gamma_j^{Born} = -\frac{e^2}{2kT} \frac{1}{\varepsilon^2} \frac{\partial \varepsilon}{\partial n_j} \sum \frac{n_i z_i^2}{r_i} \tag{5.17}$$

For the ions, the equation is unchanged:

$$\ln \gamma_i^{Born} = \frac{e^2}{2kT} \left(\frac{1}{\varepsilon} - \frac{1}{\varepsilon_w} \right) \frac{z_i^2}{r_i} \tag{5.18}$$

where ε_w is the dielectric constant of water. If the dielectric constant is made salt concentration dependent, this produces an extra term in Equation (5.18). In Figure 5.6 the influence of the additional terms on the activity coefficients of the solvents is

shown for the system water + 1-propanol + NaCl at 298.1 K for an equimolar mixture of water and 1-propanol.

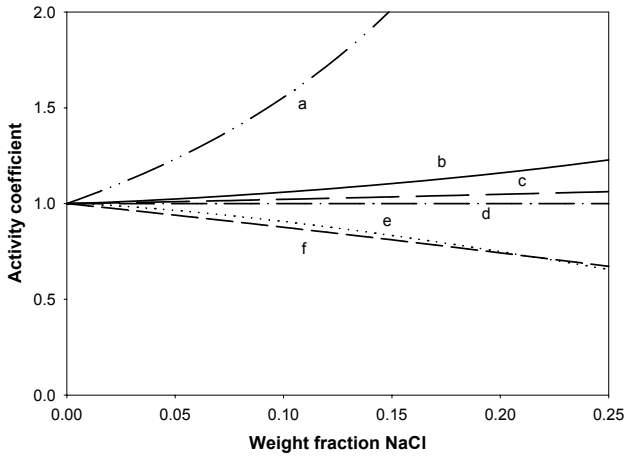

Figure 5.6: Pitzer-Debye-Hückel (PDH) and Born contributions to the solvent activity coefficients in a mixture with equal mass fractions of water (1) and 1-propanol (2) at 298.1K, with a) γ_2^{Born} (modified), b) γ_1^{PDH} (modified), c) $\gamma_1^{PDH} = \gamma_2^{PDH}$ (original), d) $\gamma_1^{Born} = \gamma_2^{Born}$ (original) = 1, e) γ_2^{PDH} (modified), f) γ_1^{Born} (modified)

Figure 5.6 shows that in particular the new Born contribution (due to the solvent composition dependency of the dielectric constant) is of importance. To some extent it is compensated by the larger (water) or smaller (1-propanol) Pitzer-Debye-Hückel solvent activity coefficient.

In this work, initially the Brønsted-Guggenheim contribution as used by Christensen et al. (1983) was added. As discussed, it is not possible to simultaneously model mean ionic activity coefficients and LLE, when this contribution is applied. Since it was found that the results for systems with a ternary critical point are improved using a different definition of this term, the contribution was changed and a solvent composition dependent Brønsted-Guggenheim interaction parameter is proposed, using a Margules-like equation:

$$\beta_{ca} = \beta_{jk} x_j x_k \qquad \textbf{(5.19)}$$

where j and k refer to solvents and β is not salt specific.

The generalised equation for the Brønsted-Guggenheim term in the excess Gibbs energy is now:

$$\frac{G^{E,BG}}{RT} = \frac{1000}{\sum_k x_k M_k} \frac{\sum_j \sum_{k>j} \beta_{jk} x_j x_k}{T} x_a x_c \tag{5.20}$$

The activity coefficient for solvent, cation and anion is then given by:

$$\ln \gamma_j^{BG} = -\left(\frac{M_j}{\sum_k^{ns} x_k M_k} + 2 \right) \frac{1000}{\sum_k^{ns} x_k M_k} \frac{\beta_{ca}}{T} x_c x_a + \frac{1000}{T \sum_k^{ns} x_k M_k} x_c x_a \sum_k^{ns} x_k \left(\beta_{kj} + \beta_{jk} \right) \tag{5.21}$$

$$\ln \gamma_c^{BG} = \frac{1000}{\sum_j^{ns} x_j M_j} \frac{\beta_{ca}}{T} \left(x_a - 2 \cdot x_c x_a \right) \tag{5.22}$$

$$\ln \gamma_a^{BG} = \frac{1000}{\sum_j^{ns} x_j M_j} \frac{\beta_{ca}}{T} \left(x_c - 2 \cdot x_a x_c \right) \tag{5.23}$$

The contributions for the anion and the cation go to zero for pure solvents and do not represent any problem for the modelling of mean ionic activity coefficients and for low salt concentrations approaching the salt-free system, like the original contribution does. The new model was applied to a variety of electrolyte systems from literature (section 5.6) and to the experimental data in Chapter 3 (section 5.7). The model is summarized in Appendix IV. In the next sections, its results are compared with those obtained with the electrolyte NRTL model of Chen (1986).

5.6 Modelling of water + alcohol + salt systems

5.6.1 Procedure

To test the model and to compare the results with models in literature, the model was applied first to a number of data sets from literature, mainly water + alcohol + salt systems. Besides LLE data, mean ionic activity coefficient data were used in the regressions. These experimental mean ionic activity coefficients were obtained from

Robinson and Stokes (1959) and converted from molal to molar activity coefficients by (Robinson and Stokes, 1959):

$$\gamma_{\pm}^{molar} = \gamma_{\pm}^{molal} \cdot \left(1 + 0.001 \cdot \nu \cdot M_{solvent} \cdot m_{salt}\right) \quad \textbf{(5.24)}$$

where ν is the number of ions formed by the dissociation of one salt molecule. The Born radii in the model were taken from Rashin and Honig (1985). The Pitzer-Debye-Hückel closest approach parameter was fixed at 14.9, as used by Chen et al. (1982). The solution dielectric constant is calculated from the pure solvent dielectric constants using a mass fraction based mixing rule:

$$\varepsilon = \sum_j w_j' \varepsilon_j \quad \textbf{(5.25)}$$

where w_j' is the salt free mass fraction of solvent j. The pure solvent dielectric constants were obtained from Lide (1995). The solution density is calculated from the pure solvent densities assuming ideal mixing:

$$d = \frac{\sum_j x_j M_j}{\sum_k x_k M_k / d_k} \quad \textbf{(5.26)}$$

The pure solvent densities were taken from Perry (1997) and the molecular weights were used as given by Reid et al. (1987). All nonrandomness factors in the NRTL local composition model were fixed and not adjusted during the regressions. Best results were obtained when the nonrandomness factors were set at values of 0.10 (water + salt), 0.20 (solvent or water + solvent) or 0.30 (solvent + salt). The accuracy of the results is represented by average deviations, as defined by Sørensen and Arlt (1980):

$$\Delta x = \sqrt{\frac{\sum_k \sum_p \sum_i \left(x_{kpi}^{\exp} - x_{kpi}^{calc}\right)^2}{nc \times np \times nd}} \quad \textbf{(5.27)}$$

All tie-lines were given equal weight in the regressions. Although this would have largely improved the results, tie-lines near the plait point were not excluded from the regressions or given less weight to derive a more consistent and generally applicable set of parameters. If the model was found to give a good representation of the experimental data without a Brønsted-Guggenheim contribution, this parameter was fixed at zero. This was in general the case for the systems without a ternary critical

point and which showed demixing in the binary water + organic solvent subsystem. For the systems where the two solvents are fully miscible, in general a plait point exists and these systems are more difficult to model. Examples of such systems are the systems water + 1-propanol/2-propanol + salt and the system water + caprolactam + ammonium sulfate.

5.6.2 Results

In Table 5.1 results are tabulated for correlations of LLE for a number of water + alcohol + salt systems. The results were obtained by simultaneous regressions of all the data sets, including some data sets with mean ionic activity coefficients for water + salt systems. These water + salt systems are subsystems of the ternary systems in Table 5.1. The average deviations of the calculated values from the experimental mean ionic activity coefficients are given in Table 5.2. In both Table 5.1 and 5.2, the performance of the new model is compared to the results obtained with the model of Chen et al. (1986). By applying the model to a large data set of equilibrium data containing the same binary subsystems, it is believed that a more consistent set of interaction parameters is obtained, which can easier be extended to other electrolyte systems. This was indeed observed during the regressions, where the time needed for the regressions to extend the set of parameters to another salt was relatively short. In general, when moving to another salt, only the solvent/water + salt parameters were adjusted, once a set of parameters was obtained for a certain salt. A number of the data sets given in Table 5.1 has been used before in parameter regressions. The results and the parameters obtained from these regressions have been published before (Van Bochove et al., 1999) and are given in Appendix II.

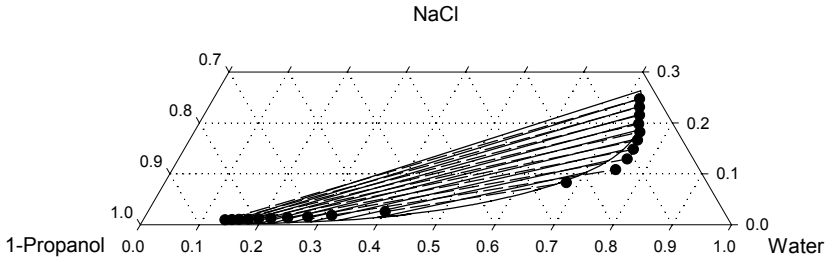

Figure 5.7: LLE for water + 1-propanol + NaCl at 298.1 K. Markers and dashed lines are experimental data (De Santis, 1976). Solid lines represent calculations with the modified extended electrolyte NRTL.

Table 5.1: Average deviations in mole percents (Δx) and mass percents (Δw) of the representation of liquid-liquid equilibria of some ternary mixed-solvent electrolyte systems at 298 K.

	Presented model		Chen's model[c]		Source[a]
	Δx (%)	Δw (%)	Δx (%)	Δw (%)	
Water + 1-propanol + NaCl	0.7	1.3	1.5	2.5	1
	1.2	1.8	1.6	2.3	2
Water + 2-propanol + NaCl	0.7	0.8	1.4	2.2	1
	0.8	1.4	2.8	4.1	2
Water + 1-butanol + NaCl	2.7	1.7	2.7	1.8	1
	2.4	1.5	2.5	1.7	3
Water + 2-butanol + NaCl	4.9	3.3	5.1	3.4	1
Water + 1-pentanol + NaCl	1.3	0.6	1.3	0.6	4
Water + 2-butanone + NaCl	2.1	0.9	2.1	0.9	3
Water + 1-propanol + NaBr	1.4	1.6	>6[b]	>8[b]	2
Water + 1-butanol + KBr	1.7	1.4	1.7	1.5	3
Water + butanone + KBr	1.9	0.8	1.9	0.9	3
Water + 1-propanol + KCl	0.9	1.5	2.2	3.0	2
Water + 1-butanol + KCl	2.2	1.9	2.2	1.5	3
Water + 2-butanone + KCl	2.1	1.0	2.1	1.0	3
Water + 1-pentanol + KCl	0.7	0.4	0.7	0.4	5
Water + 1-propanol + KF	1.0	1.1	0.9	1.3	6
Water + 2-propanol + KF	0.7	0.7	5.3	3.8	6
Water + 1-propanol +1-butanol	1.8	3.0	2.8	3.7	7
Water + 1-propanol+ 1-pentanol	1.5	2.2	1.5	2.4	8
Overall:	1.6	1.4	2.4	2.4	

[a] Source of data:1 = De Santis et al. (1976); 2 = Chou et al. (1998); 3 = Li et al. (1995); 4 = Gomis et al. (1999); 5 = Boluda et al. (2001); 6 = Wang et al. (2002); 7 = Gomis et al. (1998); 8 = Fernandez et al. (2000;)

[b] For this data set no satisfactory solution could be found

[c] Chen et al. (1986) and Aspen Technology (1999)

The binary interaction parameters for the systems in Table 5.1 are given in Appendix III, Table III.1. The temperature dependence of the binary interaction parameters obeys the equation below:

$$\tau_{ij} = \frac{A_{ij}}{T} \qquad \textbf{(5.28)}$$

In Figure 5.7 to 5.10, some of the results from Table 5.1 have been visualised. From the tables and the figures, it can be seen that the modified extended electrolyte NRTL model as presented in the previous section can handle LLE for a wide variety of

electrolyte solutions. Compared to the model of Chen et al. (1986), the model is doing better in representing the salt concentration in the organic phase and with this model it is possible to perform calculations in the vicinity of a ternary plait point. For systems not having such a plait point the difference in the performance of the model of Chen et al. (1986) and the model presented here is small. The difference for the systems, that have a plait point is larger. This is important, because the system water + caprolactam + ammonium sulfate is also having such a ternary plait point. In the next section, the model is applied to electrolyte solutions containing caprolactam.

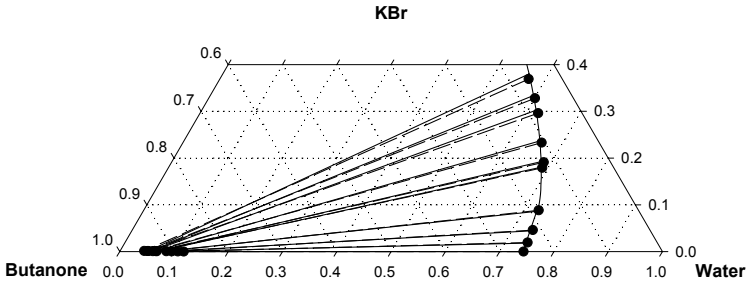

Figure 5.8: LLE for water + butanone + KBr at 298.1 K. Markers and dashed lines are experimental data (Li et al., 1995). Solid lines represent calculations with the modified extended electrolyte NRTL.

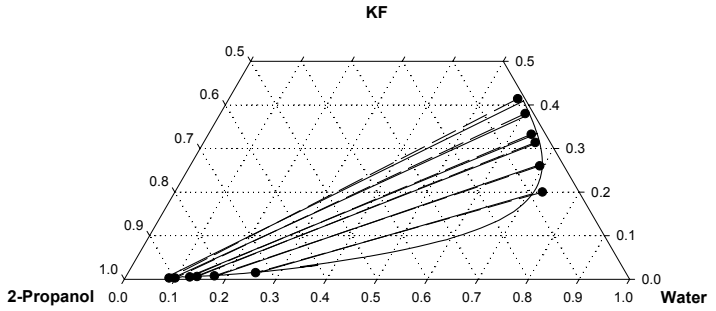

Figure 5.9: LLE for water + 2-propanol + KF at 298.1 K. Markers and dashed lines are experimental data (Wang et al., 2002). Solid lines represent calculations with the modified extended electrolyte NRTL.

Table 5.2: Relative deviations of calculated mean ionic activity coefficients at 298 K of some water + salt systems from experimental data by Robinson and Stokes (1959). Results were obtained by simultaneous regressions with the LLE presented in Table 5.1.

	Present model $\Delta\gamma$ (%)	Chen's model[a] $\Delta\gamma$ (%)
Water + NaCl	1.3	1.1
Water + NaBr	0.4	
Water + KBr	0.3	0.2
Water + KCl	0.2	0.3
Water + KF	0.6	1.0

[a] Chen et al. (1986) and Aspen Technology (1999)

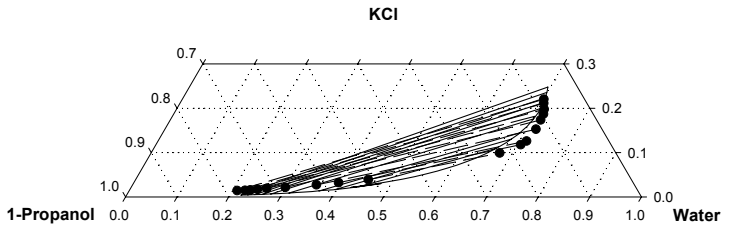

Figure 5.10: LLE for water + 1-propanol + KBr at 298.1 K. Markers and dashed lines are experimental data (Chou et al., 1998). Solid lines represent calculations with the modified extended electrolyte NRTL.

5.7 Modelling of systems containing caprolactam

5.7.1 Introduction

The modelling of the systems with water + caprolactam + solvent + ammonium sulfate is more labourious. In addition to LLE data, also LLLE data were measured, which complicates the modelling. In literature, as far as known no other work has been published on parameter regressions with many data sets including both LLE and LLLE data. In fact, the amount of literature on the modelling of LLLE using an excess Gibbs energy model is quite limited: Negahban et al. (1986, 1988) used the UNIQUAC model to correlate LLLE at 298.1 K in water + n-octane + 1-propanol + sodium chloride and water + t-butanol + tetradecane + sodium chloride systems. Garcia-Sanchez et al. (1996) and Stateva et al. (2000) also used the UNIQUAC model

to model LLLE of ternary and quaternary mixtures. Heidemann and Abdel-Ghani (2001) used the NRTL model to model LLLE in water + phenol + n-hexane.

For the caprolactam containing systems, a large number of data sets containing the same binary subsystems is available. The simultaneous modelling of all these data sets adds to the consistency of the binary interaction parameters. Since a large part of the data sets became available only during the project, the modelling was gradually extended to more data sets. At first only LLE data were available. In a later stage of the project also LLLE data were included. The binary interaction parameters had to be adjusted after the addition of every new data set to the collection of data sets used in the regression. This involves that results were obtained and published for several different combinations of experimental data sets.

The physical properties of the different components and the solution properties were obtained and calculated as for the water + alcohol + salt systems. Caprolactam was treated as a solvent. The parameters for the dielectric constant and the density were derived from water + caprolactam mixture data and are given in Appendix I.

5.7.2 Liquid-liquid equilibria

Table 5.3 compares the electrolyte NRTL model of Chen et al. (1986) with the model presented here for different systems containing caprolactam. The parameters belonging to the results presented in Table 5.3 are given in Appendix III, Table III.2. Since attempts to model LLLE using the model of Chen were not successful, the results in this table are **based on regressions of only LLE data** for both models. As will be shown later, without the introduction of a better temperature dependency of the interaction parameters τ_{ij} the inclusion of LLLE in the regressions will have a negative effect on the performance of both models for the LLE. The temperature dependence for the NRTL interaction parameters remained unchanged for the results in Table 5.3 and is given by Equation (5.28).

Table 5.3 illustrates the better performance for electrolyte solutions of the model presented here compared to the original electrolyte NRTL model (Chen et al., 1986). For some data sets the difference between the two models is insignificant. Analysis of these data sets showed that in all these cases, the experiments were carried out far from the plait point of the two-liquid phase region. The table gives the sum of squares

of the weight fractions and mole fractions for all of the data sets used and this shows again the better performance of the modified extended electrolyte NRTL. The sum of squares is given by:

$$SSQ = \sum_{k}^{nd} \sum_{p}^{np} \sum_{i}^{nc} \left(x_{kpi}^{calc} - x_{kpi}^{\exp} \right)^2 \qquad \textbf{(5.29)}$$

Table 5.3 and Figure 5.11 illustrate that simultaneously with the salt containing systems, it is possible to obtain a good description for the salt-free systems, using the same binary interaction parameters as for the same binary subsystems. This corresponds to what was found for the water + alcohol + salt systems.

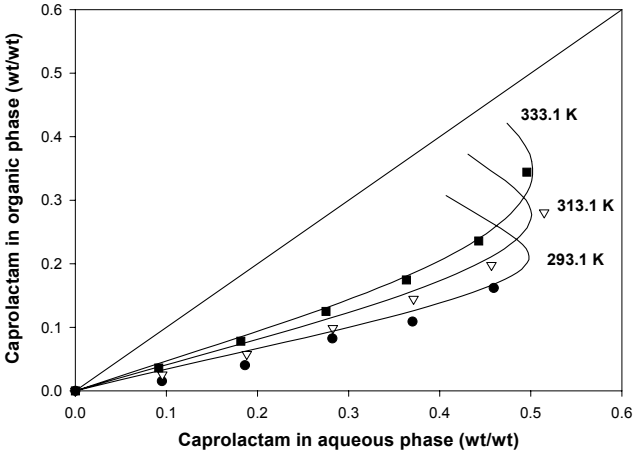

Figure 5.11: Caprolactam distribution in water + benzene at 293.1, 313.1 and 333.1 K. Markers are experimental data, lines have been calculated with the modified extended electrolyte NRTL (which for salt-free systems reduces to the original NRTL).

Figure 5.12 visualizes the performance of the model for the caprolactam distribution in water and benzene from low to high concentrations of ammonium sulfate and shows that the model can cope with concentrations up to saturation. Figure 5.13 shows the improved performance of the model for the ternary system water + caprolactam + ammonium sulfate. Similar to the results for water + propanol + NaCl a better prediction is found for the salt concentration in the organic phase and the closure of the binodal curve can be reproduced.

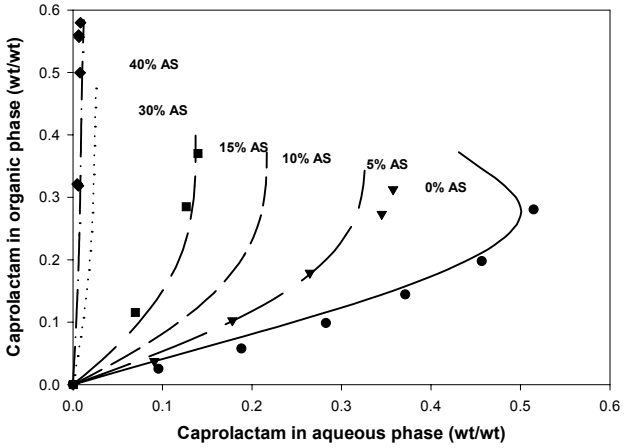

Figure 5.12: Caprolactam distribution in water + benzene at 313.1 K with different weight percents of ammonium sulfate in the bottom phase. Markers are experimental data, lines have been calculated with the modified extended electrolyte NRTL model.

It can be observed in Table 5.3 that in general the deviations in weight fractions are larger than those in mole fractions. In this respect it should be kept in mind that ammonium sulfate has a relatively high molar weight (M_w = 132 g/mole) and water a relatively low molar weight. If the deviation in weight fractions is much larger, this is an indication for the problems in reproducing the salt concentration.

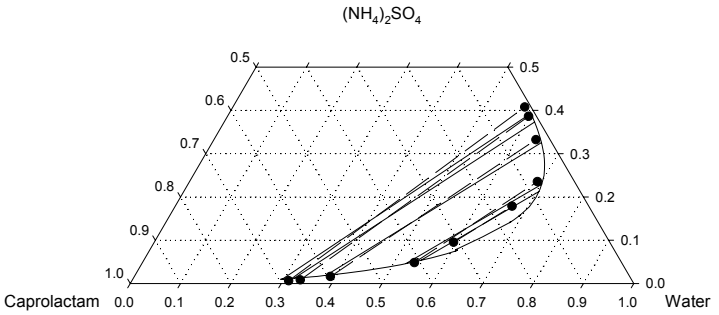

Figure 5.13: Correlation of the system water + caprolactam + ammonium sulfate at 293.1 K with the modified extended electrolyte NRTL model. Solid lines are calculated tie-lines, dashed lines with markers are experimental tie-lines.

Table 5.3: Correlation of (only) LLE of systems with water (W), caprolactam (C), solvent (B = Benzene, 1-H = 1-Heptanol, 2-H = 2-Heptanone) and ammonium sulfate (AS). Data sets marked with * were not used in the parameter regressions.

System	T	Present model		Chen's model[b]		Source[a]
	°C	Δx (%)	Δw (%)	Δx (%)	Δw (%)	
W + B + C	20	1.1	1.9	0.8	1.7	1
	40	1.7	2.3	1.2	1.8	1
	60	2.1	1.7	2.1	1.4	1
W + 1-H + C	20	2.1	3.9	1.9	4.2	
	40	1.4	3.0	1.8	3.2	
	60	2.2	4.3	2.7	4.2	
W + 2-H + C	20	1.9	2.3	1.9	2.3	
	40	1.6	1.7	2.0	1.8	
	60	2.8	2.8	3.5	3.2	
W + C + AS	20	0.9	2.7	1.4	4.4	
	20	0.6	1.7	1.1	3.1	2*
	20	1.1	2.8	1.6	4.7	3*
	30	0.3	0.8	0.7	1.3	4*
	40	0.6	1.4	1.1	3.0	
	40	0.4	0.7	1.2	2.2	5*
	50	1.5	2.4	2.1	3.5	4*
	55	1.6	2.5	2.3	3.6	1
W + C + B + AS	20	1.5	2.1	1.7	2.6	1
	40	0.9	1.1	1.1	1.4	1
	60	1.5	1.9	2.0	2.4	1
W + C + 1-H + AS	20	1.4	2.0	1.4	2.7	
	40	1.6	1.2	1.4	1.6	
	60	1.3	1.5	1.3	1.5	
W + C + 2-H + AS	20	1.8	2.8	1.8	3.1	
	40	1.3	1.5	1.2	1.5	
Sum of squares[c]		0.33	0.67	0.43	1.01	

[a] Source of literature data:
1 = De Haan and Niemann (1999)
2 = Shubtsova et al.(1975)
3 = Tettimanti and Nogradi (1960)
4 = Vecera and Sladky (1955)
5 = Gucwa and Makal (1976)

[b] Chen et al. (1986) and Aspen Technology (1999)

[c] Equation (5.29)

During the regressions it was observed that for the data sets in this section, the Brønsted-Guggenheim contribution is of lesser importance than for the water + alcohol + salt systems. Most likely this is caused by the fact that the top phases for these systems contain much more water than for the water + alcohol + salt systems. Probably, the BG-contribution is in particular important to compensate for incorrectness in the description of the **organic phase**.

The results for the systems with **1-heptanol** (Figure 5.14) are less good than for the other solvents. Attempts to improve this by adding a BG-interaction contribution for 1-heptanol + caprolactam or by changing the nonrandomness factor of water + 1-heptanol or 1-heptanol + caprolactam were not successful. Since the problem was not found for the water + alcohol + salt systems in the previous section, most likely the NRTL-model has difficulties in representing the interactions between 1-heptanol and caprolactam. This is probably due to the presence of interaction between the alcohol group and the amino group in the caprolactam molecule. The NRTL model may not be able to account properly for this interaction. (In literature no confirmation could be found for this.)

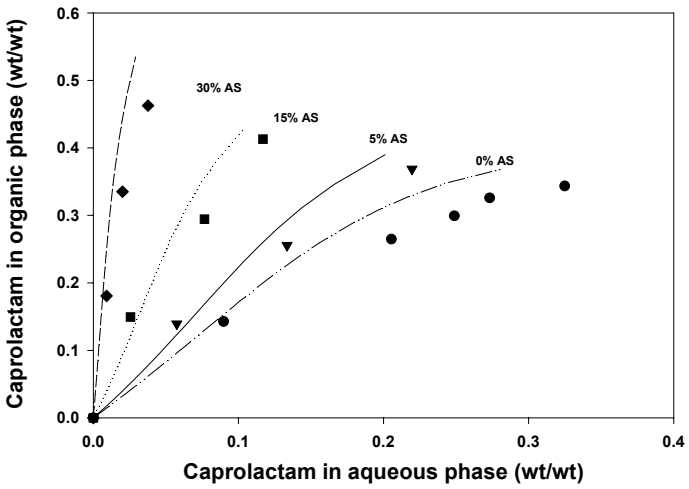

Figure 5.14: Caprolactam distribution in water + 1-heptanol at 313.1 K with different weight percents of ammonium sulfate in the bottom phase. Markers are experimental data, lines have been calculated.

5.7.3 Two- and three-liquid phase equilibria

The regressions appeared to be much more computer time consuming when LLLE data were included. Fortunately, it was found that when parameter regressions for the LLLE had been successful, the fit of LLE and also the mean ionic activity coefficients was very easy. This illustrates the fact that by correlation of LLLE a more consistent set of adjustable parameters is obtained. It could be concluded that the number of local minima in the objective function is smaller for LLLE than for LLE. In the case of parameter regressions with only LLE local minima of the objective function might be found at which the model will fail to predict a phase split into three liquid phases. The use of many data sets of different systems but with one or more common binary subsystems also improves the performance of the model and facilitates extension to more data sets.

In order to obtain a reasonable description of the LLLE at different temperatures, it was necessary to change the temperature dependence of the NRTL binary interaction parameters. The modelling was carried out with a large number of data sets, including three sets of LLLE data: the system water + benzene + caprolactam + ammonium sulfate, water + benzene + ethanol + ammonium sulfate and the system water + 2-heptanone + caprolactam +ammonium sulfate. Initially, the normal temperature dependence of the NRTL interaction parameters was used (Equation 5.28). Accurate results could be obtained by regressions with data sets at only one temperature, but subsequent application of the parameters found to all the data in the measured temperature range failed. It appeared impossible to model the LLLE at the different temperatures simultaneously without changing the temperature dependence of the binary interaction parameters. Hence, the interaction parameters are now calculated by:

$$\tau_{ij} = \frac{A_{ij} + B_{ij}\left(T - 293.15\right)}{T} \qquad \textbf{(5.30)}$$

This corresponds to the temperature dependency as used for example by Aspen Technology (1998) for the NRTL model. Initially, attempts were made to apply this equation only to a limited number of the parameters. It was found that Equation (5.30) should be applied to all of the NRTL binary interaction parameters to get a satisfactory representation of all LLLE at the temperatures measured.

The results for the various systems are given in Table 5.4 and Figure 5.15 to 5.19. Here, also two sets of results published before are given to illustrate the effect of including more data sets and including LLLE. For these results, Equation (5.28) was used for the NRTL binary interaction parameters. The last three columns in the table illustrate the performance of the model, using Equation (5.28) or using a combination of Equation (5.28) and (5.30), or using only Equation (5.30) for the NRTL binary interaction parameters. The parameters belonging to these results are given in Appendix III.3.

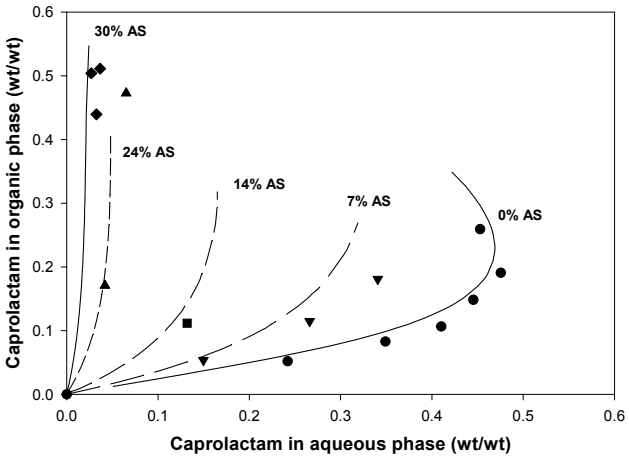

Figure 5.15: Caprolactam distribution in water + 2-heptanone at 293.1 K with different weight percents of ammonium sulfate in the bottom phase. Markers are experimental data, lines have been calculated with the modified extended electrolyte NRTL and the temperature dependence as given in Equation (5.30).

For the LLLE, the results are represented in Figure 5.16 to 5.19. Both from the tables and the figures, it can be seen that the model is able of giving a qualitatively good description of the LLLE region for the systems investigated. Quantitatively, the performance of the model is reasonable. The model has some problems correlating the experimental tie-triangles closer to the critical tie-lines. However, it is possible to predict three-phase triangles near the critical tie-lines when the overall salt concentrations are slightly changed. This large influence of small variations in the salt concentrations may also be a reason why it is so hard to correlate LLLE.

Table 5.4: Average deviations of correlations from experimental data (W = water, C = caprolactam, B = benzene, 1H = 1-heptanol, 2H = 2-heptanone, E = ethanol, AS = ammonium sulfate) using three different temperature dependencies for the NRTL binary interaction parameters. Explanation: Published results (1999, 2002) and option 1 according to Equation (5.28), option 2: Equation (5.30), but using Equation (5.28) for solvent + salt and option 3: using Equation (5.30) for all τ_{ij}'s. An asterisk indicates that the flash routine did not converge for all data points. The average deviations are given as mole percents (Δx) or weight percents (Δw).

Data set	T °C	Published 1999[a]		Published 2002[b]		Option 1		Option 2		Option 3	
		Δx	Δw	Δx	Δw	Δx	Δw	Δx	Δw	Δx	Δw
LLE											
W + C + AS	20	0.9	2.6	0.8	2.3	1.0	3.1	0.9	2.8	0.9	2.7
W + B + C	20	1.4	1.9	0.8	1.1	1.0	0.8	1.0	0.8	1.0	0.8
W + 1H + C	20	2.4	3.8	2.3	2.9	0.8	1.9	0.8	1.9	0.8	1.9
W + 2H + C	20	-	-	2.0	1.6	2.3	1.8	2.4	1.8	2.4	1.8
W + B + E	20	-	-	-	-	3.8	3.2	3.6	3.1	3.6	3.1
W + B + C + AS	20	1.7	1.8	1.1	1.0	1.0	0.8	0.9	0.6	0.9	0.6
W + 1H + C + AS	20	1.7	2.1	1.6	1.6	0.5	1.0	0.5	1.0	0.5	0.9
W + 2H + C + AS	20	-	-	1.0	1.2	1.1	1.6	1.0	1.4	1.0	1.3
W + C + AS	40	0.8	1.6	0.8	1.7	0.8	2.0	0.7	2.0	0.8	2.6
W + B + C	40	1.8	2.2	0.8	0.9	1.1	0.9	1.7	1.2	1.6	1.2
W + 1H + C	40	2.4	3.8	1.8	1.2	4.5	5.7	1.5	2.5	1.5	2.5
W + 2H + C	40	-	-	3.8	4.6	2.8	1.8	1.7	1.4	1.7	1.4
W + B + C + AS	40	1.1	1.0	0.7	1.2	1.1	1.5	0.9	0.8	1.1	1.4
W + 1H + C + AS	40	1.6	2.8	1.6	1.5	1.0	1.8	0.8	1.2	0.7	1.3
W + 2H + C + AS	40	-	-	2.5	2.9	3.7	4.5	1.8	2.2	0.8	1.5
W + B + C	60	2.3	2.0	2.3	1.9	2.8	2.3	2.5	2.9	2.5	2.9
W + C + AS	55	-	-	-	-	1.8	2.9	1.7	2.7	0.6	0.9
W + 1H + C	60	2.7	4.3	3.8	5.1	6.7	8.6	1.0	2.1	1.0	2.1
W + 2H + C	60	-	-	4.4	3.7	4.1	3.5	1.4	1.6	1.4	1.6
W + B + C + AS	60	1.6	2.0	5.5	5.7	7.6	7.4	2.2	2.0	1.7	1.5
W + 1H + C + AS	60	1.8	1.5	2.1	2.0	2.0	3.4	1.0	1.7	0.5	1.4

Table continues on next page

Table 5.4 (continued)

Data set	T °C	1999[a]		2002[b]		Option 1		Option 2		Option 3	
		Δx	Δw	Δx	Δw	Δx	Δw	Δx	Δw	Δx	Δw
LLLE											
W + B + E + AS	21	-	-	3.2	3.5	2.7	4.0	2.6	3.8	2.5	3.8
W + B + E + AS	44	-	-	-	-	16*	19*	9.2	14	3.9	4.8
W + B + E + AS	48	-	-	-	-	10*	16*	13*	18*	5*	7*
W + 2H + C + AS	20	-	-	2.0	2.7	1.6	2.7	1.5	2.3	1.5	2.2
W + B + C + AS	20	-	-	-	-	1.4	2.7	1.3	2.4	1.3	2.3
W + B + C + AS	40	-	-	-	-	7*	7*	3.0	5.0	2.1	4.0
W + B + C + AS	55	-	-	-	-	14*	13*	4*	7*	1.9	3.9
Average		1.7	2.4	2.1	2.4	3.7	4.5	2.3	3.2	1.6	2.2
SSQ						6.2	8.0	2.2	4.5	0.9	1.6
Mean ionic activity coefficients (%)											
W + AS	25	0.038		0.054		0.038		0.037		0.042	

[a] Van Bochove et al., Fluid Phase Equilib. (2000) 171, 45-58

[b] Van Bochove et al., Fluid Phase Equilib. (2002) 194-197, 1029-1044

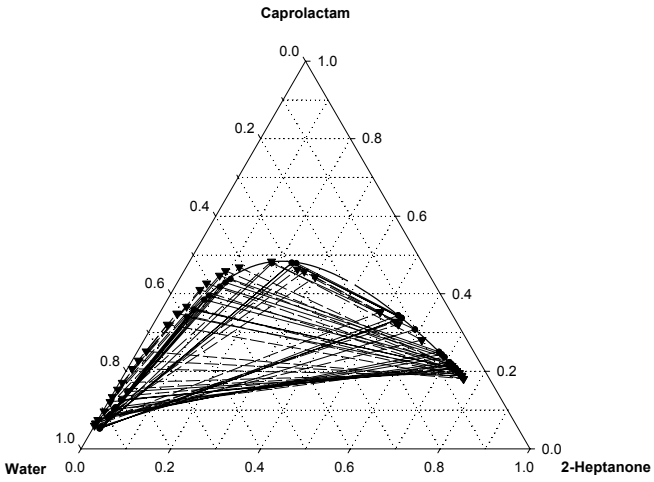

Figure 5.16: Projection of experimental LLLE (●, dashed lines) and calculated LLLE (▼, solid lines, modified extended E-NRTL) in the system water + 2-heptanone + caprolactam + ammonium sulfate at 293.1 K.

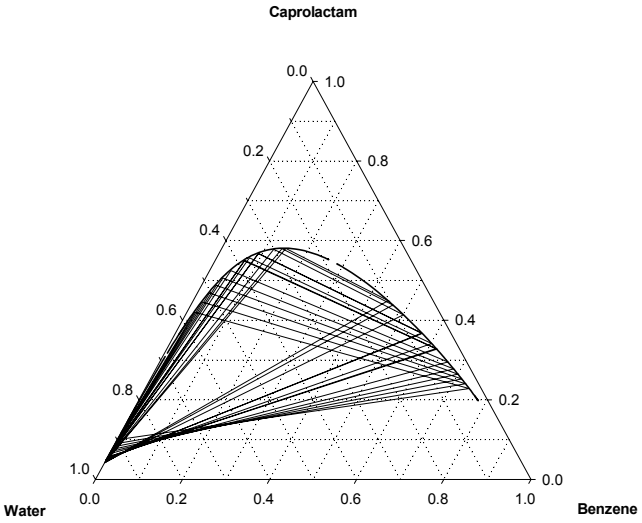

Figure 5.17: Projection of LLLE calculated with modified extended E-NRTL for water + benzene + caprolactam + ammonium sulfate at 293.1 K (The LLLE shown are correlations of the experimental LLLE in Figure 3.16)

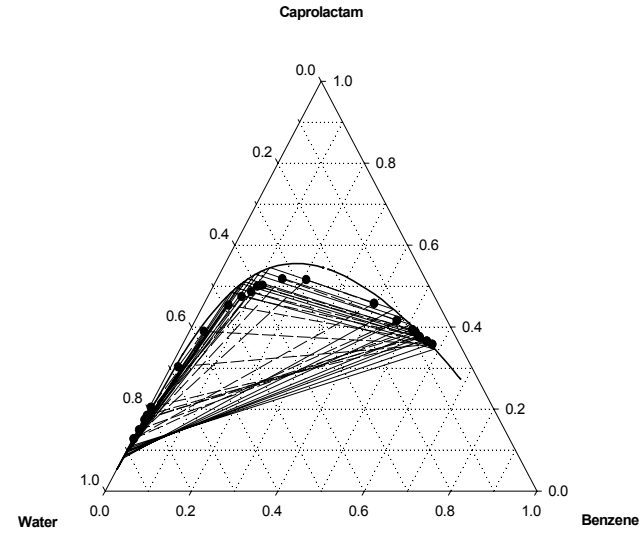

Figure 5.18: Projection of LLLE calculated with modified extended E-NRTL (solid lines) and experimental LLLE (dashed lines with markers) for the system water + benzene + caprolactam + ammonium sulfate at 313.1 K

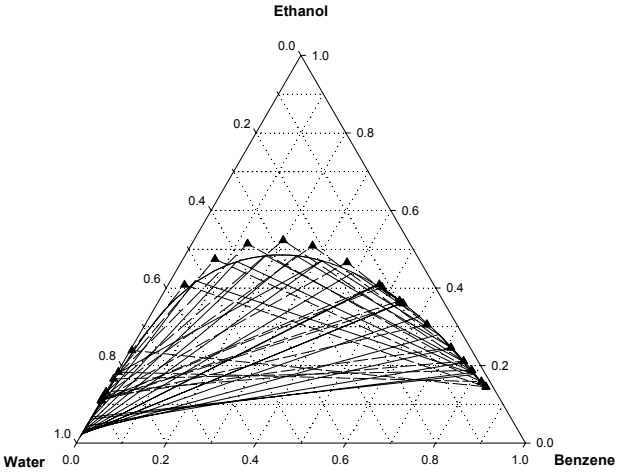

Figure 5.19: Projection of calculated LLLE (sold lines, modified extended E-NRTL) and experimental LLLE (markers and dashed lines) for the system water + benzene + ethanol + ammonium sulfate at 294 K

5.8 Comparison of Electrolyte NRTL models

Table 5.5: Comparison of the models discussed in this chapter and their representation of experimental equilibrium data.

Model	Performance
Original Electrolyte NRTL Chen et al. (1982)	Mean ionic activity coefficients: good description LLE: No convergence near plait point, LLLE: Fails to describe LLLE
Extended Electrolyte NRTL Liu andWatanasiri (1996)	Fails to describe mean ionic activity coefficients LLE: Poor representation outside experimental range LLLE: Fails to describe LLLE
Modified extended E-NRTL (This work)	Mean ionic activity coefficients: good representation LLE: Good representation of LLE, also in the neighbourhood of the plait point. LLLE: Good representation at fixed temperatures
Modified extended E-NRTL with extra temperature dependency	Good description of LLLE at different temperatures

5.9 Partial dissociation and ensemble conversion

5.8.1 Theory

It has been suggested (O'Connell, 2001) that the original electrolyte NRTL does not perform that well, because partial dissociation of the salt is not taken into account and the conversion of the McMillan-Mayer ensemble to the Lewis-Randall ensemble is ignored in the case of mixed solvents (see Chapter 2). As discussed in Chapter 2, many electrolyte theories are developed in the McMillan-Mayer framework: the solvent molecules are suppressed and replaced by a dielectric background. The only solvent properties that play a role are the dielectric constant and the solution density. The McMillan-Mayer framework delivers a Helmholtz energy. In the derivation of activity coefficients from the excess Gibbs energy (in the Lewis-Randall ensemble) T, P and n are fixed. In the derivation of activity coefficients from the Helmholtz energy T, V, the solute mole numbers and the solvent chemical potentials are fixed. The relevant Gibbs-Duhem equation is then given by Equation (2.19).

According to O'Connell (2001) the derivatives due to solvent composition dependency of the solution properties should not be taken into account because the derivation of the activity coefficients in the McMillan-Mayer ensemble should be done at a fixed solvent chemical potential. The contribution of the electrostatic term to the solvent components will be found when the Helmholtz-energy (as used in the McMillan-Mayer ensemble) is converted to the Gibbs energy as used in the Lewis-Randall ensemble. Also, according to O'Connell, it is not correct to assume full dissociation especially in the organic phase; the Brønsted-Guggenheim contribution as used in the modified extended electrolyte NRTL only serves to correct for not taking into account partial dissociation.

In this view, it is incorrect to take into account the solvent composition dependence of the dielectric constant and the density and this will lead to salting out of the solvent with the highest dielectric constant. The electrostatic contribution to the activity coefficients should be calculated from the excess Gibbs energy, which is obtained by conversion of the Helmholtz energy as given by the MM-theories. Since this would produce very complex equations, a simpler method has been proposed by O'Connell and De Cardoso (1987) using the osmotic pressure formalism, which finally leads to the following expressions:

$$\ln \gamma_i(T,P,x) = \ln \gamma_i^{'}(T,P,x) - \frac{< v_i > P_{osm}^{LRE}}{RT} \quad \textbf{(5.31)}$$

$$\ln \gamma_j(T,P,x) = \ln \gamma_j^{'}(T,P,x) + \ln \gamma_j^{LRE}(T,P,x) \quad \textbf{(5.32)}$$

where i refers to solvents and j refers to ions, γ' is the activity coefficient found from the Lewis-Randall (excess Gibbs) model, LRE refers to the long range (electrostatic) contribution from the McMillan-Mayer theory and $< v_i >$ is the average partial molar volume of solvent i in the solution. The same formulas as given above were given by Lee (2000) in a paper that discusses more thoroughly the conversion between the two ensembles.

In the work presented in this chapter, the assumptions were made that the electrostatic energy contribution is an excess Gibbs energy and that the salt was fully dissociated. To investigate how the inclusion of partial dissociation and the conversion from McMillan-Mayer to Lewis-Randall will affect the performance of the model of Chen et al. (1986) compared with the modified extended electrolyte NRTL, some calculations were carried out. First, the activity coefficients were derived using the approach as suggested by De Cardoso and O'Connell (1987). The following equations give the original Pitzer-Debye-Hückel (Equation 5.33), the converted Pitzer-Debye-Hückel solvent activity coefficient (Equation 5.34) and the Pitzer-Debye-Hückel solvent activity coefficient as used in the modified extended electrolyte NRTL (Equation 5.35).

Original Pitzer-Debye-Hückel:

$$\ln \gamma_j^{PDH} = \frac{2A_x I_x}{1+\rho\sqrt{I_x}} \quad \textbf{(5.33)}$$

"Converted" Pitzer-Debye-Hückel:

$$\ln \gamma_j^{PDH} = < v_i > \frac{1000 d_s}{M_s} \frac{2A_x I_x}{1+\rho\sqrt{I_x}} = \frac{< v_i >}{< v_s >} \frac{2A_x I_x}{1+\rho\sqrt{I_x}} \quad \textbf{(5.34)}$$

Modified extended electrolyte NRTL:

$$\ln \gamma_j^{PDH} = \frac{2A_x I_x^{3/2}}{1+\rho\sqrt{I_x}} + \frac{4I_x A_x}{\rho} \ln(1+\rho\sqrt{I_x}) \cdot \left[\frac{1}{2M_s} \frac{(M_j - M_s)}{\sum_k x_k} - \frac{n}{2d} \frac{\partial d}{\partial n_j} + \frac{3n}{2\varepsilon} \frac{\partial \varepsilon}{\partial n_j} \right] \quad \textbf{(5.35)}$$

where $<v_s>$ is the average partial molar volume of the solvent mixture (or pseudo-solvent) in the electrolyte solution. It can be seen that difference between the "incorrect traditional" approach and the "correct" approach gives (in the case of the Pitzer-Debye-Hückel equation) only a slightly different result.

Equation (5.34) is comparable to the equation derived by Macedo et al. (1990) for the extended Debye-Hückel model. The "corrected" Pitzer-Debye-Hückel solvent activity coefficient (Equation 5.34) was used with and without the assumption of partial dissociation, ignoring the influence of the salt on the solution densities and molar volumes. The assumption of partial dissociation involves the introduction of an extra component in the system: the molecular salt. If all binary interaction parameters between the molecular salt and the other components are used, this implies for a quaternary system that 9 additional parameters (including the dissociation constant) would have to be obtained by regression. Therefore, it is desirable to reduce the number of parameters.

5.8.2 Partial dissociation

Partial dissociation was introduced by calculating the chemical equilibrium (as described in Chapter 4) with a dissociation constant *K* that is obtained by regressions. Also, some new binary interaction parameters were regressed that account for the interaction of other components with the molecular salt. For the choice of the new binary interaction parameters, some options are available. Three options were studied in more detail and are given in Table 5.6. The results given there were obtained by simultaneous regressions of 5 data sets of LLE for water + alcohol + NaCl systems, 2 data sets of salt-free systems and mean ionic activity coefficients for water + NaCl, all at 298.1 K. The data set water + caprolactam + ammonium sulfate was not included, since in that system two aqueous phases are present and partial dissociation cannot be assumed to play a role. This was confirmed by some calculations on partial dissociation for this system: Assuming partial dissociation does not change the quality of the correlation. For the regressions that led to the result in Table 5.6, different initial values for the dissociation constant were tried, ranging from hardly any dissociation to almost full dissociation. The best results are presented in Table 5.6.

The three options in Table 5.6 concern the way the NRTL interaction parameters of the molecular salt are treated. The first option is following the approach by Chen et

al. (1999) introducing only the binary interaction parameters between the cation-anion pair and the undissociated salt. However, this hardly improves the result; the table shows that only a minor improvement can be reached this way. A more logical option seems to introduce molecular salt - organic solvent parameters: It can be expected that the dissociation fraction will be the lowest in the organic phase. Doing this for the systems water + alcohol + NaCl, where the alcohol is one of 1-propanol, 2-propanol, 1-butanol or 2-butanol, good results are obtained for the systems water + 1-propanol/2-propanol + NaCl. However, the results for the systems water + 1-butanol/2-butanol are still unsatisfactory with an average absolute deviation of more than 0.04. The difference between the systems with the propanols and the butanols is the binary phase split of the water-alcohol subsystem and the very low (<0.001 kg/kg) concentrations of salt in the organic phase. A third option is to introduce interaction parameters of the salt with all other components. This produces results that are much better, but it is questionable if this is achieved by a physically more correct description of the salt, or simply by the addition of many new adjustable parameters. The latter seems most likely.

The values for the dissociation fraction for the system water + 2-propanol + NaCl range from 0.00006 to 0.008 in the organic phase and from 0.98 to 0.92 in the aqueous phase. For the systems with the butanols, the dissociation fraction is around 0.01 for the organic phase and around 0.995 in the aqueous phase. (These dissociation fractions are based on the result from the last column in Table 5.6.)

Of course, it is also interesting to see how the assumption of partial dissociation affects the performance of the modified E-NRTL. For this reason, calculations were carried out with different initial values for the dissociation constant and different options for dealing with the interaction parameters of the molecular salt. Remarkably, no improvement was found assuming partial dissociation and the dissociation constant tended to go to high values in the regressions (and thus full dissociation). In Table 5.7, a typical result is given, with and without partial dissociation. In the latter case, all NRTL binary interaction parameters with the salt were included and it can be seen that even 15 additional parameters do not lead to a significant improvement.

Table 5.6: Influence of the assumption of partial dissociation on the results obtained with the electrolyte NRTL model of Chen et al. (1986) for a collection of LLE data sets of water + alcohol + salt systems at 298.1 K. Average deviations from experimental data in weight percents (Δw) and mole percents (Δx) as defined by Equation (5.27).

	Full dissociation		Option 1		Option 2		Option 3	
	Δx	Δw	Δx	Δw	Δx	Δw	Δx	Δw
Water + 1-propanol + NaCl[a]	1.7	2.6	1.5	2.1	1.2	1.5	1.2	1.5
Water + 2-propanol + NaCl[a]	1.3	2.1	1.0	1.4	1.1	1.1	1.1	1.1
Water + 1-butanol + NaCl[a]	2.9	1.6	3.0	1.6	2.9	1.7	2.9	1.6
Water + 2-butanol + NaCl[a]	5.1	3.4	5.3	3.4	5.1	3.4	5.1	3.4
Water + 1-pentanol + NaCl[b]	1.3	0.6	1.4	0.6	1.3	0.6	1.3	0.6
Water + 1-propanol + 1-butanol[c]	2.5	3.5	2.5	3.4	2.3	3.3	2.3	3.3
Water + 1-propanol + pentanol[d]	1.4	2.3	1.4	2.3	1.4	2.3	1.4	2.3
Sum of squares	0.3	0.2	0.3	0.2	0.3	0.2	0.3	0.2
Mean ionic activity coefficient Water + NaCl[e]	0.7		0.7		0.7		0.7	
Extra adjustable parameters	0		3		11		15	

Source of data: [a] De Santis et al. (1976); [b] Gomis et al. (1999); [c] Gomis et al. (1998); [d] Fernandez et al. (2000); [e] Robinson and Stokes (1959)

Comparison of Table 5.6 and Table 5.7 show that the modified extended electrolyte NRTL is doing better than the original model for the systems studied. This is still the case if partial dissociation is included for the model of Chen. Larger improvements, particularly for the water + butanol systems, could be obtained for both the modified and original E-NRTL when the mean ionic activity coefficients of water + NaCl were not included in the parameter regressions; in this case the mean ionic activity coefficients went to very large and unrealistic values. This could be an indication that the Born-contribution is too large. This contribution only has effect on the activity coefficients in the organic phase. Since for the flash calculations only the ratio of the ionic activity coefficients is important, too large activity coefficients in the organic phase have to be compensated by larger activity coefficients in the aqueous phase. If these are fixed at the experimental values, this is not possible.

Table 5.7: Modelling results for a collection of LLE data sets of water + alcohol + salt systems at 298.1 K, showing the effect of taking into account ensemble conversion and partial dissociation. Average deviations from experimental data are given in weight percents (Δw) and mole percents (Δx).

	New model		New model + part. diss		Chen + conversion		Chen + conversion+ part. diss	
	Δx	Δw	Δx	Δw	Δx	Δw	Δx	Δw
Water + 1-propanol + NaCl[a]	0.7	1.2	0.7	1.3	1.7	2.6	1.4	1.6
Water + 2-propanol + NaCl[a]	0.3	0.5	0.8	0.9	1.3	2.1	1.0	1.2
Water + 1-butanol + NaCl[a]	2.8	1.6	2.8	1.6	2.9	1.7	2.9	1.7
Water + 2-butanol + NaCl[a]	5.0	3.4	5.0	3.4	5.1	3.4	5.1	3.4
Water + 1-pentanol + NaCl[b]	1.3	0.6	1.3	0.6	1.3	0.6	1.3	0.6
Water +1-propanol + 1-butanol[c]	2.3	3.2	1.8	3.0	2.5	3.5	2.3	3.3
Water + 1-propanol + pentanol[d]	1.4	2.3	1.4	2.3	1.4	2.3	1.4	2.3
Sum of squares (Eq.)	0.3	0.2	0.3	0.2	0.3	0.2	0.3	0.2
Mean ionic activity coefficient Water + NaCl[e]	0.7		0.7		0.7		0.8	
Extra adjustable parameters	0		15		0		15	

Source of data: [a] De Santis et al. (1976); [b] Gomis et al. (1999); [c] Gomis et al. (1998); [d] Fernandez et al. (2000); [e] Robinson and Stokes (1959)

5.8.3 Ensemble conversion

Some calculations were performed to investigate the influence of taking into account the conversion from the McMillan-Mayer ensemble to the Lewis-Randall ensemble. First, regressions were carried out using only the "converted" Pitzer-Debye-Hückel contribution (Equation 5.34) without assuming partial dissociation. The results in this case are comparable to those obtained for the original electrolyte NRTL. Then partial dissociation was introduced. In Table 5.7 some typical results are given for the results thus obtained. It can be seen that the combination of ensemble conversion and partial dissociation gives a better result than only partial dissociation. The latter is again better than the original electrolyte NRTL model. It should be kept in mind that the better results with assuming partial dissociation involved the introduction of many new adjustable parameters, which will mainly account for this improvement.

Secondly, including the chemical equilibrium is computationally quite intensive. The time required for the regressions increases with a factor 5 or more. The best results are still obtained with the modified extended electrolyte NRTL: The model performs better, requires much less computation time and does not involve too many additional adjustable parameters. The suggestion that the assumption of full dissociation is the reason of a less good performing electrolyte NRTL model could not be substantiated here.

6. Mean Spherical Approximation

In chapter 6 some work carried out with models based on the Mean Spherical Approximation theory is discussed. In particular attention is paid to a model based on a combination of NRTL and MSA, to the nonprimitive MSA and to the extended electrolyte equation of state, that also incorporates MSA theory.

6.1 Principles

As discussed in Chapter 2, the solution for the pair correlation function can only be derived if there is an additional relation between the direct correlation function C_{ij} and the pair correlation function g_{ij}. These relations are the closure relations, like the Hypernetted Chain approximation and the Percus-Yevick approximation. Another integral equation, especially designed for electrolyte solutions, is the Mean Spherical Approximation or MSA (Lee, 1988).

The Mean Spherical Model was originally proposed as a model for Ising ferromagnets. In 1966, it was generalized for continuum systems by Lebowitz and Percus. They extended the mean spherical model to lattice gases. In the lattice model molecules of a mixture of gases are arranged on a regular lattice and the properties of the mixture are calculated from the possible positions of the molecules. Lebowitz and Percus went over from a lattice gas to a continuum fluid by approximating a continuum fluid by a lattice gas with infinitely small lattice spacing.

In the Mean Spherical Approximation theory (MSA), the total correlation function and the direct correlation function of Ornstein and Zernike satisfy the following conditions:

$$h_{ij}(r_{ij}) = g_{ij}(r_{ij}) - 1 = -1 \qquad for\ r \le \sigma_{ij} \tag{6.1}$$

$$C_{ij}(r) = -\beta u_{ij}(r) \qquad for\ r > \sigma_{ij} \tag{6.2}$$

$$\sigma_{ij} = \frac{1}{2}\left(\sigma_i + \sigma_j\right) \tag{6.3}$$

where $\beta=1/kT$, σ_i is the hard core diameter of molecule i, σ_{ij} is the distance of closest approach and u_{ij} is the pair potential. Equation (6.1) is an exact relation. This equation implies that it is impossible for a molecule to penetrate in the hard core of another molecule. The relation for C_{ij} is only valid for $r\rightarrow\infty$, but in the MSA theory it is used as an approximation for all $r>\sigma_{ij}$. For hard spheres, MSA corresponds with the Percus-Yevick theory for hard sphere fluids. Together, Equation (6.1) and (6.2) provide the information to solve the Ornstein-Zernike equation.

In the case of electrolytes, the MSA model can be solved both in the primitive model for electrolytes (McMillan-Mayer ensemble) as in a nonprimitive model. The difference between these models lies in the definition of the pair potential u_{ij}. In addition, in the primitive model i and j in Equation (6.1) to (6.3) refer to only ions, whereas in the nonprimitive models they refer to all components including solvents.

6.2 Primitive MSA model

6.2.1 Solutions of the primitive MSA model

Following the primitive model of electrolytes (MM-ensemble), the solvent molecules are replaced by a dielectric background. In Equation (6.3) σ_i and σ_j now refer to the hard sphere diameter of the hydrated ions of type i and j, respectively. The pair potential u_{ij} in a dielectric medium with dielectric constant ε is given by the electrostatic interaction potential:

$$u_{ij}^{*}(r)=\frac{z_i z_j e^2}{\varepsilon r} \qquad \textbf{(6.4)}$$

This model has been solved for a system of ions with equal diameters (the restricted primitive model) and for a system with ions of different size. Waisman and Lebowitz (1970, 1972a, 1972b) solved the MSA for the restricted primitive model. In the restricted primitive model the cations and anions are charged hard spheres of equal size and charge. Waisman and Lebowitz found explicit analytical expressions for the thermodynamic properties such as the internal energy and the Helmholtz energy A:

$$\frac{A^{MSA}}{VkT}=\frac{3x^2+6x-2(1+2x)^{3/2}+2}{12\pi\sigma^3} \qquad \textbf{(6.5)}$$

with:

$$x^2 = \kappa^2\sigma^2 = \frac{4\pi\sigma^2}{\varepsilon kT}\sum_{j=+,-}\rho_j q_j^2 \qquad \textbf{(6.6)}$$

where κ is the Debye-Hückel parameter and $\sigma = \sigma_i = \sigma_j$. This solution has been shown to provide satisfactory results for the prediction of osmotic coefficients of simple electrolytes. However, assuming equal diameters is quite unrealistic. In the not restricted primitive model the cations and anions are treated as charged hard spheres of unequal diameters. This model has been solved by Blum (1975) and Blum and Hoye (1977). The only restriction they used, is the electroneutrality condition: $\sum\rho_j z_j = 0$. Their solution is an one parameter model, where the only parameter is Γ, the shielding parameter. Like for κ in the Debye-Hückel-theory, the reciprocal of this parameter is a characteristic length. The shielding parameter is given by the following set of equations:

$$\Gamma^2 = \frac{\pi e^2}{\varepsilon kT}\sum_j \rho_j \left(\frac{z_j - \frac{\pi}{2\Delta}\sigma_j^2 P_n}{1+\Gamma\sigma_j} \right)^2 \qquad \textbf{(6.7)}$$

$$\Omega = 1 + \frac{\pi}{2\Delta}\sum_k \frac{\rho_k\sigma_k^3}{1+\Gamma\sigma_k} \qquad \textbf{(6.9)}$$

$$P_n = \frac{1}{\Omega}\sum_k \frac{\rho_k\sigma_k z_k}{1+\Gamma\sigma_k} \qquad \textbf{(6.8)}$$

$$\Delta = 1 - \frac{\pi}{6}\sum_k \rho_k\sigma_k^3 \qquad \textbf{(6.10)}$$

where P_n is the coupling parameter (of electrostatic effects to geometric effects), Δ is the volume fraction of the solvent and Ω is some unspecified parameter. The summations are over the number of ions. The shielding parameter or inverse shielding length Γ has to be determined by iteration. A good starting value would be $\kappa/2$. For $\sigma_+ = \sigma_-$ the solution of Blum is consistent with the Waisman-Lebowitz solution. The internal energy and the Helmholtz energy in the solution of Blum and Hoye are given by:

$$\frac{U^{MSA}}{VkT} = \frac{e^2}{\varepsilon kT}\left(\Gamma\sum_i \frac{\rho_i z_i^2}{1+\Gamma\sigma_i} + \frac{\pi}{2\Delta}\Omega P_n^2\right) \tag{6.11}$$

$$\frac{A^{MSA}}{VkT} = \frac{U^{MSA}}{VkT} + \frac{\Gamma^3}{3\pi} \tag{6.12}$$

6.2.2 Activity coefficients

The primitive MSA single-ion activity coefficient γ_i is obtained from the Helmholtz energy by:

$$\ln\gamma_i^{MSA} = \beta\frac{\partial A^{MSA}}{\partial\rho_i} \tag{6.13}$$

resulting in:

$$\ln\gamma_i^{MSA} = -\frac{e^2}{\varepsilon kT}\frac{\Gamma z_i^2}{1+\Gamma\sigma_i} - \frac{\pi e^2}{\varepsilon kT}\frac{P_n}{2\Delta}\left(\frac{2z_i\sigma_i}{1+\Gamma\sigma_i} - \frac{\pi P_n\sigma_i^3}{2\Delta(1+\Gamma\sigma_i)} + \frac{\pi P_n\sigma_i^3}{6\Delta}\right) \tag{6.14}$$

The ionic activity coefficient is built up from two contributions. The first contribution is a Debye-Hückel like term and accounts for the long range electrostatic interactions. The second term describes the short range electrostatic interactions and reflects the shielding ability according to the size of the ions. If concentration dependent dielectric constants or ionic diameters are used, additional terms are required since a correct derivation would introduce the derivatives to the concentration in the relation for the activity coefficient as given by Simonin (1996).

The primitive MSA model was first applied to aqueous electrolyte solutions without including nonelectrostatic terms in the calculation of the activity coefficients. This led to large errors for concentrated solutions. MSA could be applied to calculate mean and single-ion activity coefficients activity coefficients, but the agreement with experimental results was only satisfactory for dilute aqueous electrolyte solutions, even when concentration dependent ionic diameters were used (Corti, 1987). Using only the MSA contribution for the calculation of ionic activity coefficients corresponds to assuming that the contribution of the salt is restricted to the contribution arising from the charges of the ions. Therefore, including the contribution from the uncharged reference system is necessary: the hard sphere contributions.

Humffray (1983) introduced the addition of a hard sphere contribution and found that it greatly improved the results for aqueous solutions of sodium chloride and calcium chloride.

$$\ln \gamma_i = \ln \gamma_i^{MSA} + \ln \gamma_i^{HS} \tag{6.15}$$

Usually, the hard sphere contribution is calculated with the Carnahan-Starling equation for mixtures of unequally sized hard spheres as derived by Mansoori et al. (1971):

$$Z = \frac{\left(1+\xi+\xi^2\right)-3\xi\left(y_1+y_2\xi\right)-\xi^3}{\left(1-\xi\right)^3} \tag{6.16}$$

where Z is the compressibility factor and ξ, y_1 and y_2 are functions of the size of the spheres and the composition of the mixture. The Helmholtz energy can be obtained from this equation. Subsequently, the activity coefficient can be derived from the Helmholtz energy. The equations are rather complex, but fortunately the expression for the activity coefficient has been derived and been simplified by Simonin et al. (1996, 1997):

$$\ln \gamma_i^{HS} = -\ln\left(1-X_3\right)+\sigma_i \frac{3X_2}{1-X_3}+\sigma_i^2 F_2+\sigma_i^3 F_3 \tag{6.17}$$

$$F_2 = \frac{3X_1}{1-X_3}+\frac{3X_2^2}{X_3\left(1-X_3\right)^2}+\frac{3X_2^2}{X_3^2}\ln\left(1-X_3\right) \tag{6.18}$$

$$F_3 = \frac{1}{1-X_3}\left(X_0-\frac{X_2^3}{X_3^2}\right)+\frac{3X_1X_2-X_2^3/X_3^2}{\left(1-X_3\right)^2}+\frac{2X_2^3}{X_3\left(1-X_3\right)^2}-\frac{2X_2^3}{X_3^3}\ln\left(1-X_3\right) \tag{6.19}$$

$$X_n = \frac{\pi}{6}\sum \rho_j \sigma_j^n \tag{6.20}$$

The equation gets more complicated when concentration dependent ionic diameters are used, as shown by Simonin (1996).

6.2.3 Primitive MSA vs. Debye-Hückel

The MSA mean ionic activity coefficient can be obtained from Equation (6.12) and (6.13). When this mean ionic activity coefficient is compared with the mean ionic activity coefficient from the Debye-Hückel theory (DH) and the Extended Debye-Hückel theory (EDH), a striking resemblance is found:

$$\ln \gamma_{\pm}^{DH} = -\frac{|z_c z_a| e^2}{2\varepsilon kT}\kappa \qquad \textbf{(6.21)}$$

$$\ln \gamma_{\pm}^{EDH} = -\frac{|z_c z_a| e^2}{2\varepsilon kT}\frac{\kappa}{1+\kappa a} \qquad \textbf{(6.22)}$$

$$\ln \gamma_{\pm}^{MSA} = \ln \gamma_{\pm}^{HS} - \frac{e^2\Gamma}{\varepsilon kT}\sum_i \frac{(\rho_i/\rho) z_i^2}{1+\Gamma\sigma_i} - \frac{(\alpha P_n \Omega)^2}{8\rho}\left[\frac{1}{\Omega\Delta} + \frac{1}{(\Omega\Delta)^2}\right] \qquad \textbf{(6.23)}$$

Since the Debye-Hückel theory considers ions as point charges, the hard sphere term immediately drops out from the expression for the MSA mean ionic activity coefficient. For low concentrations the third term, the short term electrostatic interaction term, may be ignored. Thus, for low concentrations only the long range electrostatic contribution is important. Obviously, the MSA can be seen as an extension of the Debye-Hückel theory: for low numerical concentrations and zero diameter the MSA shielding parameter approaches ½κ. In this case the MSA activity coefficient is equal to the Debye-Hückel activity coefficient. The difference between the Debye-Hückel model and the MSA model also becomes clear from the assumptions made for their derivation from statistical mechanics:

MSA:

$$h_{ij}(r_{ij}) = g_{ij}(r_{ij}) - 1 = -1 \qquad for\ r \le \sigma_{ij} \qquad \textbf{(6.24)}$$

$$C_{ij}(r) = -\beta u_{ij}(r) \qquad for\ r > \sigma_{ij} \qquad \textbf{(6.25)}$$

DH:

$$C_{ij}(r) = -\beta u_{ij}(r) \qquad for\ all\ r \qquad \textbf{(6.26)}$$

The Debye-Hückel model neglects the excluded volume effects: ions can approach each other to a zero distance. It may be concluded from this comparison that the MSA theory is a more physically correct extension of the Debye-Hückel theory, which in contrary to the Debye-Hückel theory takes into account ion size effects. This is particularly important in mixed solvents since "salting out" is closely associated with ion sizes.

6.2.4 Some applications of the MSA theory

Many published applications of the Mean Spherical Approximation are concerned with predicting of osmotic coefficients. In this section a short summary is given of some published applications of the MSA theory. (In the publications discussed, the hard sphere contribution is included in the MSA.)

- Triolo et al. (1976, 1978) used the solution of the MSA by Blum to fit experimental osmotic coefficients of a collection of monovalent salts at concentrations of 0 to 2 M. They used the Newton-Raphson method to solve the shielding parameter. No correction was used for the conversion of Lewis-Randall to McMillan-Mayer ensemble. Triolo et al. fitted the predictions to experimental data by adjusting the hard core diameter of one ion. The Percus-Yevick approximation was used for the reference osmotic coefficient. Later, this work was improved by using a hard core diameter as a function of density (but not of temperature) and by making the dielectric constant density (concentration) dependent. The differences between theory and experiments appeared to be within the uncertainties of the experimental values.
- Simonin et al. (1996, 1997) used the MSA for several pure ionic solutions of nonassociating salts (alkalihalides and acids). Here, the variation of the dielectric constant and the cation diameter with concentration is taken into account explicitly for the calculation of the activity coefficient, using simple expressions. Good fittings for activity coefficients and osmotic coefficients were obtained in the concentration range 0 up to 15 mole/kg for strong electrolytes. In addition to this, the model was applied to mixtures of two and three salts, resulting in rather good agreement with experimental results.
- Lee (1996) combined the MSA theory with a UNIFAC model to form a so-called ElecGC model (Group Contribution method with ELECtrostatic contribution). This model was applied successfully to a multisalt multisolvent mixture (>20 components) for the calculation of vapour-liquid equilibria. Lee uses the MSA activity coefficient plus a Born contribution for the ionic activity coefficients. The expression for the ionic activity coefficients does not contain a molecular UNIFAC contribution. The neutral components were modelled using a molecular UNIFAC model, combined with an MSA contribution to account for the electrostatic influence on the molecular components. This electrostatic contribution is related to the osmotic coefficient and was obtained from integration of the Gibbs-Duhem equation

from a hypothetical neutral solution to the real situation. The resulting equation for the **molecular** species j is:

$$\ln \gamma_j = \ln \gamma_j^{UNIFAC} + \frac{1}{\sum_j \rho_j}\left[\frac{\Gamma^3}{3\pi} + \frac{\pi e^2}{2\varepsilon kT}\left(\frac{P_n}{\Delta}\right)^2 - \frac{\Pi^{HS}}{RT}\right] \qquad \textbf{(6.27)}$$

- Wu and Lee (1992) used a comparable method in 1992 for the calculation of vapour-liquid equilibria of mixed solvent electrolyte systems. They used the MSA mean ionic activity coefficient for LiCl in a mixture of methanol and water. They used the Gibbs-Duhem relation for the calculation of the activity coefficients of the molecular species by numerical integration from a low salt concentration to the desired concentration. Therefore, a hypothetical chain of osmotic cells was constructed with increasing salt concentrations. The activity coefficients of the salt-free solution were calculated from a UNIQUAC model. The pseudo-solvent approach of Gering and Lee (1989) was used. The physical properties of the solvents are averaged to those of one pseudo-solvent. The ionic diameters in this pseudo-solvent were averaged from diameters fitted to data of LiCl in the individual solvents. The conversion from the McMillan-Mayer to the Lewis-Randall ensemble was ignored.
- A modification of the MSA has been published by Gering et al. (1989), the so-called EXP-MSA. In this model an exponential factor is added to the hard sphere radial distribution function. The EXP-MSA theory was successfully used to predict osmotic coefficients and activity coefficients for various (multisolvent) 1:1 electrolyte systems.
- So far there are no publications on applying the MSA to liquid-liquid equilibria

6.3 Nonprimitive MSA

The primitive model of the Mean Spherical Approximation has been extended to a nonprimitive model by Planche and Renon (1981) and by Blum and Wei (1987) resulting in two different models. They solved the MSA for a model where the solvent molecules are considered as hard spheres of different sizes. So the solvent mixture is not replaced by a dielectric background. Other approaches combined (primitive) MSA and a model for dipoles to perturb a model for hard spheres. Several papers were published discussing perturbation models for electrolyte solutions.

6.3.1 Perturbation models

This approach consists of using the Mean Spherical Approximation equation as derived for the primitive model, but with an extra Helmholtz contribution to account for the dipolar forces. The dipole interactions are introduced using the perturbation method. Perturbation theory is based on the idea that the properties of a fluid can be described as those of a simpler fluid (the reference system, usually a hard sphere fluid) plus some corrections. Its advantage is that the calculations are more straightforward than with the iterative procedures used in the numerical calculation of integral equations. The main disadvantage is that the perturbation expansion usually converges too slow when applied to electrolyte solutions. Some work has been published on this subject ranging from rather simple models to complex equations, differing in the interactions that are accounted for (dipole-dipole, ion-dipole, dispersion, quadrupolar, induced interaction energies), the reference system and in the order to which the perturbation expansion is evaluated.

So far, mainly ionic activity coefficients and osmotic coefficients have been described using a perturbed mean spherical approximation model. The most successful models are those published by Jin and Donohue (1988), Cong et al. (1996), Liu et al. (1999) and Wu et al. (1994). The latter combined a perturbed hard sphere equation of Mansoori et al. (1971) with an unperturbed primitive MSA model to solve the divergence problem. The same technique was used by Liu et al. (1999), who combined electrolyte perturbation theory and MSA theory with the statistical associating fluid theory (SAFT) and found good results for a large number of mean ionic activity coefficients of water + salt systems. In the model of Jin and Donohue (1988), the short-range interactions are calculated using the perturbed anisotropic-chain-theory (PACT) and the long-range interactions are calculated from a perturbation expansion of the primitive MSA. In this model, only the number of expressions for the Helmholtz energy already sums up to ten terms. A relatively simple but successful application of MSA perturbation was given by Copeman and Stein (1987) who developed a perturbed hard sphere MSA equation of state and reported good results for some LLE, with deviations within 6%.

6.3.2 MSA model of ions and dipoles (Blum and Wei)

The most fundamental and (most nonprimitive) method of solving the MSA for electrolyte solutions has been published by Blum and Wei (1987). They first solved the Mean Spherical Approximation model for a mixture of dipolar hard spheres without ions. Later they solved the MSA for a mixture of ions of equal charge and diameter and a dipolar solvent with the same diameter as the ions and for a mixture of ions of different charge and diameter and one dipolar solvent, all with different diameters. In the nonprimitive MSA of Blum and Wei (1987) the electrolyte system consists of a mixture of a number of charged hard spheres with a charge ez_i and one solvent s with a hard core diameter and a dipole moment μ. The pair potentials u for $r>\sigma_{ij}$ are given by:

$$u_{ij} = \frac{z_i z_j e^2}{4\pi\varepsilon_0 r} \tag{6.28}$$

$$u_{ss} = -\sqrt{\frac{10}{3}}\frac{\mu^2 \Phi^{112}}{4\pi\varepsilon_0 r^3} \tag{6.29}$$

$$u_{is} = \frac{z_i e \mu \Phi^{011}}{4\pi\varepsilon_0 r^2} \tag{6.30}$$

where s refers to the solvent and the angular function Φ_{mnl} accounts for the orientation of the dipole moment μ; $4\pi\varepsilon_0$ is a factor that returns in the solution of the MSA but is left out in several publications for unclear reasons, however it is required for the equations to be dimensionally correct. If the pair potentials given are used with the common MSA assumptions, a set of nonlinear equations is obtained:

$$\sum_{i=ion} \rho_i (a_i^0)^2 + \rho_s (a_s^1)^2 = \alpha_0^2 \tag{6.31}$$

$$-\sum_{i=ion} \rho_i a_i^0 k_{si}^{10} + a_s^1 (1 - \rho_s k_s^{11}) = \alpha_1^2 = \alpha_0 \alpha_2 \tag{6.32}$$

$$(1 - \rho_s k_s^{11})^2 + \rho_s \sum_{i=ion} \rho_i (k_{si}^{10})^2 = y_1^2 + \rho_s \alpha_2^2 \tag{6.33}$$

where the three equations represent respectively ion-ion interactions, ion-dipole interactions and dipole-dipole interactions. The α-values stand for the ion strength (α_0) and the strength of the dipole (α_2) and contain only input values. The other variables

in the equations above can be expressed using three characteristic parameters Γ, B_{10} and b_2 which are related again to the interactions between ion-ion, ion-dipole and dipole-dipole, respectively. The three parameters have to be calculated by solving the three equations above by numerical iteration. The expressions for the other variables are complex functions of Γ, B_{10} and b_2 and will not be given here. The MSA internal energy and the ionic chemical potential are given by:

$$\frac{\beta E}{V} = \frac{1}{4\pi}\left(\alpha_0^2 \sum_i \rho_i z_i N_i - 2\alpha_0\alpha_2\rho_s B_{10} - 2\alpha_2^2\rho_s b_2/\sigma_s^3\right) \qquad \textbf{(6.35)}$$

$$\beta\mu_i^{MSA} = \frac{z_i}{4\pi}\left(\alpha_0^2 N_i - \alpha_0\alpha_2\rho_s m_i\right) \qquad \textbf{(6.34)}$$

The nonprimitive MSA of Blum and Wei (1987) reduces to the primitive MSA of Blum (1975) for small solvent diameters and infinite dilution. Adjustable parameters are the hard sphere diameters of all components, the solvent density and the dipole moment μ of the solvent. The nonprimitive MSA has been applied for the study of mean ionic activity coefficients and vapour pressures by Li et al. (1996) and Liu et al. (1998).The ion-dipole MSA model was tested and found able of giving a successful representation of the vapour pressure of water (Li et al., 1996). It was also used to calculate the mean ionic activity coefficient of single aqueous electrolyte solutions with fair accuracy (average relative deviation: <4%).

The analytic solution for a multi-component mixture of ions of different size and charge and a multi-component mixture of different sized diameters has not been given yet in literature and is believed to be too complicated. Therefore, the only possibility to use the nonprimitive Mean Spherical Approximation model of Blum and co-workers for mixed solvent electrolyte solutions, is by using equal diameters and by defining an effective dipole moment for all the solvent molecules.

6.3.3 Electrolyte equation of state (Fürst and Renon)

More empirical but easier to use is the approach by Fürst and Renon (1993). Their equation of state is based on the so-called Hard Spheres with Dirac and Coulomb attractive forces model (HSDC-model) of Planche and Renon (1981). In the model of Planche and Renon, molecule-molecule and ion-molecule attractive forces, ion-ion Coulombic interaction and hard sphere repulsion among all particles are assumed.

Dipolar interactions and other short-range interactions are assumed to be Dirac functions at the surface of the molecules or ions. The interaction potential u_{ij} for all species (where i and j refer to both ions and neutral molecules) is given by:

$$\beta u_{ij}(r) = \frac{\beta}{4\pi\varepsilon_0\varepsilon}\frac{z_i z_j e^2}{r} + \frac{W_{ij}}{2\pi r N}\delta'(r-\sigma_{ij}) \quad for\, r > \sigma_{ij} \tag{6.36}$$

$$\beta u_{ij}(r) = \infty \; for\, r < \sigma_{ij} \tag{6.37}$$

where δ is the Dirac function. The hard spheres are either ions or solvent molecules. The last term is new compared to the primitive MSA model. This contribution is a short range contribution that consists for a part of a hard sphere repulsion and for the other part was meant to take into account multipolar interactions, quantified by the interaction parameter W_{ij}. Since $\delta'(x) = -\delta(x)/x$, this term is attractive for all values of $W_{ij}>0$, which makes this contribution corresponding to a sticky spheres model. The advantage of using this term is that it only contains one parameter and that by using a Dirac distribution the integral calculations are made easier (Ball, 1984).

The solution obtained by Planche and Renon was modified by Ball et al. (1985). They derived a set of analytical expressions that is more easy to work with than the original equations. For W_{ij} an empirical relation is used, introducing four new adjustable parameters. If the interaction parameters W_{ij} are zero, the model reduces to the primitive MSA of Blum (1975). The obtained model was applied to a large number of data sets of osmotic coefficients of water + salt systems up to 6 mole/kg. Passarello and Fürst (1996) applied the model of Ball to VLE of water + nitric acid + nitric acid anhydride with good results.

Based on the expressions of Planche and Renon (1981) and Ball et al. (1985), Fürst and Renon (1993) developed an equation of state for electrolyte solutions by combining them with a nonelectrolyte part from the Soave-Redlich-Kwong equation of state of Schwartzentruber et al. (1989). Later the model was extended to mixed solvent solutions by Zuo et al. (2000a, 2000b). The SRK-equation of state of Schwartzentruber et al. (1989) is given by:

$$\frac{P}{RT} = \frac{1}{v-b} - \frac{a^{SR}}{RT(v+c)(v+b+2c)} \tag{6.38}$$

where v is the molar volume, a^{SR} is the energy parameter and b is the co–volume. The c is a volume translation, as suggested by Peneloux et al. (1982), and ensures that the solution of this equation for the (saturated) liquid phase gives the proper molar volume. This volume translation is made such that the prediction of the liquid molar volume is improved without affecting the phase equilibrium calculations. For the pure solvents, the energy parameter and the co-volume are given by:

$$a_i^{SR} = \frac{1}{9\left(2^{1/3}-1\right)}\frac{\left(RT_{ci}\right)^2}{P_{ci}}\left[1+m\left(\omega_i\right)\left(1-\sqrt{T_{ri}}\right)-p_{1,i}\left(1-T_{ri}\right)\left(1+p_{2,i}T_{ri}+p_{3,i}T_{ri}^2\right)\right]^2 \quad \textbf{(6.39)}$$

$$m(\omega_i) = 0.48508 + 1.55171\omega_i - 0.15613\omega_i^2 \quad \textbf{(6.40)}$$

$$b_i = \frac{2^{1/3}-1}{3}\frac{RT_{ci}}{P_{ci}} - c_i \quad \textbf{(6.41)}$$

In these equations the subscript c refers to a critical property, subscript r refers to a reduced property and ω is the acentric factor. The polar parameters $p_{k,i}$ are adjusted to the pure component vapour pressures. If the polar parameters are set to zero the original SRK-EOS is obtained.

To extend this equation to electrolyte solutions, Fürst and Renon (1993) added an electrostatic contribution consisting of a long-range MSA-term and a short range electrostatic term, based on the model of Ball et al. (1985):

$$\frac{P^{SR2}}{RT} = -\sum_k\sum_l \frac{x_k x_l W_{kl}}{\left(v - \frac{N\pi}{6}\sum_i x_i\sigma_i^3\right)^2} \quad \textbf{(6.42)}$$

$$\frac{P^{MSA}}{RT} = -\frac{\alpha^2}{4\pi\varepsilon}\frac{\partial\varepsilon}{\partial V}\sum_j \frac{n_j z_j^2 \Gamma}{1+\Gamma\sigma_j} - \frac{\Gamma^3}{3\pi N_A} \quad \textbf{(6.43)}$$

where W_{ij} is the binary interaction parameter given by:

$$W_{cs} = \lambda_3\sigma_c^S + \lambda_4 \quad \textbf{(6.44)}$$

$$W_{ca} = \lambda_5\left(\sigma_c^S + \sigma_a^P\right)^4 + \lambda_6 \quad \textbf{(6.45)}$$

where σ_c^S is the Stokes diameter of the cation in the solvent and σ_a^P is the anionic Pauling diameter. A mixing rule is used to calculate W_{ij} for mixed solvents. The screening parameter Γ is given by

$$4\Gamma^2 = \alpha^2 \sum_i \frac{x_i}{v} \left(\frac{z_i}{1+\Gamma\sigma_i} \right)^2 N_A \qquad \textbf{(6.46)}$$

Further details about the parameters and variables are given in the papers by Zuo et al. (2000a, 2000b). In the SRK-part the influence of the ions was included in the co-volume b and in the volume translation c for the mixture by:

$$b = b_m + b_{ion} = b_m + \sum_i^{ion} x_i b_i \qquad \textbf{(6.47)}$$

$$c = c_m + c_{ion} = \sum_j^m x_j c_j + 0 \qquad \textbf{(6.48)}$$

where m refers molecular components and ion refers to ionic components. The co-volume for the ions is assumed to be zero. The ionic co-volumes are calculated by:

$$b_c = \lambda_1 \left(\sigma_c^{S(aq)} \right)^3 + \lambda_2 \qquad \textbf{(6.49)}$$

$$b_a = \lambda_1 \left(\sigma_a^P \right)^3 + \lambda_2 \qquad \textbf{(6.50)}$$

where $\sigma_c^{S(aq)}$ is the Stokes diameter of the cation in water and σ_a^P is the anionic Pauling diameter. The coefficients λ are different for different types of anions and are obtained from vapour pressures of water + salt systems. To calculate the a_m^{SR} and b_m for a mixed solvent, Zuo et al. (2000a) incorporated the mixing rules of Wong and Sandler (1992) with the UNIQUAC excess Gibbs energy model. A modification of the UNIQUAC model of Abrams and Prausnitz (1975) is used.

In a recent publication Zuo et al. (2000b) presented an extension of the work of Fürst and Renon to model LLE of mixed-solvent electrolyte solutions. They added a Born term to the existing equation of state. For the Born radius they used the same radius as used in the SR2-contribution, but multiplied by a correction factor f:

$$r_i = f\sigma_i \qquad \textbf{(6.51)}$$

Zuo applied the new EOS to liquid-liquid equilibria of 12 water + alcohol + salt systems found in literature. The dielectric constant was made salt concentration dependent. Most of the parameters required could be obtained from LLE of the salt-free system and from VLE data. The average deviation of the calculated data from the experimental LLE data was 0.8% without any parameters adjusted from ternary data.

6.4 Applying the primitive MSA model (NRTL-MSA)

This section deals with the work on the primitive Mean Spherical approximation theory as described by Van Bochove (1998)

6.4.1 Mean ionic activity coefficients in the MSA

The MSA mean ionic coefficient is built up from three terms: a long range electrostatic contribution (LRE), a short range electrostatic contribution (SRE) and a hard sphere contribution (HS). The extent to which these contributions contribute to the activity coefficient is dependent on the salt concentration and the ionic diameters. To examine this, calculations were carried out for the system water-NaCl and the individual contributions were studied. The diameters of the anion and the cation were fixed at respectively the Pauling diameter (see later) of 0.36 nm and a fitted diameter from literature (Corti, 1987) and the concentration of sodium chloride, expressed in moles salt per kg solvent, was varied from 0 to 5 mol//kg. This produced the results presented in Figure 6.1.

From the calculations it can be concluded that the long range electrostatic contribution is dominant at lower concentrations. The hard sphere contribution is getting more important at increasing concentration and with increasing cation diameter. The short range electrostatic contribution is small and has a parabolic form with a minimum when the ionic diameters are equal. The electrostatic contributions to $\ln(\gamma_{\pm})$ are negative and thus lower the activity coefficient. The hard sphere contribution is positive (repulsive) and enlarges the ionic activity coefficient.

An important question arising when using the MSA model is the value of the ionic diameter to use. This should be the hard core diameter of the hydrated ion: the diameter of the sphere that cannot be penetrated by another ion. This diameter is not given in literature and hard to determine. The effective diameter of an ion is dependent on the type of solvents present and the ion concentration. Generally, the effective anion and cation diameters decrease as the concentration increases. This is due to decreased availability of the solvent molecules for the secondary hydration shell ($r > \sigma_{water}$) and compression of the entire solvation shell. Articles on the MSA report the use of the Pauling diameter or a fitted diameter. In some publications, like Simonin

et al. (1997), a concentration dependent diameter is used, where the ionic diameter may vary with both salt concentrations and solvent ratios (Gering et al., 1989).

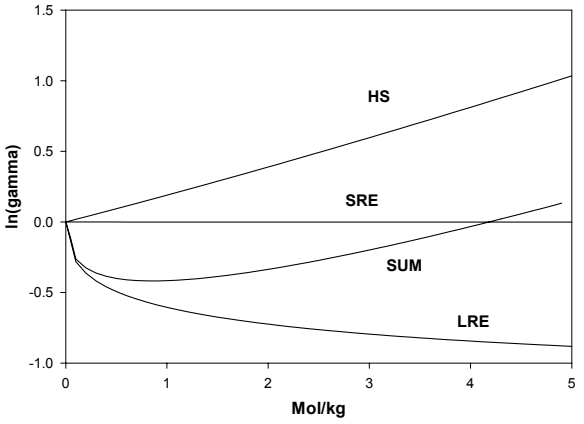

Figure 6.1: Contributions of the individual terms for the MSA mean ionic activity coefficient for water + NaCl at 298 K (HS = Hard sphere contribution, SRE = short-range electrostatic term, LRE = long-range electrostatic term, SUM = HS + SRE + LRE.

Nightingale (1959) has published three different ionic diameters for a large number of ions. They are:

- Pauling diameter: This diameter has been calculated from the interatomic distances from crystallographic data
- Stokes diameter: This diameter has been calculated from conductance experiments by the relations of Stokes and Einstein.
- Hydrated diameter: This is an effective hydrated diameter, calculated from a solvation model by Nightingale (1959)

Rashin and Honig (1985) have given radii of the dielectric cavities formed by the ions. These radii were used by them to reproduce experimental hydration enthalpies, using the Born model of ion hydration, with fairly good results. Table 6.1 gives ionic diameters for some selected ions.

Table 6.1: Comparison of ionic diameters in water (in nm)

Ion	Pauling[a]	Stokes[a]	Hydrated[a]	Cavity[b]
Na^+	0.190	0.368	0.716	0.336
Cl^-	0.362	0.242	0.664	0.387
Li^+	0.120	0.476	0.764	0.263
Ca^{2+}	0.198	0.620	0.824	0.372
NH_4^+	0.296	0.250	0.662	0.426
SO_4^{2-}	0.480	0.460	0.758	
Zn^{2+}	0.148	0.698	0.860	0.267

[a] Nightingale (1959);
[b] Rashin and Honig (1985)

In many publications a Pauling diameter is used for the anion and a fitted diameter for the cation. This is explained from the fact that the anion is generally hydrated to a smaller extent than the cation, because the association between anion and hydrogen is generally much weaker than the association between cation and oxygen. Therefore, the anion can be assumed to remain unhydrated. Calculations of mean ionic activity coefficients with MSA + hard sphere contribution showed that the Pauling diameter is too small for the NaCl-water system. In fact it is too small for all systems studied, except water + ammonium sulfate, which shows a behaviour different from the other electrolytes. The use of Stokes diameters or the ionic cavity diameters can be assumed to account more for the influence of the solvent on the diameter and does produce better results.

To test the performance of the Mean Spherical Approximation model, mean ionic activity coefficients were calculated for systems of NaCl, $CaCl_2$, $(NH_4)_2SO_4$ and $ZnSO_4$ + water. The objective of this choice of the electrolytes was to see if the MSA can cope with different classes of electrolytes (1:1, 1:2, 2:1, 2:2). The experimental ionic activity coefficients were obtained from Robinson and Stokes (1959) and converted to molar activity coefficients by Equation (5.23). In Figure 6.2 the results of the calculations are shown. The anionic diameters were fixed at the Pauling diameter, the cationic diameter was obtained from regression of the experimental data (Na^+: 0.31 nm, Ca^{2+}: 0.67 nm, Zn^{2+}: 0.23 nm, NH_4^+: 0.05 nm.)

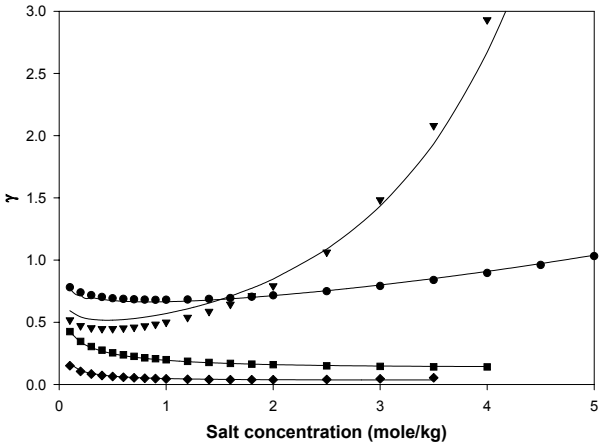

Figure 6.2: Experimental (markers) and calculated (lines) mean ionic activity coefficients for water + salt systems at 298 K. (● = NaCl, ▼ = $CaCl_2$, ■ = $(NH_4)_2SO_4$, ◆ = $ZnSO_4$)

It can be seen in Figure 6.2 that for the salt + water systems given a good description can be obtained with the primitive MSA model + hard sphere contribution.

6.4.2 Modelling of LLE of electrolyte solutions

As discussed earlier in this Chapter, the MSA theory gives a physically more correct description of the electrostatic interaction than the Debye-Hückel theory. Therefore, it was expected that a combination of the primitive MSA model and the NRTL model would perform better than the existing electrolyte NRTL models. Two options were studied to combine MSA theory with NRTL theory: MSA + molecular NRTL and MSA + electrolyte NRTL. These options are further discussed below.

Model 1: MSA + molecular NRTL

The first attempt in modelling liquid-liquid equilibria of electrolyte systems with an NRTL-MSA model was to follow the approach by Lee (1996). He used a molecular UNIFAC model for the calculation of the activity coefficients for the molecular species and the MSA for the calculation of the ionic activity coefficients. From Gibbs-

Duhem integration he derived an expression for the electrostatic contribution to the molecular species (Equation 6.26). A Born expression was added to the ionic activity coefficient. Using this so called ElecGC model, Lee could successfully describe vapour-liquid equilibria of a multicomponent mixture.

Here, the corresponding combination of the NRTL and the MSA model was chosen. The molecular NRTL of Renon and Prausnitz (1968) was used for the activity coefficients of the neutral species. The MSA activity coefficient (including the hard sphere term) is used for the description of the ionic activity coefficients. First, to get an impression if the molecular NRTL could handle the system without electrostatic terms it was tried to model the system with the molecular NRTL where NaCl was accounted for as an uncharged molecular component. It was found that satisfactory results for water + alcohol + salt systems were only obtained if at least one of the nonrandomness factors was adjusted by parameter regressions.

For the combination of a molecular NRTL with MSA and ionic hard sphere contribution, initially fixed ionic diameters were used, that were obtained by the least squares regression with experimental ionic activity coefficients (previous section). Since this did not seem to work, the diameters were also fitted, it was tried to use solvent dependent diameters that were mixed on mass fraction basis and it was tried to use concentration dependent diameters which required programming of additional terms in the MSA and Born activity coefficients, containing the derivatives of the diameter to the concentration. None of these approaches led to satisfactorily results. Assuming partial dissociation or accounting for the salt effect on the solution density did not improve the results.

Model 2: NRTL-MSA model

For combination with the local composition contribution of the electrolyte NRTL, the hard sphere contribution that is commonly used with the primitive MSA model is omitted. It was assumed that the short range interactions of the NRTL implicitly include the hard sphere repulsion of the ions. The hard sphere contribution was not present in the original MSA model, but was introduced later to obtain better fits of mean ionic activity coefficients and osmotic coefficients in concentrated aqueous solutions.

A model was proposed in which the local composition contribution from the electrolyte NRTL model and the MSA model are combined. The Born equation is used

again for the reference states. Stokes diameters were used for the MSA ionic diameters. Calculations were carried out on a data set of LLE of water + alcohol + salt systems at 298.1 K. The results were than compared with results of the original model of Chen et al. (1986), using the same initial values for the interaction parameters. It was found that both models give the same results. Apparently, the description of the electrostatic forces is only of minor importance and inadequacies in the model are compensated by small changes in the NRTL binary interaction parameters. It was concluded that although the MSA theory is physically more correct, the replacement of the Debye-Hückel contribution with an expression derived from primitive MSA theory does not lead to improvements in the performance of the model.

6.5 Applying the nonprimitive MSA model (Blum and Wei)

Since the results of Li et al. (1996) looked promising, the work with the NP-MSA was started by trying to reproduce their work. Therefore, the equations as summarized by Li et al. were programmed. Newton-Raphson iteration was used to solve the three characteristic parameters from the three equations that were scaled and made dimensionless for more rapid convergence. While programming and testing some mistakes were found in the publication of Li et al. (1996). Therefore the equations for the chemical potential were derived again from the solution found by Blum and Wei (1987b). For the reference state of the ions, it is common to use the infinite dilution state in water. This was also used here, but it had to be approached by extrapolations from calculations at low concentrations (10^{-6} mole/mole) since attempts to derive an analytic expression were not successful.

The routine for the NP-MSA was then used to reproduce internal energies given by Li et al. (1996). After some difficulties it was possible to approach the internal energies as found by Li et al. and those calculated from molecular simulations by Eggebrecht and Ozler (1990). However, although it was possible to get more or less the same results for the chemical potentials, attempts to reproduce the mean ionic activity coefficients as found by Li et al. (1996) and Liu et al. (1998) have failed. The activity coefficients calculated are usually much too small and change too rapidly with ionic concentration. According to the theory, for a zero dipole the non-primitive MSA has to approach the primitive MSA. This was checked and appeared to be the case.

Also, at zero ionic concentration the model should reduce to the Wertheim equation for the dielectric constant, this was also the case.

Two issues may contribute to the problems discussed here. Firstly, the choice of the initial values for the parameters Γ, b_2 and B_{10} and secondly the choice of the reference state. This was confirmed by professor Li (2001) who was asked for assistance. However, his computer programme was not available anymore. He advised not to use the model as described by Li et al. (1996), because it uses the same diameter for the same ion in different salts, which decreases the accuracy. The most recent paper from the group of professor Li on this subject is the one of Liu (1998) that does use different ionic diameters in different salts. In this paper also a SAFT contribution is used to account for hydrogen bond association. The low limit of the model used by Li is also the reference state and is 0.1 M. Li is now trying to improve the performance of the model in the low concentration region, but has not succeeded yet.

Because of these experiences, the work on the nonprimitive MSA model of Blum and Wei (1987) has not been continued and the decision was made to apply the extended electrolyte equation of state of Fürst and Renon (1993) instead.

6.6 Applying the extended electrolyte equation of state

Because the extended electrolyte equation of state seems a promising model for the correlation and prediction of VLE and LLE, it is worthwhile to apply this equation of state to the experimental data on water + caprolactam + solvent + ammonium sulfate systems as given in Chapter 3. This way, a comparison can be made between two fundamentally different methods of phase equilibrium calculations: the activity coefficient approach and the equation of state approach.

The equations for the electrolyte equation of state have been discussed in section . The electrolyte equation of state and its mixing rules have been developed and extended in a series of publications. The version programmed and used in this work is the one given by Zuo et al. (2000a, 2000b). To test the model, attempts were made to reproduce the results given by Zuo et al. (2000a) for vapour pressures of solvent + salt solutions and vapour-liquid equilibria of mixed-solvent electrolyte solutions. After solving some obscurities in the publication, it was possible to reproduce the vapour pressure calculations. Reproduction of the results on vapour-liquid equilibria was less

successful, but after repeated consultation of one of the authors, Dr. Zuo, it seems most likely that these problems were caused by using different sources of physical property data of the components. Similar observations were made for the liquid-liquid equilibrium calculations reported by Zuo et al. (2000b).

For the modelling of the experimental LLE data for the caprolactam containing systems with the electrolyte equation of state, none of the adjustable parameters were available yet in the literature and therefore had to be obtained otherwise. The critical properties of the components were taken from Reid et al. (1987). For caprolactam estimations were used, that were obtained from DSM and are given in Appendix I. The polar parameters for the various components were obtained from fits of the pure component vapour pressures as given by the polynomials by Reid et al. (1987) to the SRK-equation of Schwartzentrüber. The polar parameters are given in Appendix V, Table V.1.

The UNIQUAC interaction parameters for the Wong-Sandler mixing rule are obtained from regressions of the LLE of the nonelectrolyte systems with the (nonelectrolyte part of the) the electrolyte equation of state. In this case, two options are possible: the normally used expression for the interaction parameters (Equation 6.52) and the slightly different equation used by Zuo et al. (2000b), Equation (6.53):

$$\lambda_{ji} = \exp\left(-\tau_{ij}\right) \qquad \textbf{(6.52)}$$

$$\lambda_{ij} = \exp\left(-\tau^{0}_{ji} - \theta_j \theta_i \tau^{1}_{ji}\right) \qquad \textbf{(6.53)}$$

where θ_i is the surface fraction, τ_{ji} and τ_{ji}^{0} and τ_{ji}^{1} are unsymmetrical and symmetrical interaction parameters, respectively. It can be seen that in Equation (6.53) λ_{ij} is treated as a function of composition and one extra parameter per solvent pair has to be obtained by regression. For the representation of the LLE of the nonelectrolyte systems, this additional parameter is not really necessary as can be seen in Table 6.2. The interaction parameters for the data in this table are given in Appendix V.

To obtain binary interaction parameters (for the SR2 contribution) for solvent + salt, the procedure used by Zuo et al. (2000b) is to calculate these parameters from vapour pressure data of the solvent + salt systems. Unfortunately, it is not possible to find these data for the required solvent + ammonium sulfate systems. Calculations of mean

ionic activity coefficients of water + ammonium sulfate showed that in this case the parameters given by Zuo et al. (2000a, 2000b) for water + halide systems could satisfy. The average relative deviation found was 2.8 wt%. For the organic solvent + ammonium sulfate systems the values had to be found differently. Not only the salt is different, but also the organic solvents are very different from those in the systems used by Zuo et al., who gave parameters for halide + alcohol systems. Therefore, these parameters were obtained by regression of the ternary systems water + caprolactam + ammonium sulfate at 293 K, 313 K and 328 K.

To reduce the number of adjustable parameters, the interaction parameters for benzene, 1-heptanol, 2-heptanone and caprolactam + ammonium sulfate were assumed to be equal. The cationic diameter in the organic components was obtained in a similar way as the SR2 interaction parameters. Zuo et al. obtained the cationic Stokes diameters from conductivity data of the salt in the solvent concerned. However, conductivity data of ammonium sulfate in the required organic solvents were not available in literature.

Table 6.2: Average deviations[a] between experimental and calculated LLE of caprolactam containing systems. Representation of LLE using the electrolyte equation of state, applying two different equations for the UNIQUAC interaction parameter.

System	T	Equation (6.52)		Equation (6.53)	
	˚C	Δx (%)	Δw (%)	Δx (%)	Δw (%)
Water + benzene + caprolactam	20	1.5	1.7	1.5	1.3
	40	1.2	0.8	1.6	0.8
	60	1.9	2.1	1.3	1.9
Water + 1-heptanol + caprolactam	20	2.4	2.5	1.7	2.5
	40	2.0	2.7	1.3	2.4
	60	2.1	3.3	1.4	3.1
Water + 2-heptanone + caprolactam	20	1.9	1.8	2.5	2.6
	40	0.9	1.0	0.9	1.1
	60	1.7	2.8	1.5	2.3
Overall average deviation		1.7	2.1	1.5	2.0

[a] As defined by Equation (5.27)

All values for the interaction parameters used here, are given in Appendix V, Table V.3. For the modelling of the systems containing ammonium sulfate, initially Equation (6.53) was used and the SR2 interaction parameters for water were unchanged.

However, no satisfactory results could be obtained this way. Three options were then available to improve the performance of the model:

- Applying Equation (6.53) for the UNIQUAC interaction parameters
- Adjusting the SR2-interaction parameters for salt + water
- Considering caprolactam as a different type of component as the solvents and obtain different values for caprolactam +salt than for solvents + salt.

In case of the first option the number of adjustable parameters increases with the number of solvent +solvent binaries. Initially, it was attempted to use the results as obtained for the salt-free systems given in Table 6.2 and then to adjust only the SR2-interaction parameters for nonaqueous solvent + salt systems, but no satisfactory results could be obtained this way. Therefore, the procedure followed was to regress the ternary systems to obtain initial values for the interaction parameters and subsequently to use the quaternary systems to slightly adjust them. The results thus obtained can be found in Table 6.3. The adjusted parameters are given in Appendix V.

The second and third option mentioned give comparable results. With the second option the number of adjustable parameters increases with two. Only λ_5 and λ_6 were adjusted. Adjusting λ_3 and λ_4 did not give better results and complicated the regressions by causing numerical problems. It can be seen that moderately accurate results are obtained this way. Remarkably, for this option it was not necessary to include the UNIQUAC interaction parameters in the regression. The parameters from the salt-free regressions could be used. By including the mean ionic activity coefficients, it was taken care of that the mean ionic activity coefficients would have realistic values. For the third option the number of adjustable parameters is increased with four. In this case adjustion of the UNIQUAC parameters was not required.

For all three options the correction factor for the Born radius had to be obtained by regressions from the quaternary equilibrium data. Looking at Table 6.3, it can be seen that the first option gives the best results, however with more parameters. Figure 6.3 shows the results from option one for the system water + caprolactam + ammonium sulfate at 40˚C. It shows that the model largely overpredicts the region of demixing. In comparison with the original electrolyte NRTL model (Chen et al., 1986) the model gives a better prediction of the salt concentration in the organic phase.

Table 6.3: Correlation of LLE of systems with water (W), caprolactam (C), solvent (B = Benzene, 1-H = 1-Heptanol, 2-H = 2-Heptanone) and ammonium sulfate (AS), with the three options discussed in the text. Average deviations[b] are given as mass percents Δw or mole percents Δx.

System	T	Option 1		Option 2		Option 3		
	°C	Δx	Δw	Δx	Δw	Δx	Δw	
W + B + C	20	2.2	3.1	2.9	2.8	2.9	2.8	a
	40	2.0	2.1	2.7	1.4	2.7	1.4	a
	60	2.9	2.0	4.0	2.4	4.0	2.4	a
W + 1-H + C	20	1.3	2.6	1.6	2.8	1.6	2.8	
	40	1.5	3.0	1.4	3.0	1.4	3.0	
	60	1.6	4.0	1.7	4.0	1.7	4.0	
W + 2-H + C	20	3.5	3.5	3.8	3.1	3.8	3.1	
	40	2.0	1.7	3.2	1.2	3.2	1.2	
	60	2.1	2.1	4.0	3.5	4.0	3.5	
W + C + AS	20	1.3	4.5	1.5	4.8	1.3	4.1	
	40	1.0	3.7	1.2	3.9	1.0	3.1	
	55	0.9	1.7	1.2	2.2	0.6	1.4	a
W + C + B + AS	20	1.5	2.6	2.7	3.3	3.6	3.6	a
	40	1.8	1.4	2.7	2.0	3.5	2.1	a
	60	5.3	4.6	6.3	5.1	6.3	4.5	a
W + C + 1-H + AS	20	1.1	1.8	0.9	2.0	1.0	2.0	
	40	1.3	1.9	1.6	2.1	1.3	1.9	
	60	1.4	2.1	1.8	2.3	1.5	2.3	
W + C + 2-H + AS	20	1.3	3.0	2.4	4.4	2.8	4.6	
	40	4.2	4.3	4.7	5.3	1.8	3.8	
Average		2.0	2.8	2.6	3.1	2.5	2.9	
Adjustable parameters[c]		25[c]		24[d]		26[d]		

[a] Source of equilibrium data: De Haan and Niemann (1999)

[b] See Equation (5.27)

[c] All parameters were optimized simultaneously using the data for all systems in Table 5.3

[d] The 14 parameters fot the salt-free systems were optimized separately. See Table 6.2 and Appendix V, Table V.3

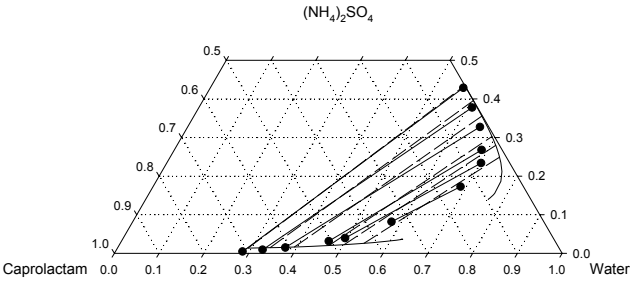

Figure 6.3: Representation of LLE for water + caprolactam + ammonium sulfate at 313.1 K, calculated with the electrolyte equation of state. Markers and dashed lines are experiments, solid lines are calculated.

6.7 Discussion

From the models based on MSA theory discussed in this chapter, only the extended electrolyte equation of state, could give reasonable results. However, even in this case some problems were found. The predictive value of the model was reduced by the lack of relevant experimental data and by the need to adjust parameters for a better performance of the model. In Table 6.4 a comparison is made of the best results for the LLE of caprolactam containing systems as obtained with the extended electrolyte equation of state, the electrolyte NRTL model of Chen et al. (1986) and the modified extended electrolyte NRTL model presented in this work. Also, the difference is shown in the number of parameters that have to be obtained by regressions with the experimental data itself. The table clearly shows that from the calculations presented in this work, the best results are obtained when the modified extended electrolyte NRTL model is used.

Table 6.4: Correlation of LLE of systems with water (W), caprolactam (C), solvent (B = Benzene, 1-H = 1-Heptanol, 2-H = 2-Heptanone) and ammonium sulfate (AS) using the modified extended electrolyte NRTL (M-E-NRTL), original electrolyte NRTL[b] (E-NRTL) or extended electrolyte equation of state (AEEOS)

System	T	M-E-NRTL		E-NRTL[b]		AEEOS		
	°C	Δx	Δw	Δx	Δw	Δx	Δw	
W + B + C	20	1.1	1.9	0.8	1.7	2.2	3.1	a
	40	1.7	2.3	1.2	1.8	2.0	2.1	a
	60	2.1	1.7	2.1	1.4	2.9	2.0	a
W + 1-H + C	20	2.1	3.9	1.9	4.2	1.3	2.6	
	40	1.4	3.0	1.8	3.2	1.5	3.0	
	60	2.2	4.3	2.7	4.2	1.6	4.0	
W + 2-H + C	20	1.9	2.3	1.9	2.3	3.5	3.5	
	40	1.6	1.7	2.0	1.8	2.0	1.7	
	60	2.8	2.8	3.5	3.2	2.1	2.1	
W + C + AS	20	0.9	2.7	1.6	4.7	1.3	4.5	
	40	0.6	1.4	1.2	3.3	1.0	3.7	
	55	1.6	2.5	2.2	3.4	0.9	1.7	a
W + C + B + AS	20	1.5	2.1	1.7	2.6	1.5	2.6	a
	40	0.9	1.1	1.1	1.4	1.8	1.4	a
	60	1.5	1.9	2.0	2.4	5.3	4.6	a
W + C + 1-H + AS	20	1.4	2.0	1.4	2.7	1.1	1.8	
	40	1.6	1.2	1.4	1.6	1.3	1.9	
	60	1.3	1.5	1.3	1.5	1.4	2.1	
W + C + 2-H + AS	20	1.8	2.8	1.8	3.1	1.3	3.0	
	40	1.3	1.5	1.2	1.5	4.2	4.3	
Average deviation		1.5	2.2	1.7	2.6	2.0	2.8	
Adjustable parameters		25		24		25		

[a] Source of data: De Haan and Niemann (1999)

[b] Chen et al. (1986) and Aspen Technology (1999)

7. Conclusions and Outlook

This thesis discusses both experiments and calculations that are of importance for the modelling of the extraction process of caprolactam. In this extraction process liquid-liquid equilibria are present of mixtures containing the salt ammonium sulfate in the range of concentrations from low up to saturation. Good understanding of these liquid-liquid equilibria is essential for the simulation and design of this process and similar processes with mixed solvent electrolyte solutions present.

For the experimental work, the procedure was to prepare a mixture that was expected to show demixing and to equilibrate this mixture in a thermostated vessel. The vessel has sample ports for each phase, from which samples were taken which were analysed by gaschromatography, Karl-Fischer titration and titration with bariumperchlorate. Liquid-liquid equilibria for water + caprolactam + ammonium sulfate and water + benzene + caprolactam were determined and compared with literature data. Good agreement was found. After that, experiments were carried out on the liquid-liquid equilibria of the ternary and quaternary systems containing caprolactam, water, solvent and ammonium sulfate at 293 K, 313 K and 333 K. As the solvents 1-heptanol and 2-heptanone were chosen. The experiments with these solvents show that the mutual solubility of water and the organic solvent can be increased by the addition of caprolactam. When enough caprolactam is added, the systems water + solvent + caprolactam can be brought to a critical point and to full miscibility.

At higher temperatures the solubility of caprolactam in both the organic solvent and water increases. The solubility of caprolactam in the organic solvent increases more rapidly than the solubility in water, as can be seen from the change in the slope of the tie-lines and the slope of the distribution curves of caprolactam. The region in which demixing occurs becomes smaller at higher temperatures. Depending on the solvent used, the caprolactam is distributed in a certain ratio between the two phases. It was found that the solubility of caprolactam in 1-heptanol was much higher than the solubility in benzene and 2-heptanone. In the case of 1-heptanol, also at lower temperatures most caprolactam dissolves in the organic phase. The experiments with 2-heptanone show an almost similar phase behaviour as benzene, but the region in which demixing occurs is smaller. Therefore, for the (backward) extraction of caprolactam 2-heptanone will be more suitable than 1-heptanol.

Addition of salt to the two-phase system leads to salting-out of the caprolactam from the aqueous phase to the organic phase. Almost all the salt will dissolve in the aqueous phase. The hydration of all the ions will reduce the availability of the water molecules for the solvation of caprolactam and the caprolactam will prefer to dissolve in the organic phase. At high ammonium sulfate concentrations nearly all caprolactam will dissolve in the organic phase. This effect was observed for each of the solvents investigated.

For benzene and 2-heptanone, also three-liquid phase equilibria were encountered and determined. The pattern of the phase behaviour was studied at different temperatures and salt concentrations. At a certain caprolactam and salt concentration, the bottom phase in a two–phase system of water + solvent + caprolactam + ammonium sulfate will split up into two identical liquid phases, resulting in a three-liquid phase equilibrium. With increasing salt concentration, the bottom phase will contain less caprolactam and finally will consist of only water and ammonium sulfate. The middle phase and the top phase will become richer in caprolactam. The compositions of the middle and the top phase will approach the same values until finally they are identical. From here on, a two-liquid phase equilibrium is found. So, a progression is found with increasing salt concentration, showing a transition from two liquid phases to three liquid phases at higher salt concentrations and to two liquid phases again at still higher concentrations. For benzene the LLLE measurements were carried out at different temperatures: With increasing temperature the range of concentrations where three liquid phases are present, is shrinking and finally disappears around 331 K. The tri-critical point of the system water + benzene + caprolactam + ammonium sulfate, where the three liquid phases become identical, was not determined but its location could be estimated from the experiments.

The experimental liquid-liquid equilibrium data could successfully be correlated using an activity coefficient model based on a modified extended electrolyte NRTL model, presented in this work. The modified electrolyte NRTL model includes the solvent composition dependency of the solution properties by using mixing rules for the solution properties, which is taken into account in the derivation of the activity coefficients. In this way a better correlation is obtained of the salt concentration in the organic phase, than with the original model. One of the major shortcomings observed for the original model was the fact that it predicted too low values of the salt concentration in the organic phase. By the addition and modification of a Brønsted-Guggenheim contribution an improved representation of equilibrium data near the

solution critical point was obtained, making it possible to predict the full binodal curve. The results of the model are better than those obtained with the original electrolyte NRTL model (Chen et al., 1986) as has been shown for a large number of water + solvent + salt systems and for the systems containing caprolactam.

The modelling of three-liquid phase equilibria puts a high demand on the consistency of the model. However, a qualitatively good representation could be obtained of experimental three-liquid phase equilibrium data for the systems water + 2-heptanone + caprolactam + ammonium sulfate, water + benzene + caprolactam + ammonium sulfate and water + benzene + ethanol + ammonium sulfate. Using the model, it is possible to predict the location of the critical tie-lines, but the quality of the values obtained is only reasonable. Attempts to use the original electrolyte NRTL (Chen et al., 1986) to describe LLLE were unsuccessful.

A disadvantage of the extended electrolyte NRTL model is the lack of physical background and the large number of adjustable parameters that has to be obtained by regression of experimental data. Therefore, it would be desirable to have a more fundamental model with more predictive qualities. To this end, some additional calculations were performed using primitive Mean Spherical Approximation (MSA) theory, using nonprimitive MSA theory and using an electrolyte equation of state, incorporating MSA theory. None of these models showed results comparable to or better than the results obtained with the extended electrolyte NRTL model. Best results were obtained with the extended electrolyte equation of state, but this model still requires a lot of research to be done before it can be used as a substitute for the electrolyte NRTL model. The main problem of this equation of state is that it requires a relatively large amount of different types of data for the salt, which represents a problem in the case of ammonium sulfate. In that case the values have to be obtained by regression of equilibrium data, which reduces the predictive value of the model.

Outlook

The area of thermodynamics of demixing in electrolyte solutions still requires much research. As also follows from this work new and appealing electrolyte models are published, but often do not provide enough accuracy and flexibility to be used in industry. For use in industry, models like the extended electrolyte NRTL model are much more suitable. The modification of the extended electrolyte NRTL model

presented in this work enables a better description of the relevant phase equilibria in the extraction process of caprolactam. This work will make it easier to simulate and to optimize extraction processes with salts present, like the extraction process of caprolactam. It is the expectation that this model could be of use also in many other extraction processes involving concentrated electrolyte solutions. To investigate this, application of the model to other systems is desirable.

Due to the increasing interest for biotechnological processes, there will be a need for models that can cope with the kind of systems that are present in these processes. These systems usually involve many charged species such as salts and proteins. Also, partitioning of components in a mixture by the addition of salt is a common separation technology for biologically active molecules that degrade at higher temperatures. In both cases models are required that describe mixed electrolyte systems, that make it possible to calculate the many complex equilibria and that account for association. Therefore, it is recommended to extend the field of research of the current research project to this kind of processes. To reduce the number of adjustable parameters in the model, it is also desirable to investigate the possibility of using a kind of group contribution approach for the NRTL interaction parameters. Unfortunately, this also requires a lot of experimental equilibrium data of various kinds of systems.

It is believed that in the future more fundamental models like the Mean Spherical Approximation will become more important, although the results published in this report do not point in this direction. The major drawback of models like the electrolyte NRTL model is that they have many adjustable parameters with doubtful physical meaning. Therefore, a model with more predictive power, based on more physical background is highly desirable. A model based on nonprimitive MSA theory could be of use here, if an analytical solution is available.

Appendices

I. Selected physical properties
II. Water + alcohol + salt systems
III. Adjustable parameters Electrolyte NRTL
IV. Modified Extended Electrolyte NRTL model
V. Parameters AEEOS

Appendix I: Selected physical properties

Born radii

Table I.1: Born radii as used in the Electrolyte NRTL models (Rashin and Honig,1985)

Ion	NH_4^+	K^+	Na^+	SO_4^{2-}	Cl^-	F^-	Br^-
Radius (nm)	0.213	0.217	0.168	0.300	0.193	0.142	2.087

Dielectric constant: $\varepsilon_r = A + B \cdot T + C \cdot T^2 + D \cdot T^3$ [-]

with T in K

Table I.2: Dielectric constants as a function of temperature. The polynomial coefficients are as given by Lide (1995), except for caprolactam which were calculated from experimental data of water + caprolactam mixtures.

	A	B	C	D
		K^{-1}	K^{-2}	K^{-3}
Water	249.21	-0.79069	7.2997E-4	
Benzene	2.6706	-0.91648E-03	-.14257E-5	
1-Heptanol	60.662	-.24049	.25155E-3	
2-Heptanone	38.348	-.12531	.12005E-3	
Caprolactam	233.047	-0.7985	0.00074	
Methanol	193.41	-0.92211	1.2839E-3	
Ethanol	151.45	-.87020	.19570E-2	-0.15512E-5
1-Propanol	98.045	-0.3686	3.6422E-4	
2-Propanol	104.16	-0.41011	4.2049E-4	
1-Butanol	105.78	-0.50587	8.4733E-4	-0.48841E-6
2-Butanol	138.50	-0.75146	1.4086E-3	-0.89512E-6
1-Pentanol	73.397	-0.28165	2.8427E-4	
Butanone	15.457	0.090152	-0.271E-3	

Density: $d = \frac{M_w \cdot A}{B^{1+(1-T/C)^D}}$ [kg/m^3]

with M_w in mol/kg and T in K

Table I.3: Liquid densities as a function of temperature. The polynomial coefficients are as given by Perry (1997), except for caprolactam which were calculated from experimental data of water + caprolactam mixtures.

	A	B	C	D
	mol/m^3		K	
Water	5.4590	0.30542	647.13	0.08100
Benzene	1.0162	0.26550	562.16	0.28212
1-Heptanol	.60481	0.26320	631.90	0.27300
2-Heptanone	.56213	0.23385	576.00	0.26180
Caprolactam	3.66956	0.533137	608.295	0.998512
Methanol	2.2880	0.26850	512.64	0.24530
Ethanol	1.6480	0.27627	513.92	0.23310
1-Propanol	1.2350	0.27136	536.78	0.24000
2-Propanol	1.2400	0.27342	508.30	0.23530
1-Butanol	0.9650	0.26660	563.05	0.24419
2-Butanol	0.9660	0.26064	536.05	0.27460
1-Pentanol	0.8164	0.26730	586.15	0.25060
Butanone	0.9377	0.25035	535.50	0.29964

Critical properties caprolactam:

Critical temperature : 855.00 K
Critical pressure : 52.080 bar
Critical volume : 0.35088 $m^3/kmol$
Acentric factor : 0.259

Appendix II: Water + alcohol + salt systems

Results for water + alcohol + salt systems, published as: G.H. van Bochove, G.J.P. Krooshof, Th.W. de Loos, Fluid Phase Equilib. (2000) 171, 45-58

Table II.1: Average deviations in mole fractions (Δx) and mass fractions (Δw) of the representation of some liquid-liquid equilibria of ternary mixed solvent electrolyte systems at 298 K.

	Present model		Chen's model		Source[a]
	Δx (%)	Δw (%)	Δx (%)	Δw (%)	
Water + 1-propanol + NaCl	0.7	1.2	1.6	2.2	1
Water + 2-propanol + NaCl	0.3	0.4	1.7	2.3	1
Water + 1-butanol + NaCl	2.2	1.3	2.9	1.6	1
Water + 2-butanol + NaCl	4.7	3.1	4.8	3.0	1
Water + 1-pentanol + NaCl	1.2	0.5	1.1	0.5	3
Water + butanone + NaCl	2.1	0.9	2.1	1.6	3
Water + 1-butanol + KBr	1.7	1.1	1.5	1.2	3
Water + butanone + KBr	1.3	0.7	1.4	0.7	3
Water + 1-butanol + KCl	2.2	1.3	2.2	1.3	3
Water + butanone + KCl	1.7	0.8	1.7	0.8	3

[a] Source of data: 1 = De Santis et al., 1976
2 = Gomis et al., 1999
3 = Li et al., 1995

Table II.2: Mean ionic activity coefficients at 298 K of some water + salt systems. Results were obtained by simultaneous regressions with the LLE presented in table 1. Experimental data from Robinson and Stokes (1959)

	Present model	Chen's model
	$\Delta\gamma_{\pm}$ (%)	$\Delta\gamma_{\pm}$ (%)
Water + NaCl	6.0	10.0
Water + KBr	1.4	3.4
Water + KCl	0.7	0.8
Water + $(NH_4)_2SO_4$	4.2	5.2

Table II.3: Parameters for the systems in Table II.1 and II.2. NRTL nonrandomness factors α were fixed at values of 0.10 (water-salt), 0.20 (solvent or water-solvent) or 0.30 (solvent-salt).

Component 1	Component 2	Presented model			Chen's model	
		τ_{12}	τ_{21}	β_{12} kg·K/mol	τ_{12}	τ_{21}
Water	1-Propanol	1.591	0.375	589.5	1.25	0.489
Water	2-Propanol	1.859	0.018	2008.5	0.585	0.595
Water	1-Butanol	4.688	-0.763	-	4.897	-0.904
Water	2-Butanol	3.751	-0.669	-	3.845	-0.758
Water	1-Pentanol	5.736	-0.522	-	5.562	-0.565
Water	Butanone	2.773	0.250	-	2.777	0.257
Water	NaCl	-11.12	-1.092	-	-13.00	-1.971
Water	KCl	-14.94	26.98	-	-14.43	23.07
Water	KBr	-11.07	-0.552	-	-14.87	-0.686
1-Propanol	NaCl	-9.676	30.00	-	-7.875	0.193
2-Propanol	NaCl	-11.59	10.37	-	-5.353	2.290
1-Butanol	NaCl	-4.559	1.418	-	-8.202	0.356
2-Butanol	NaCl	-4.501	3.059	-	-5.797	2.454
1-Pentanol	NaCl	-7.691	1.401	-	-10.70	6.803
Butanone	NaCl	-5.719	0.626	-	-5.962	1.795
1-Propanol	1-Butanol	-4.519	3.088	-	-4.716	1.444
1-Butanol	KBr	-7.608	28.19	-	-5.396	2.159
Butanone	KBr	-4.422	-0.989	-	-4.248	-0.226
1-Butanol	KCl	-10.86	29.98	-	-8.939	6.719
Butanone	KCl	-3.854	1.632	-	-4.019	1.937

Appendix III: Adjustable parameters Electrolyte NRTL

III.1 Parameters for Table 5.1 & 5.2

Table III.1: Parameters for the systems in Table 5.1 and 5.2. NRTL nonrandomness factors α_{ij} were fixed at values of 0.10 (water-salt), 0.20 (solvent or water-solvent) or 0.30 (solvent-salt). NRTL binary interaction parameters τ are given by: $\tau_{ij} = A_{ij}/T$.

Component 1	Component 2	Presented model			Chen's model	
		A_{12}	A_{21}	β_{12}	A_{12}	A_{21}
		K	K	kg·K/mol	K	K
Water	1-Propanol	507.1	90.4	346.2	286.6	297.8
Water	2-Propanol	569.5	-5.7	1835.5	-55.2	839.7
Water	1-Butanol	1316.1	-209.2	-	1325.2	-216.9
Water	2-Butanol	1089.8	-188.1	-	1103.5	-198.3
Water	1-Pentanol	1615.4	-153.0	-	1646.4	-154.4
Water	Butanone	797.8	110.4	-	802.2	107.6
Water	NaCl	-3374.9	-106.9	-	-5343.9	-200.6
Water	KCl	-2893.0	257.8	-	-6683.7	2.1
Water	KBr	-5804.8	14.8	-	-6938.4	-71.5
Water	KF	-3713.5	-118.3	-	-10000.0	-396.0
Water	NaBr	-3366.4	-294.3	-		
1-Propanol	NaCl	-2913.2	4519.8	-	-1689.7	715.8
2-Propanol	NaCl	-3480.9	1262.6	-	-1612.9	697.7
1-Butanol	NaCl	-1216.2	1654.5	-	-2173.2	125.8
2-Butanol	NaCl	-1150.0	735.8	-	-1902.2	480.6
1-Pentanol	NaCl	-2550.7	5000.0	-	-3862.5	-49.5
Butanone	NaCl	-1639.9	-86.1	-	-1936.3	-92.2
1-Propanol	NaBr	-2128.6	-762.2	-		
1-Propanol	KCl	-2069.4	3345.7	-	-1754.3	638.5
1-Butanol	KCl	-1773.2	2200.3	-	-3121.9	1324.3
Butanone	KCl	-1050.0	1683.0	-	-1915.9	328.3
1-Pentanol	KCl	-1803.2	2540.6	-	-3220.9	-134.0
1-Propanol	KF	-3346.0	977.7	-	-3042.2	-718.1
2-Propanol	KF	-3822.5	2086.1	-	-3035.2	527.8
1-Propanol	1-Butanol	-1355.0	3254.0	-	-1436.2	914.1
1-Propanol	1-Pentanol	-1730.2	893.5	-	-1912.6	506.7
1-Butanol	KBr	-1794.9	933.3	-	-2185.6	917.2
Butanone	KBr	-1255.1	-279.6	-	-1534.3	-44.4

III.2 Parameters for Table 5.3

Table III.2: NRTL binary interaction parameters for the systems in Table 5.3. All nonrandomness factors (α) are fixed at 0.20, except those with caprolactam, which were fixed at 0.30. NRTL binary interaction parameters τ are given by: $\tau_{ij} = A_{ij}/T$.

Component 1	Component 2	Presented model			Chen's model	
		A_{12}	A_{21}	β_{12}	A_{12}	A_{21}
		K	K	kg·K/mol	K	K
Water	Benzene	1390.6	813.4	-	1407.1	887.7
Water	1-Heptanol	1756.3	-70.4	-	1899.2	-80.2
Water	2-Heptanone	1543.5	226.5	-	1530.3	229.9
Water	Caprolactam	1193.2	-671.4	231.2	1096.4	-666.7
Benzene	Caprolactam	-222.9	-4.7	-	-417.9	175.1
1-Heptanol	Caprolactam	-559.6	147.6	-	4392.3	-837.1
2-Heptanone	Caprolactam	-110.8	21.2	-	-137.6	27.4
Water	$(NH_4)_2SO_4$	2937.9	-1407.6	-	2752.3	-1315.1
Benzene	$(NH_4)_2SO_4$	4278.9	3323.4	-	3785.0	3235.2
1-Heptanol	$(NH_4)_2SO_4$	1606.1	7267.7	-	4069.1	995.9
2-Heptanone	$(NH_4)_2SO_4$	1273.6	5046.2	-	5241.6	1853.1
Caprolactam	$(NH_4)_2SO_4$	546.4	3454.3	-	855.4	3673.5

III.3 Parameters for Table 5.4

Parameters Table 5.4, Van Bochove et al., 1999

Table III.3: NRTL binary interaction parameters for the systems in Table 5.4. All nonrandomness factors (α) are fixed at 0.20, except those for solvent + caprolactam, which were fixed at 0.30. NRTL interaction parameters τ are given by: $\tau_{ij} = A_{ij}/T$.

Component 1	Component 2	Presented model		
		A_{12} K	A_{21} K	β_{12} kg·K/mol
Water	Benzene	1383.5	696.3	-
Water	1-Heptanol	1876.7	-39.8	-
Water	Caprolactam	1171.0	-649.4	29.65
Benzene	Caprolactam	-296.5	153.5	-
1-Heptanol	Caprolactam	953.8	-734.6	-
Water	$(NH_4)_2SO_4$	2888.4	-1369.4	-
Benzene	$(NH_4)_2SO_4$	4074.0	3232.9	-
1-Heptanol	$(NH_4)_2SO_4$	1620.9	4819.1	-
Caprolactam	$(NH_4)_2SO_4$	576.0	3598.2	-

Parameters Table 5.4, Van Bochove et al., 2002

Table III.4: NRTL binary interaction parameters for the systems in Table 5.4. All nonrandomness factors (α) are fixed at 0.20, except those for solvent + caprolactam, which were fixed at 0.30. NRTL interaction parameters τ are given by: $\tau_{ij} = A_{ij}/T$.

Component 1	Component 2	A_{12} K	A_{21} K	β_{12} kg·K/mol
Water	Benzene	1841.7	798.8	-
Water	1-Heptanol	1990.7	-16.7	-
Water	2-Heptanone	1668.2	218.1	-
Water	Ethanol	237.7	-254.4	136.5
Water	Caprolactam	1274.5	-706.1	137.9
Benzene	Caprolactam	-326.9	203.5	-
1-Heptanol	Caprolactam	842.1	-681.6	-
2-Heptanone	Caprolactam	69.9	-93.1	-
Benzene	Ethanol	290.2	-164.4	-
Water	$(NH_4)_2SO_4$	3025.2	-1421.5	-
Benzene	$(NH_4)_2SO_4$	4070.7	3232.6	-
1-Heptanol	$(NH_4)_2SO_4$	1150.1	3218.5	-
2-Heptanone	$(NH_4)_2SO_4$	1605.6	9.5	-
Ethanol	$(NH_4)_2SO_4$	1161.5	1742.0	-
Caprolactam	$(NH_4)_2SO_4$	487.9	3156.8	-

Parameters Table 5.4

Table III.5: NRTL binary interaction parameters for the systems in Table 5.4, option 1. All nonrandomness factors (α) are fixed at 0.20, except those for solvent + caprolactam, which were fixed at 0.30. NRTL interaction parameters τ are given by: $\tau_{ij} = A_{ij}/T$.

Component 1	Component 2	A_{12} K	A_{21} K	β_{12} kg·K/mol
Water	Benzene	1799.9	711.4	-
Water	1-Heptanol	1873.2	-79.1	-
Water	2-Heptanone	1586.4	208.2	-
Water	Ethanol	310.1	-188.1	838.1
Water	Caprolactam	1209.4	-661.5	361.2
Benzene	Caprolactam	-275.3	232.4	-
1-Heptanol	Caprolactam	-782.2	1020.4	-
2-Heptanone	Caprolactam	30.1	-37.7	-
Benzene	Ethanol	458.5	-158.9	-
Water	$(NH_4)_2SO_4$	2928.9	-1380.8	-
Benzene	$(NH_4)_2SO_4$	3525.3	3441.7	-
1-Heptanol	$(NH_4)_2SO_4$	934.2	951.1	-
2-Heptanone	$(NH_4)_2SO_4$	692.7	1043.2	-
Ethanol	$(NH_4)_2SO_4$	1169.0	1651.5	-
Caprolactam	$(NH_4)_2SO_4$	546.6	3127.9	-

Table III.6: NRTL binary interaction parameters for the systems in Table 5.4, option 2. All nonrandomness factors (α) are fixed at 0.20, except those for solvent + caprolactam, which were fixed at 0.30. NRTL parameters τ are given by: $\tau_{ij} = A_{ij}/T + B_{ij}(1\text{-}293.1/T)$.

Component 1	Component 2	A_{12} K	A_{21} K	B_{12}	B_{21}	β_{12} kg·K/mol
Water	Benzene	1793.3	713.2	1.160	-0.782	-
Water	1-Heptanol	1876.1	-77.5	3.067	-1.398	-
Water	2-Heptanone	1569.8	216.1	2.289	0.685	-
Water	Ethanol	309.2	-188.2	2.398	-0.403	839.5
Water	Caprolactam	1195.5	-662.2	2.318	-0.851	368.2
Benzene	Caprolactam	276.0	235.8	-2.026	-1.652	-
1-Heptanol	Caprolactam	794.6	1015.1	-6.263	19.15	-
2-Heptanone	Caprolactam	28.0	-38.1	-4.396	0.908	-
Benzene	Ethanol	461.9	-158.2	-9.107	-0.127	-
Water	$(NH_4)_2SO_4$	2922.1	-1384.7	-	-	-
Benzene	$(NH_4)_2SO_4$	3529.8	3440.8	-	-	-
1-Heptanol	$(NH_4)_2SO_4$	1158.1	1068.0	-	-	-
2-Heptanone	$(NH_4)_2SO_4$	804.2	1133.2	-	-	-
Ethanol	$(NH_4)_2SO_4$	1169.3	1653.0	-	-	-
Caprolactam	$(NH_4)_2SO_4$	537.8	3167.4	-	-	-

Table III.7: NRTL binary interaction parameters for the systems in Table 5.4, option 3. All nonrandomness factors (α) are fixed at 0.20, except those for solvent + caprolactam, which were fixed at 0.30. NRTL interaction parameters τ are given by: $\tau_{ij} = A_{ij}/T + B_{ij}(1-293.1/T)$.

Component 1	Component 2	A_{12} K	A_{21} K	B_{12}	B_{21}	β_{12} kg·K/mol
Water	Benzene	1793.3	713.2	1.16	-0.782	-
Water	1-Heptanol	1876.1	-77.7	3.072	-1.404	-
Water	2-Heptanone	1570.4	216.3	2.286	0.676	-
Water	Ethanol	317.9	-187.3	3.363	-1.399	788.3
Water	Caprolactam	1194.6	-662.2	2.323	-0.849	367.8
Benzene	Caprolactam	-276.3	235.6	-2.031	-1.652	-
1-Heptanol	Caprolactam	-793.1	1021.0	-6.186	19.62	-
2-Heptanone	Caprolactam	28.0	-38.1	-4.384	0.893	-
Benzene	Ethanol	463.4	-155.4	-9.170	-0.127	-
Water	$(NH_4)_2SO_4$	2922.2	-1384.7	2.647	-2.050	-
Benzene	$(NH_4)_2SO_4$	3529.9	3440.7	24.81	-0.520	-
1-Heptanol	$(NH_4)_2SO_4$	1126.4	1014.7	-3.638	-7.641	-
2-Heptanone	$(NH_4)_2SO_4$	800.6	1132.1	-4.017	20.98	-
Ethanol	$(NH_4)_2SO_4$	1171.1	1659.2	-2.542	-8.270	-
Caprolactam	$(NH_4)_2SO_4$	534.7	3162.9	5.406	-52.98	-

III.3 Parameters for Table 5.5

Table III.8: Parameters for the results in Table 5.5 for the electrolyte NRTL model with full dissociation and with partial dissociation, using interaction parameters for ion pair and molecular salt. NRTL interaction parameters τ are given by: $\tau_{ij} = A_{ij}/T$.

Component 1	Component 2	No dissociation		Option 1		
		A_{12}	A_{21}	A_{12}	A_{21}	α_{12}
		K	K	K	K	
Water	1-Propanol	402.2	169.8	37.1	658.2	0.2
Water	2-Propanol	10.5	657.9	398.6	186.6	0.2
Water	1-Butanol	1408.9	-241.2	1403.5	-238	0.2
Water	2-Butanol	1098.7	-191.4	1093.2	-186.5	0.2
Water	1-Pentanol	1663.3	-164.7	1663.0	-163.0	0.2
Water	NaCl	4137.3	-113.5	-4195.6	-116.1	0.1
1-Propanol	NaCl	1758.4	710.7	-1812.8	520.2	0.3
2-Propanol	NaCl	1889.9	112.7	-1946.8	28.1	0.3
1-Butanol	NaCl	-2152.5	205.5	-2467.4	41.8	0.3
2-Butanol	NaCl	-1777.4	1089.2	-1797.6	1255.3	0.3
1-Pentanol	NaCl	-2502.4	884.9	-3137.7	296.3	0.3
1-Propanol	1-Butanol	-1303.7	751.1	-1311.2	817.3	0.2
1-Propanol	1-Pentanol	-1792.1	601.1	-1796.8	643.3	0.2
NaCl (m)	NaCl			-3144.7	-173.9	0.2
ln K				1.76		

Table III.9: Parameters for the results in Table 5.5 for the electrolyte NRTL model with partial dissociation, using interaction parameters for solvent + molecular salt (option 2). or for all components + molecular salt (option 3). NRTL interaction parameters τ are given by: $\tau_{ij} = A_{ij}/T$.

Component 1	Component 2	Option 2		Option 3		
		A_{12}	A_{21}	A_{12}	A_{21}	α_{12}
		K	K	K	K	
Water	1-Propanol	402.5	226.6	402.4	226.8	0.2
Water	2-Propanol	67.0	649.8	67.8	649.3	0.2
Water	1-Butanol	1382.4	-231.9	1382.1	-231.7	0.2
Water	2-Butanol	1098.8	-191.0	1098.7	-191.0	0.2
Water	1-Pentanol	1632.0	-161.2	1632.6	-161.1	0.2
Water	NaCl	-4158.7	-117.0	-4158.2	-116.9	0.1
1-Propanol	NaCl	-1914.4	852.1	-1915.0	851.5	0.3
2-Propanol	NaCl	-1995.7	88.0	-1996.1	89.5	0.3
1-Butanol	NaCl	-2288.1	191.1	-2275.9	200.6	0.3
2-Butanol	NaCl	-1774.6	1117.8	-1792.2	1065.3	0.3
1-Pentanol	NaCl	-3003.2	655.2	-3149.9	637.6	0.3
1-Propanol	1-Butanol	-1335.0	1036.0	-1336.2	1041.4	0.2
1-Propanol	1-Pentanol	-1834.7	811.9	-1834.7	810.7	0.2
Water	NaCl (m)			-2.8	-0.7	0.2
1-Propanol	NaCl (m)	120.1	-489.0	132.7	-489.5	0.2
2-Propanol	NaCl (m)	653.7	-451.2	662.7	-448.9	0.2
1-Butanol	NaCl (m)	1710.0	1508.2	1821.5	1322.2	0.2
2-Butanol	NaCl (m)	1836.6	2340.3	2096.6	1699.7	0.2
1-Pentanol	NaCl (m)	1528.0	2279.0	1451.7	2352.2	0.2
NaCl (m)	NaCl			-3.0	0.2	0.2
ln K		1.22		1.22		

Table III.10: Parameters for the results in Table 5.6 for the electrolyte NRTL model with full dissociation and with partial dissociation, using interaction parameters for all components + molecular salt (option 3). The nonrandomnessfactors are as given in Table III.8. NRTL interaction parameters τ are given by: $\tau_{ij} = A_{ij}/T$.

Component 1	Component 2	full dissociation			partial dissociation		
		A_{12} K	A_{21} K	β_{12} kgK/mol	A_{12} K	A_{21} K	β_{12} kgK/mol
Water	1-Propanol	496.6	110.2	455.6	483.6	128.6	560.8
Water	2-Propanol	547.5	37.4	2083.9	563.3	12.7	1881.9
Water	1-Butanol	1378.5	-231.1	-	1391.8	-236.5	-
Water	2-Butanol	1083.5	-184.4	-	1092.8	-189.7	-
Water	1-Pentanol	1619.1	-160.1	-	1629.3	-161.5	-
Water	NaCl	-3319.9	-89.7	-	-3332.3	-98.0	-
1-Propanol	NaCl	-2838.3	9647.7	-	-2859.1	8686.8	-
2-Propanol	NaCl	-3470.3	1967.6	-	-3446.8	1779.0	-
1-Butanol	NaCl	-1264.8	355.0	-	-1562.7	221.5	-
2-Butanol	NaCl	-1184.9	652.8	-	-1185.0	669.1	-
1-Pentanol	NaCl	-1684.4	2025.1	-	-1693.0	895.0	-
1-Propanol	1-Butanol	-1317.3	1017.7	-	-1284.4	936.5	-
1-Propanol	1-Pentanol	-1741.3	883.3	-	-1755.0	869.4	-
Water	NaCl (m)				19.3	-18.5	-
1-Propanol	NaCl (m)				-847.1	-155.1	-
2-Propanol	NaCl (m)				-176.0	-160.6	-
1-Butanol	NaCl (m)				-144.8	1867.6	-
2-Butanol	NaCl (m)				1132.8	1545.1	-
1-Pentanol	NaCl (m)				-132.8	1544.9	-
NaCl (m)	NaCl				-756.8	-19.2	-
ln K						3.78	

Table III.11: Parameters for the results in Table 5.6 for the electrolyte NRTL model with ensemble conversion with full dissociation and with partial dissociation. Nonrandomness factors are as given in Table III.8. NRTL interaction parameters τ are given by: $\tau_{ij} = A_{ij}/T$.

Component 1	Component 2	full dissociation		partial dissociation	
		A_{12}	A_{21}	A_{12}	A_{21}
		K	K	K	K
Water	1-Propanol	401.3	170.5	396.4	223.7
Water	2-Propanol	0.6	680.7	60.5	663.6
Water	1-Butanol	1410.0	-241.7	1387.9	-233.6
Water	2-Butanol	1097.7	-191.0	1102.0	-192.7
Water	1-Pentanol	1658.1	-163.9	1631.2	-161
Water	NaCl	-4182	-115.8	-4149.0	-122
1-Propanol	NaCl	-1706.6	562.6	-1895	677.4
2-Propanol	NaCl	-1796.4	88.0	-2010.2	109.2
1-Butanol	NaCl	-2136.4	147.0	-2251.1	165.2
2-Butanol	NaCl	-1745.8	951.3	-1812.0	844.5
1-Pentanol	NaCl	-3718.3	9870.0	-2174.4	1026
1-Propanol	1-Butanol	-1301.5	745.4	-1328.2	973.4
1-Propanol	1-Pentanol	-1800.9	601.3	-1826.4	779.6
Water	NaCl (m)			-382.9	-108.4
1-Propanol	NaCl (m)			-54.2	-744.5
2-Propanol	NaCl (m)			-172.1	-574
1-Butanol	NaCl (m)			2708.6	2517.9
2-Butanol	NaCl (m)			1802.7	1597.4
1-Pentanol	NaCl (m)			2042.5	1154.8
NaCl (m)	NaCl			-2539.7	-2030
ln K					3.56

Appendix IV: Modified Extended Electrolyte NRTL model

Complete model:

$$G^E = G^{E,NRTL} + G^{E,PDH} + G^{E,Born} + G^{E,BG}$$

NRTL local composition contribution
(Here simplified to only one salt)

$$\frac{G^E}{RT} = \sum_m X_m \frac{\sum_j X_j G_{jm} \tau_{jm}}{\sum_k X_k G_{km}} + X_c \frac{\sum_j X_j G_{jc} \tau_{jc}}{\sum_k X_k G_{kc}} + X_a \frac{\sum_j X_j G_{ja} \tau_{ja}}{\sum_k X_k G_{ka}} - x_c \ln\left(\gamma_c^\infty\right) - x_a \ln\left(\gamma_a^\infty\right)$$

$$X_j = C_j x_j \qquad (C_j = Z_j \; for \; ions, C_j = 1 \; for \; solvents)$$

$$\alpha_{jc} = \alpha_{ja} = \alpha_{cj} = \alpha_{aj} = \alpha_{j,ca}$$

$$\tau_{jc} = \tau_{ja} = \tau_{j,ca}$$

$$\tau_{cj} = \tau_{aj} = \tau_{ca,j}$$

$$\tau_{ji} = \left(g_{ji} - g_{ii}\right)/RT$$

$$G_{ji} = \exp\left(-\alpha_{ji}\tau_{ji}\right)$$

Pitzer-Debye-Hückel contribution:

$$\frac{G^{E,PDH}}{RT} = -\left(\sum_n^{nc} x_n\right) \frac{4A_x I_x}{\rho} \ln(1 + \rho\sqrt{I_x})$$

$$I_x = \frac{1}{2}\sum_i^{ion} x_i z_i^2$$

$$A_x = \frac{1}{3}\sqrt{\frac{1000}{M_s}}\sqrt{2\pi N_A d}\left(\frac{e^2}{\varepsilon kT}\right)^{3/2}$$

$$\varepsilon = \sum_j w_j ' \varepsilon_j$$

$$d = \frac{\sum_j x_j M_j}{\sum_k x_k M_k / d_k}$$

Born contribution

$$\frac{G^{E,Born}}{RT} = \frac{e^2}{2kT}\left(\frac{1}{\varepsilon} - \frac{1}{\varepsilon_w}\right)\sum_i^{ion} \frac{x_i z_i^2}{r_i}$$

Brønsted-Guggenheim contribution

$$\frac{G^{E,BG}}{RT} = \frac{1000}{\sum_k x_k M_k} \frac{\sum_j \sum_{k>j} \beta_{jk} x_j x_k}{T} x_a x_c$$

Appendix V: Parameters AEEOS

Table V.1: Polar parameters for the SRK part of the electrolyte equation of state.

Component	p_1	p_2	p_3	$c_i \times 10^{-5}$ m^3/mol
Water[a]	0.023175	4.6462	-8.8079	0.60473
Benzene	0.000865	5.4135	-6.5154	0.93308
1-Heptanol	-1.2838	-2.7776	1.9251	2.3232
2-Heptanone	-0.000426	-0.9014	-37.54	4.3951
Caprolactam	0.04638	-19.566	20.54	1.800

[a] As given by Zuo et al., 2000a.

Table V.2: UNIQUAC binary interaction parameters for the results obtained with the electrolyte equation of state as given in Table 6.2, with two types of expressions for λ_{ij}

Component 1	Component 2	Equation 6.52		Equation 6.53		
		τ_{12}	τ_{21}	τ_{12}^0	τ_{21}^0	τ_{12}^1
Water	Benzene	1.6773	1.7831	1.5461	25.8246	-1.167
Water	1-Heptanol	0.7038	1.8709	1.0200	1.2585	1.0114
Water	2-Heptanone	0.9370	2.0304	1.1866	2.5531	0.6027
Water	Caprolactam	-0.3113	3.0171	-0.0356	-0.2931	0.2617
Benzene	Caprolactam	0.7659	-0.1644	-0.5996	0.4284	0.2100
1-Heptanol	Caprolactam	1.2121	-0.5996	0.3829	-0.8612	0.5576
2-Heptanone	Caprolactam	1.2191	-0.4367	0.6468	-0.5387	0.1953

Table V.3: UNIQUAC binary interaction parameters for the results obtained with the electrolyte equation of state as given in Table 6.3

Component 1	Component 2	Option 1			Option 2 & 3[a]	
		τ_{12}^0	τ_{21}^0	τ_{12}^1	τ_{12}	τ_{21}
Water	Benzene	1.1857	2.6302	-2.4492	1.6773	1.7831
Water	1-Heptanol	0.7409	1.6962	0.2282	0.7038	1.8709
Water	2-Heptanone	1.1403	2.2729	-0.7247	0.9370	2.0304
Water	Caprolactam	0.3388	0.9615	0.0980	-0.3113	3.0171
Benzene	Caprolactam	0.0945	0.1915	-0.4594	0.7659	-0.1644
1-Heptanol	Caprolactam	0.4709	-0.5857	0.4101	1.2121	-0.5996
2-Heptanone	Caprolactam	0.7713	-0.417	0.0731	1.2191	-0.4367

[a] These values were not adjusted by regressions with salt containing systems

Table V.4: Adjusted parameters for the results with the electrolyte equation of state as given in Table 6.3. Bold values were given by Zuo et al. (2000b)

System	Variable	Option 1	Option 2	Option 3	Units
AS in water	λ_3	**3.51E-05**	**3.51E-05**	**3.51E-05**	$m^3\ mol^{-1}\ Å^{-1}$
	λ_4	**6.00E-06**	**6.00E-06**	**6.00E-06**	m^3/mol
	λ_5	**-3.21E-08**	-2.84E-08	**-3.21E-08**	$m^3\ mol^{-1}\ Å^{-4}$
	λ_6	**-1.89E-05**	-9.40E-06	**-1.89E-05**	m^3/mol
AS in solvent	λ_3	8.24E-05	7.25E-05	4.95E-05	$m^3\ mol^{-1}\ Å^{-1}$
	λ_4	-4.22E-04	-3.93E-04	-3.99E-04	m^3/mol
	λ_5	-7.16E-09	-5.45E-09	5.48E-10	$m^3\ mol^{-1}\ Å^{-4}$
	λ_6	-4.03E-04	-2.77E-04	-9.50E-05	m^3/mol
AS in caprolactam	λ_3			6.87E-05	$m^3\ mol^{-1}\ Å^{-1}$
	λ_4			-4.43E-04	m^3/mol
	λ_5			3.97E-09	$m^3\ mol^{-1}\ Å^{-4}$
	λ_6			3.47E-04	m^3/mol
AS in solvent	σ	8.14	9.05	10.2	Å
water/benzene/cap	f	1.00	1.40	2.00	-
water/1-heptanol/cap	f	1.00	1.26	1.20	-
water/2-heptanone/cap	f	2.00	2.00	2.00	-
water/caprolactam	f	1.42	1.62	2.00	-

Cited literature

Abovsky, V. Y. Liu, S. Watanasiri, Fluid Phase Equilib., 150-151 (1998) 277-286

Abrams, D.S., J.M. Prausnitz, AIChE J. 21, 1 (1975) 116-128

Anderko, A., P. Wang, M. Rafal, Fluid Phase Equilib., 194-197 (2002) 123-142

Aspen Technology. Inc., Physical property methods & models, ASPEN PLUS Manual, release 10, Cambridge (1998)

Austgen, D.M., G.T. Rochelle, X. Peng, C.C. Chen, Ind. Eng. Chem. Res. 28 (1989) 1060-1073

Aznar, M., R.N. Araujo, J.F. Romanato, G.R. Santos, S.G. d'Avila, J. Chem. Eng. Data, 45 (2000) 1055-1059

Balaban, A., G. Kuranov, N. Smirnova, Fluid Phase Equilib., 194-197 (2002) 717-728

Ball, F.X., Evaluation de nouveax modeles pour la representation des ecarts a l'idealité des solutions d'electrolytes fortes, PhD-thesis ENSTA France (1984)

Ball, F.X., H. Planche, W. Furst, H. Renon, AIChE J., 31, 8 (1985) 1233-1240

Blum, L., Mol. Phys., 30, 5 (1975) 1529-1535

Blum, L., J.S. Hoye,, J. Phys. Chem., 81, 13 (1977), 1311-1316.

Blum, L. , D.Q. Wei, J. Chem. Phys. 87, 1 (1987) 555-565.

Bochove, G.H. van, Measurements and modelling of liquid-liquid equilibria of caprolactam + water + solvent + ammonium sulfate systems, MSc-thesis TU-Delft (1998)

Bocko. P., Fluid Phase Equilib.,4 (1980) 137-150

Boluda, N., V. Gomis, F. Ruiz, M.D. Saquette, N. Barnes, Fluid Phase Equilib., 179 (2001) 269-276

Bromley, L.A., AIChE J., 19 (1973) 313-320

Cardoso, J.E. de M., J.P. O'Connell, Fluid Phase Equilib., 33 (1987) 315-326

Cheluget, E.L., S. Marx, M.E. Weber, J.H. Vera, J. Sol. Chem., 23, 2 (1994) 275-305

Chen, C.C., H.I. Britt, J.F. Boston, L.B. Evans, AIChE J., 28, 4 (1982) 588-596

Chen, C.C., L.B. Evans, AIChE J., 32, 3 (1986) 444-454

Chen, C.C., Y. Zhu, L.B. Evans, Biotechnology Progress, 5, 3 (1989) 111-118

Chen, C.C., P.M. Mathias, H. Orbey, AIChE J., 45, 7 (1999) 1576-1586

Chen, C.C., P.M. Mathias, AIChE J., 48, 2 (2002) 194-200

Chou, T.J., A. Tanioka, H.C. Tseng, Ind. Eng, Chem. Res., 37 (1998) 2039-2044

Christensen, C., B. Sander, A. Fredenslund, P. Rasmussen, Fluid Phase Equilib., 13 (1983) 297-309

Cong, W., Y. Li, J. Lu, J. Sol. Chem., 25, 12 (1996) 1213-1226

Conway, B.E., Ionic hydration in chemistry and biophysics, Amsterdam (1981)

Copeman, T.W., F.P. Stein, Fluid Phase Equilib., 35 (1987) 165-187

Corti, H.R., J. Phys. Chem., 91 (1987), 686-689

Cruz, J.L., H. Renon, AIChE Jounal, 24,5 (1978) 817-830

Debye, P., E. Hückel. Physik. Z., 24 (1924) 185

Eggebrecht, J., P. Ozler, J. Chem. Phys., 93 (1990) 2004-2015

Fernandez, M.J.,V. Gomis, M. Ramos, F. Ruiz, J. Chem. Eng. Data, 45 (2000) 1053-1054

Fisher, G., Chemical Marketing Reporter, November 20, 2000

Friedman, H.L., J. Sol. Chem., 1, 5 (1972) 387-431

Fürst, W., H. Renon, AIChE J., 39, 2 (1993) 335-343

Garcia-Sanchez, F., J. Schwartzentruber, M.N. Ammar, H. Renon, Fluid Phase Equilib. 121 (1996) 207-225

Gering, K.L., L.L. Lee, L.H. Landis, Fluid Phase Equilib., 48 (1989) 111-139

Gomis, V. F. Ruiz, M. Ramos-Nofuentes, M.J. Fernández-Torres, Fluid Phase Equilib., 149 (1998) 139-145

Gomis, V., F. Ruiz, N. Boluda, D. Saquete, J. Chem. Eng. Data, 44 (1999) 918-920

Grunwald, E., Thermodynamics of molecular species, New York (1997)

Gucwa, A.J., K. Makal, J. Azymczak, Przemysl Chemiczny, 55, 8 (1976) 420

Guggenheim, E.A., Phil. Mag., 19 (1935) 588-643

Haan, A,B. de, S. Niemann, Paper presented at International Solvent Extraction Conference, Barcelona, Spain, July 11-16, 1999

Haase, K., Measurements of liquid-liquid equilibria of water + ε-caprolactam + ammonium sulfate + solvent systems, M.Sc.-thesis TU-Berlin (1997)

Haghtalab, A., J.H. Vera, AIChE J., 34, 5 (1988) 803-813

Haghtalab, A., B. Mokhtarani, Fluid Phase Equilib., 180 (2001) 139-149

Heidemann, R.A., R.M. Abdel-Ghani, Chem. Eng. Science, 56 (2001) 6873-6881

Hildebrand, J., J.Phys.Colloid.Chem., 53 (1949) 944

Humffray, A.A., J. Phys. Chem., 87 (1983) 5521-5522

Jaretun, A., G. Aly, Fluid Phase Equilib., 163 (1999) 175-193

Jin, G., M.D. Donohue, Ind. Eng. Chem. Res., 27 (1988) 1073-1084

Kahlweit, M., R. Strey, P. Firman, D. Haase, J. Jen, R. Schomäcker, Langmuir, 4 (1988) 499-511

Knickerbocker, B.M., C.V. Pesheck, H.T. Davis, L.E. Scriven, J. Phys. Chem, 86, 3 (1982) 393-400

Knickerbocker, B.M., C.V. Pesheck, H.T. Davis, L.E. Scriven, J. Phys. Chem, 83, 15 (1979) 1984-1990

Koak, N., Some computational and experimental aspects of polymer solution phase behaviour, PhD- thesis University of Calgary (1997)

Lang, J.C., B. Widom, Physica 81A (1975) 190-213

Lebowitz, J.L. and J.K. Percus, Phys. Rev., 144, 1 (1966), 251-258.

Lee, L.L., Molecular Thermodynamics of Nonideal Fluids, Boston (1988)

Lee, L.L., Proceedings of the 75th GPA annual convention (1996) 92-101

Lee, L.L., J. Mol. Liq. 87 (2000) 129-147

Li, C., Y. Li, J. Lu, L. Yang, Fluid Phase Equilib. 124 (1996) 99-110

Li, J.D., H.M. Polka, J. Gmehling, Fluid Phase Equilib., 94 (1994) 89-114

Li, Y., personal communication Th.W. de Loos (2001)

Li, Z., Y. Tang, Y. Liu, Y. Li, Fluid Phase Equilib., 103 (1995) 143-153

Lide, R. (Ed.), CRC Handbook of chemistry and Physics, 76th ed., Boca Raton (1995)

Liu, Y., A.H. Harvey, J.M. Prausnitz, Chem. Eng. Commun., 77 (1989a) 43-66

Liu, Y., U. Gren, M. Wimby, Fluid Phase Equilib., 53 (1989b) 269-277

Liu, Y., S. Watanasiri, Fluid Phase Equilib., 116 (1996) 193-200

Liu, Y., S. Watanasiri, Chem. Eng. Progr., 10 (1999) 25-42

Liu, W.B., Y.G. Li, J.F. Lu, Fluid Phase Equilib., 158-160 (1999) 595-606

Liu, W.B, Z.P. Liu, Y.G. Li, J.F. Lu, Fluid Phase Equilib., 178 (2001) 45-71

Loehe, J.R., M.D. Donohue, AIChE J., 43 (1997) 180-195

Macedo, E.A., P. Skovborg, P. Rasmussen, Chem. Eng. Science, 45, 4 (1990) 875-882

Mansoori, G.A., N.F. Carnahan, K.E. Starling, T.W.Leland, J. Chem. Phys., 54, 4 (1971) 1523-1525

Mazo, R.M. and C.Y.Mou, In: Activity Coefficients in Electrolyte Solutions, K.S. Pitzer (Ed), 2nd Ed., Boca Raton (1991)

Michelsen, M.L., Fluid Phase Equilib., 9 (1982) 1-40

Michelsen, M.L., Computers Chem. Engng., 18, 7 (1994) 545-550

McMillan, W.G. J.E. Mayer, J. Chem. Phys., 13, 7 (1945) 276-305

Mock, B., L.B. Evans, C.C. Chen, AIChE J., 32, 10 (1986) 1655-1664

Morachevskii, A.G., V.E. Sabinin, Zh. Prikladnoi Khimii, 33, 8 (1960) 1775

Navis, R., Bepaling van vloeistof - vloeistof evenwichten van het systeem caprolactam / benzeen / water / ammoniumsulfaat, Student report DSM Research, Geleen (1996)

Negahban, S., G.P. Willhite, S.M. Walas, M.J, Michnick, Fluid Phase Equilib., 32 (1986) 49-61

Negahban, S., G.P. Willhite, S.M. Walas, SPE Reservoir Engineering, August (1988) 1017-1024

Nightingale, E.R., J. Phys. Chem., 63 (1959), 63, 1381-1387

O'Connell, J.P., personal communication Th.W. de Loos (2001)

Olaya, M.M., A. Botella, A. Marcilla, Fluid Phase Equilib., 157 (1999) 197-211

Pająk, M., J. Piotrowicz, W. Skrzypiński, Przemysl Chemiczny, 70, 2 (1991) 72-74

Passarello, J.P., W. Fürst, Fluid Phase Equilib., 116 (1996) 177-184

Peneloux, A., E. Rauzy, R. Freze, Fluid Phase Equilib., 8 (1982) 7-23

Peng, Q., Z. Li, Y. Li, Fluid Phase Equilib. 97 (1994) 67-80

Perry, R. (Ed.), Perry's Chemical Engineer's Handbook, 7th ed., New-York (1997)

Pfennig, A., A. Schwerin, Ind. Eng. Chem. Res., 37 (1998) 3180-3188

Phoenix, A.V., R.A. Heidemann, Fluid Phase Equilib. 150-151 (1998) 255-265

Pitzer, K.S., J. Phys. Chem., 77 (1973) 268-277

Pitzer, K.S., J. Am. Chem. Soc., 102, 9 (1980) 2902-2906

Pitzer, K.S., Thermodynamics, 3rd Edition, New-York (1995)

Planche, H., Modele moleculaire de representation des proprietes thermodynamiques des corps polaires, de leurs melanges et des solutions d'electrolytes, PhD-thesis ENSTA, France (1982)

Planche, H., H. Renon, J. Phys. Chem., 85 (1981) 3924-3929

Prausnitz, J.M., R.N. Lichtenthaler, E. Gomes de Azevedo, Molecular Thermodynamics of Fluid-Phase Equilibria, 3rd edition, New-Yersey (1999)

Press, W.H., S.A. Teukolsky, W.T. Vetterling, B.P. Flannery, Numerical Recipes in FORTRAN 77: The art of scientific computing, 2nd edition, New-York (1997)

Rafal, M., J.W. Berthold, N.C. Scrivner, S.L. Grise, Models for electrolyte solutions. In: S.I. Sandler (Ed.) Models for thermodynamic and phase equilibria calculations, New York (1994)

Rashin, A.A., B. Honig, J. Phys. Chem., 89, 26 (1985) 5588

Reid, R.C., J.M. Prausnitz, B.E. Poling, The properties of gases and liquids, 4th Ed., New York (1987)

Renon, H., J.M. Prausnitz, AIChE J., 14,1 (1968) 135-144

Renon, H., Fluid Phase Equilib., 30 (1986) 181-195

Riedel-de Haën, 'Hydranal manual', Seelze (1994)

Ritz, J., H. Fuchs, H. Kieczka, W.C. Moran. In: Ullmann's Encyclopedia of Industrial Chemistry, 6th Edition, Electronic release, Weinheim (1999)

Robinson, R.A., R.H. Stokes, Electrolyte solutions, London (1959)

Rowlinson, J.S., F.L. Swinton, Liquids and Liquid Mixtures, 3rd Ed., London (1983)

Sander, B., Extended UNIFAC/UNIQUAC models for 1) Gas solubility calculations and 2) Electrolyte solutions, PhD-thesis Technical University of Denmark (1984)

Sander, B., A. Fredenslund, P. Rasmussen, Chem. Eng. Science, 41, 5, (1986) 1171-1183

Santis, R. de, L. de Marelli, P.N. Muscetta, Chem. Eng. J., 11 (1976) 207-214

Schwartzentrüber, J., H. Renon, S. Watanasiri, Fluid Phase Equilib. 52 (1989) 127-134

Shubtsova, I.G., N.I. Nikurashina, S.E. Chepurnova, Russ. J.Phys.Chem., 49, 1 (1975a) 33-35

Shubtsova, I.G., N.I. Nikurashina, S.K. Rybalov, Russ. J. Phys. Chem., 49, 1 (1975b) 35-37

Simonin, J.P, L. Blum, P. Turq, J. Phys. Chem., 100 (1996) 7704-7709

Simonin, J.P., J. Phys. Chem. B, 101 (1997) 4313-4320

Simons, A.J.F., N.F. Haasen, Extraction of caprolactam, In: T.C. Lo, Baird, M.H.I., and Hanson, C. (Eds.), Handbook of Solvent Extraction, Malabar (1991) 557-566

Smith, J.M., H.C. van Ness, Introduction to Chemical Engineering Thermodynamics, 4th Edition, New York (1987)

Snell-Ettre (Ed.), Encyclopedia of industrial chemical analysis, vol. 8, 116, New York (1969)

Sørensen, J.M., T. Magnussen, P. Rasmussen, A. Fredenslund, Fluid Phase Equilib., 2 (1979) 297-309

Sørensen, J.M., W. Arlt, Liquid-Liquid Data Equilibrium Collection, DECHEMA, Frankfurt (1980)

Stateva, R.P., G.S. Cholakov, A.A. Galushko, W.A. Wakeham, Chem. Eng. Science, 55 (2000) 2121-2129

Stokes, R.H., In: Activity Coefficients in Electrolyte Solutions, K.S. Pitzer (Ed), 2nd Ed., Boca Raton (1991)

Tettimanti, K., M. Nogradi, J. Sawinski, J. Periodica Polytechnica, 4 (1960a) 201-218

Tettimanti, K., M. Nogradi, J. Periodica Polytechnica, 5, 1 (1960b) 15-23

Thomsen, K, P. Rasmussen, R. Gani, Chem. Eng. Science, 51, 14 (1996) 3675-3683

Thomsen, K., P. Rasmussen, Book of abstracts PPEPPD 2001, Kurashiki, Japan (2001)

Triolo, R., J.R. Grigera, L.Blum, J. Phys. Chem., 80, 17 (1976), 1858-1861.

Triolo, R., L. Blum, M.A. Floriano, J. Chem. Phys., 67, 12 (1978) 5956-5959.

Vecera, S., J. Sladky, Coll. Czechoslov. Chem. Commun., 20 (1955) 557

Waisman, E., J.L. Lebowitz, J. Chem. Phys., 52 (1970) 4307-4309

Waisman, E., J.L. Lebowitz, J. Chem. Phys., 56, 6 (1972a) 3086-3093

Waisman, E., J.L. Lebowitz, J. Chem. Phys., 56, 6 (1972b) 3093-3099

Walas, S.M., Phase equilibria in chemical engineering, London (1985)

Wang, J., Y. Zhang, Y. Wang, J. Chem. Eng. Data, 47 (2002) 110-112

Wijtkamp, M., Progress report May 1996, Delft (1996)

Wijtkamp, M., G.H. van Bochove, Th.W. de Loos, S. Niemann, Fluid Phase Equilib., 158-160 (1999) 939-947

Wilson, G.M., J. Am. Chem. Soc., 36 (1964) 127

Wong, D.S.H., S.I. Sandler, Ind. Eng. Chem. Res., 31 (1992) 2033-2039

Wu, J., J. Lu, Y. Li, Fluid Phase Equilib., 101 (1994) 121-136

Wu, R.S, L.L. Lee, Fluid Phase Equilib., 78 (1992) 1-24

Yan, W., M. Topphoff, C. Rose, J. Gmehling, Fluid Phase Equilib., 162 (1999) 97-113

Zerres, H., J.M. Prausnitz, AIChE J., 40, 4 (1994) 676-691

Zhu, Y., L.B. Evans, C.C. Chen, Biotechnol. Prog., 6 (1990) 266-272

Zuo, Y-X., W. Fürst, Fluid Phase Equilib., 150-151 (1998) 267-275

Zuo, J.Y., D. Zhang, W. Fürst, Fluid Phase Equilib., 175 (2000a) 285-310

Zuo, J.Y., D. Zhang, W. Fürst, AIChE J., 46, 11 (2000b) 2318-2329

Zuo, J.Y., D. Zhang, E.H. Stenby, Chem. Eng. Commun., 184 (2001) 175-192

–, Chemical Week, August 29, 2001

List of symbols

a	Radius
a_i^{SR}	Energy parameter
A	Debye-Hückel parameter
A_{ij}	NRTL binary interaction parameter
A^E	Excess Helmholtz energy
b_i	Molar co-volume
b_2	MSA parameter
B_{10}	MSA parameter
B_{ij}	NRTL binary interaction parameter
c_i	Volume translation parameter
C_{ij}	Direct correlation function
D	Tangent plane distance
d_i	Density
e	Electronic charge
F	Objective function
f_i	Fugacity
f	Born correction
G^E	Molar excess Gibbs energy
g_{ij}	Pair correlation function
g_{ij}	Minimization function
g_{ij}	Interaction function
h_{ij}	Total correlation function
I	Ionic strength
I_x	Ionic strength (mole fraction scale)
k	Boltzmann constant
K_{ij}	Distribution coefficient
K	Dissociation constant
M_i	Molecular weight
N	Number of particles
N_A	Avogadro's number
nc	Number of components
nd	Number of datapoints
np	Number of phases
n	Mole number
p_i	Polar parameter
P	Pressure
P_n	MSA coupling parameter

q_i	Charge
Q	Michelsen objective function
r	Radius or distance
R	Universal gas constant
SSQ	Sum of squares
T	Temperature
u_{ij}	Interaction potential
U	Internal energy
v	Stoichiometric coefficient
v	Molar volume
$<v>$	Average molar volume
V	Volume
w_i	Weight fraction
W	Weight factor
W_{ij}	SR2 interaction parameter
x	Mole fraction
x	Distance
X	Local mole fraction
z	Charge number
z	Overall composition
Z	Compressibility factor

Greek symbols:

α	Dissociation fraction
α_{ij}	Nonrandomness factor
α	MSA interaction parameter
β	Phase fraction
β_{ij}	Brønsted-Guggenheim interaction parameter
β	Boltzmann factor = 1/kT
δ	Dirac function
Δ	Solvent volume fraction
Δx	Average deviation in mole fractions
Δw	Average deviation in weight fractions
ε	Dielectric constant ($\varepsilon = 4\pi \cdot 8.8542 \times 10\text{-}12 \cdot \varepsilon_r$)
γ	Activity coefficient
$\gamma_{\pm}$	Mean ionic activity coefficient
Γ	MSA shielding parameter
κ	Debye-Hückel shielding parameter
θ	Surface fraction

θ	Stability function
λ	Step size
λ	SR2 interaction parameter
λ_{ij}	UNIQUAC interaction parameter
μ_i	Chemical potential
μ	Dipole moment
Ξ	Partition function
Π	Osmotic pressure
ρ	Numeric density
ρ	Closest approach parameter
σ_i	Diameter
σ_{ij}	Distance of closest approach
τ_{ij}	Binary interaction parameter
ϕ_i	Fugacity coefficient
ϕ_i	Volume fraction
Φ_{mnl}	Angular function
ψ	Electrostatic potential
ω	Acentric factor
Ω	MSA parameter

Acknowledgements

This thesis would not be complete without acknowledgements to all those who contributed to either (1) the work reported or (2) the stimulating environment in which it was created. I want to thank all those people who feel they contributed in one way or both ways. However, I will use this opportunity to thank some people in person.

For their contribution to the work reported in this thesis, I would like to thank the following persons:

- Firstly, Theo de Loos, who was my supervisor during my graduation project as a student, who stimulated me to do a PhD-project and guided me when I did this PhD-work. Theo, thank you for more than five years of wonderful cooperation and support.
- For his contribution, I also want to thank Gerard Krooshof from DSM Research. It was good to have your enthusiasm and contributions during our meetings.
- Also, I want to thank professor Jakob de Swaan Arons, for giving me the opportunity to start this PhD-project and for the interesting discussions.
- Many thanks to Mark Wijtkamp for setting up the experiments and the experimental procedure.
- For half a year, Zhou Huan helped me with the experiments on the three-liquid phase equilibria with benzene. Thanks!
- Eugene Straver was always there when I needed help with the analytical work. Thank you Eugene.

For the good feelings I have when I look back to the period I spent in the group of Applied Thermodynamics, not the work is the most important, but the atmosphere and environment in which this work was carried out is determinative. Therefore, I owe thanks to many colleagues:

Special thanks go to Diana Nanu, with whom I shared an office for almost three years: *Diana ai fost cea mai buna colega de birou, pe care mi-o puteam dori.* Thank you for your nice company, your support and much more.

I want to thank Miranda for her help and cooperation in many activities and for her friendship during all four years of my PhD-project.

Wim and Theo I thank for the many pleasant discussions while drinking coffee or water, but especially for their moral support in many matters and their interest in more than just my work.

I thank also Ali and Sona, the "lunch partners", for the nice discussions.

I want to thank Eugene for many enjoyable discussions and help, at university or during our "excursions" into Delft.

Of course, I cannot mention everyone here, but I also want to thank all other colleagues and students that were part of our group for shorter or longer periods. Many of them came from abroad: from Romania, from Portugal, from Canada, from Spain and so on. That mix of cultures and nationalities in the group is something I have always enjoyed very much. Once again: Thanks to all of you!

Tenslotte wil ik mijn ouders bedanken die mij al die jaren op de achtergrond gesteund hebben van HTS naar TU tot promotie bij de TU, wat uiteindelijk resulteerde in dit proefschrift.

Gerard

List of publications

Bochove, G.H. van, Measurements and Modelling of Liquid-Liquid Equilibria of Caprolactam + Water + Solvent + Ammonium Sulfate Systems, MSc-thesis TU-Delft (1998)

Wijtkamp, M., G.H. van Bochove, Th.W. de Loos, S. Niemann, *Measurements and modeling of liquid-liquid equilibria of water + caprolactam + electrolyte + organic solvent systems*, poster presentation at PPEPPD 1998, April 26-May 1, 1998, Noordwijkerhout, The Netherlands

Wijtkamp, M., G.H. van Bochove, Th.W. de Loos, S. Niemann, *Measurements of liquid-liquid equilibria of water + ε-caprolactam + electrolyte + organic solvent systems*, Fluid Phase Equilibria (1999) 158-160, 939-947

Bochove, G.H. van, G.J.P. Krooshof, Th.W. de Loos, *A New Version of the Extended Electrolyte NRTL Theory to Model Liquid-Liquid Equilibria of Ternary and Quaternary Mixed-Solvent Electrolyte Systems*, presentation Annual Meeting AIChE 1999, Dallas, USA

Bochove, G.H. van, G.J.P. Krooshof, Th.W. de Loos, *Modelling of Liquid-Liquid Equilibria of Mixed Solvent Electrolyte Systems Using the Extended Electrolyte NRTL*, Fluid Phase Equilibria (2000) 171, 45-58

Loos, Th.W. de, G.H. van Bochove, G.J.P. Krooshof, *Two- and Three-Liquid Phase Equilibria of the System Water + 2-Heptanone + Caprolactam + $(NH_4)_2SO_4$*, presentation at Thermodynamics 2001, April 4-6, 2001, Bristol, UK

Bochove, G.H. van, G.J.P. Krooshof, Th.W. de Loos, *Two- and Three-Liquid Phase Equilibria of the System Water + 2-Heptanone + Caprolactam + $(NH_4)_2SO_4$: Experiments and Modelling*, presentation at PPEPPD 2001, May 20-25, 2001, Kurashiki, Japan

Bochove, G.H. van, G.J.P. Krooshof, Th.W. de Loos, *Two- and Three-Liquid Phase Equilibria of the System Water + 2-Heptanone + Caprolactam + $(NH_4)_2SO_4$: Experiments and Modelling*, Fluid Phase Equilibria (2002) 194-197, 1029-1044

Bochove, G.H. van, H. Zhou, Th.W. de Loos, *Three-Liquid Phase Equilibria in Water + Benzene + Caprolactam + Ammonium Sulfate Mixtures*, poster presentation at AIChE Annual Meeting 2002, November 3-8, 2002, Indianapolis, USA

Zhou, H., G.H. van Bochove, Th.W. de Loos, *Three-Liquid Phase Equilibria in Water + Benzene + Caprolactam + $(NH_4)_2SO_4$ Mixtures*, AIChE Journal, in press (2003)

Curriculum Vitae

28 September 1973	Born in Oud-Beijerland
1985-1991	Secondary school at the Guido de Bres, Rotterdam
5 June 1995	VWO diploma
1991-1995	HTS Dordrecht, Dordrecht Chemical Technology (B.Sc.)
20 July 1995	Graduated
1995-1998	Delft University of Technology, Delft Chemical Engineering (M.Sc.)
27 August 1998	Graduated cum laude
1998-2002	PhD.-project at the Laboratory for Applied Thermodynamics and Phase Equilibria, Delft University of Technology, Delft
from October 2002	Working as a scientist at PURAC biochem BV, Gorinchem